

12-2018

HYPOTHALAMIC CIRCUITS IN THE CONTROL OF FEEDING AND EMOTIONAL BEHAVIORS

Leandra Mangieri

Follow this and additional works at: https://digitalcommons.library.tmc.edu/utgsbs_dissertations

 Part of the [Behavioral Neurobiology Commons](#), [Medicine and Health Sciences Commons](#), and the [Molecular and Cellular Neuroscience Commons](#)

Recommended Citation

Mangieri, Leandra, "HYPOTHALAMIC CIRCUITS IN THE CONTROL OF FEEDING AND EMOTIONAL BEHAVIORS" (2018). *UT GSBS Dissertations and Theses (Open Access)*. 903.
https://digitalcommons.library.tmc.edu/utgsbs_dissertations/903

This Dissertation (PhD) is brought to you for free and open access by the Graduate School of Biomedical Sciences at DigitalCommons@TMC. It has been accepted for inclusion in UT GSBS Dissertations and Theses (Open Access) by an authorized administrator of DigitalCommons@TMC. For more information, please contact laurel.sanders@library.tmc.edu.

HYPOTHALAMIC CIRCUITS IN THE CONTROL OF FEEDING AND EMOTIONAL
BEHAVIORS

by

Leandra R. Mangieri, M.S.

APPROVED:

Qingchun Tong, Ph.D.
Advisory Professor

Andrew Bean, Ph.D.

Michael Beierlein, Ph.D.

Benjamin Arenkiel, Ph.D.

Vihang Narkar, Ph.D.

APPROVED:

Dean, The University of Texas
MD Anderson Cancer Center UTHealth Graduate School of Biomedical Sciences

HYPOTHALAMIC CIRCUITS IN THE CONTROL OF FEEDING AND EMOTIONAL
BEHAVIORS

A

DISSERTATION

Presented to the Faculty of

The University of Texas

MD Anderson Cancer Center UTHealth

Graduate School of Biomedical Sciences

in Partial Fulfillment

of the Requirements

for the Degree of

DOCTOR OF PHILOSOPHY

by

Leandra R. Mangieri, M.S.
Houston, Texas

December, 2018

Dedication

This work is dedicated to my loving and supportive family, my friends, and cats.

Acknowledgments

First and foremost, I sincerely and emphatically thank Dr. Tong for his extraordinary mentorship, guidance and support throughout my graduate education. His intense enthusiasm and love for teaching has always been a true inspiration and motivation for me to pursue the highest degree of achievement. I will always treasure our exciting conversations that sparked intellectual curiosity and critical thinking, and helped me develop critical skills in experimental design and hypothesis generation. Dr. Tong is truly a brilliant scientist who loves what he does, and an exemplar for young scientists who aspire to do something great with their careers.

I also sincerely thank my lab mates in the Tong lab, especially Yuanzhong Xu, Ryan Cassidy, and former lab members Yungang Lu, Eun Ran Kim, Shengjie Fan, and Zhaofei Wu. They have all provided tremendous direction and support for my projects, taught me laboratory techniques and helped me with any experimental technical issues. Importantly, I would like to acknowledge and graciously thank Yungang Lu for his excellent collaborative support with electrophysiology experiments.

I am also very grateful for the support and friendship of everyone (current and past members) in the Institution of Molecular Medicine's department of Metabolic and Degenerative Diseases. I would like to especially thank Dr. Nick Justice, and his lab, Zhiying Jiang and Shiva Rajamanickam for their support and guidance on my projects. I thank Zhiying Jiang tremendously for her enthusiastic collaborative effort on electrophysiology experiments.

I would also like to express my sincerest gratitude for the members (including Dr. Tong) who participated in my graduate committee: Dr. Andrew Bean, Dr. Vihang Narker, Dr.

Michael Beierlein and Dr. Ben Arenkiel. They have challenged me and provided all the necessary support to guide me successfully throughout graduate training. I sincerely acknowledge the critical support of Dr. Ben Arenkiel as a co-mentor for my NIH fellowship. His guidance and collaborative support on projects have tremendously aided my success throughout my graduate school years.

I also thank Dr. Sheng Zhang and Dr. Kartik Venkatachalam for the opportunity to rotate in their labs, and early support during my graduate training. They provided excellent mentorship and imparted critical knowledge and skills that were essential for my learning experience. Relatedly, I would also like to express many thanks to the faculty at MD Anderson Cancer Center UTHealth Graduate School of the Biomedical Sciences and Neuroscience Program for the excellent education I was able to receive from outstanding researchers who imparted their knowledge in the classroom in an enjoyable, productive and informative way. Special thanks go to Deans Michelle Barton and Michael Blackburn for crafting an outstanding graduate school experience for students.

I would also like to express my gratitude to the staff at GSBS and my department who effortlessly work to make student's lives as smooth as possible. They provide all the necessary support to aid in career development, grant writing, social networking, and more, which are all essential aspects of the graduate school experience. In particular, I would like to thank Amanda Williamson for her hard work and dedication to the Neuroscience Program. She has always worked tirelessly to help put together highly enjoyable and educational events, like the annual program retreat.

I sincerely express great thanks as well to the scholarship donors and evaluation committees who bestowed upon me the honor to be a recipient of awards, including the Dee S. and Patricia Osborne Endowed Scholarships in the Neurosciences, Wei Yu Family

Endowed Scholarship, and Roberta M. and Jean M. Worsham Endowed Fellowship in Behavioral Neurosciences. I also graciously thank the National Institute of Health-National Institute on Drug Abuse (NIDA) for the honor to receive an F31 fellowship for my graduate training.

Last, but certainly not least, I would like to thank my family and the friends I've made in graduate school, for their support and all the color they add to my life.

Hypothalamic Circuits in the Control of Feeding and Emotional Behaviors

Leandra Rosa Mangieri, M.S.

Advisory Professor: Qingchun Tong, Ph.D.

Feeding results from the integration of both nutritional and affective states, and is guided by complex neural circuitry in the brain. The hypothalamus is a critical center controlling feeding and motivated behaviors. We found that targeted photostimulation of projections from the lateral hypothalamus (LH) to the paraventricular hypothalamus (PVH) in mice elicited voracious feeding and repetitive self-grooming behavior. GABA neurotransmission in the LH→PVH circuit mediated the evoked feeding behavior, and elicited behavioral approach, whereas glutamate release promoted repetitive self-grooming, which was stress-related in nature. Optogenetic inhibition of LH^{GABA}→PVH circuit reduced feeding after fasting, whereas photostimulation abruptly stopped ongoing self-grooming and immediately elicited feeding. Oppositely, optogenetic inhibition of LH^{Glutamate}→PVH circuit reduced repetitive self-grooming, whereas photostimulation suppressed fast-refeeding in exchange for repetitive self-grooming. Optogenetically activating and silencing PVH neurons directly recapitulated these findings, and demonstrated the necessity of glutamatergic PVH neurons in mediating the competition between self-grooming and feeding. Together, these results provided evidence that the mutually exclusive nature of feeding and self-grooming behaviors are in part mediated by distinct components in the LH→PVH circuit.

Interestingly, photostimulating PVH neurons with greater intensity promoted transitions from grooming to frantic escape-jumping, suggesting scalability of stress-related behaviors mediated by PVH neural activity. Because evoked jumping resembled attempts to escape, we posited PVH neurons mediate defensive responses. Validating this,

photostimulating PVH neurons induced avoidance and increased locomotion, two classic behavioral indicators of active defense strategies. Anterograde tracing showed that PVH neurons densely projected to the midbrain region in and surrounding the ventral tegmental area (VTA), a brain region well-known for its roles in motivated behaviors. Indeed, photostimulation of PVH→midbrain projections produced escape behaviors and conditioned place aversion. Combined optogenetic and chemogenetic experiments showed that glutamatergic-midbrain neurons were required for escape behaviors. Further, glutamatergic-midbrain neurons displayed increased neural population activity *in vivo* during a fear-provoking situation, validating a role for this population in processing threat.

Taken together, our work reveals novel hypothalamic circuits in the control of feeding, emotional valence, and behaviors related to stress and defense. These findings shed light on possible neural mechanisms underlying complex disease states characterized by feeding abnormalities, anxiety and fear.

Table of Contents

Approval Sheet.....	i
Title Page.....	ii
Dedication.....	iii
Acknowledgments.....	iv
Abstract.....	vii
Table of Contents.....	ix
List of Figures.....	xiv
List of Tables.....	xviii
Abbreviations.....	xix
Chapter 1. Background and Significance.....	1
Introduction.....	2
Homeostatic feeding: hypothalamus and brainstem.....	3
<i>Arcuate Nucleus</i>	3
<i>Paraventricular Hypothalamus</i>	6
<i>Lateral Hypothalamus</i>	10
<i>Other hypothalamic sites and connections with the brainstem</i>	13
Non-homeostatic feeding and emotional regulation.....	17
<i>The Lateral Hypothalamus in Reward and Other Behaviors</i>	18

<i>Arc^{AgRP} Neurons in Feeding-Related Behaviors and Emotion</i>	21
<i>The PVH, VMH, and Brainstem Neurons Produce Diverse Behaviors and Emotional States</i>	22
Tools for Interrogating Neural Circuits Underlying Behavior.....	26
<i>Cre-LoxP Technology</i>	26
<i>Optogenetics</i>	27
<i>Designer Receptors Exclusively Activated by Designer Drugs (DREADDs)</i>	29
<i>Deep Brain Imaging in vivo</i>	30
Significance.....	31
Chapter 2. A Neural Basis for Antagonistic Control of Feeding and Compulsive Behaviors	34
Summary.....	35
Introduction.....	35
Results.....	37
LH→PVH projections directly synapse on a common subset of PVH neurons.....	37
Activation of LH→PVH fibers induces feeding and self-grooming.....	40
Glutamate release from LH→PVH fibers in self-grooming behavior.....	45
PVH neurons mediate feeding and self-grooming behavior.....	49

LH→PVH projections in physiologic feeding and grooming.....	54
Antagonistic control of feeding and grooming by LH→PVH projections.....	57
Activation of PVH neurons on self-grooming versus feeding.....	60
Discussion.....	66

Chapter 3. Defensive Behaviors Driven by a Hypothalamic-Midbrain

Circuit.....	71
Summary.....	72
Introduction.....	73
Results.....	74
Activation of PVH neurons elicits escape behavior associated with increased flight and negative valence.....	74
PVH projections to the midbrain area drive escape behavior and avoidance.....	78
Activation of PVH→midbrain circuit suppresses food intake due to intense avoidance and promotes aversion learning.....	84
Glutamatergic midbrain neurons are activated by PVH projections to drive escape behavior.....	87
Population dynamics of glutamatergic midbrain neurons during a fearful and aversive situation.....	93
Discussion.....	95

Chapter 4. Materials and Methods	100
Methods for Chapter 2.....	101
Animal care.....	101
Surgeries and viral constructs.....	101
Brain slice electrophysiological recordings.....	103
Behavioral Experiments.....	104
Feeding and Grooming Assays.....	105
Real Time Place Preference (RTPP).....	106
Ionotropic GluR blockade experiment.....	106
Inhibition Experiments.....	107
Feeding vs. Grooming Competition Experiments.....	109
In situ hybridization (ISH).....	110
Brain tissue preparation, imaging, and post-hoc analysis.....	111
Statistics.....	112
Methods for Chapter 3.....	113
Subjects and Experimental Models.....	113
Viruses and Surgery.....	113
Acute Brain Slices Preparation and <i>in vitro</i> Electrophysiology	

Recordings.....	115
Optogenetic Experimental Parameters.....	117
Behavioral Analysis.....	117
Fiber Photometry and Modified T-maze.....	122
Immunohistochemistry and Imaging.....	123
Statistics.....	124
Chapter 5. Discussion.....	126
Bibliography.....	135
Vita.....	152

List of Figures

Figure 1. The hypothalamus is composed of several spatially clustered neural populations.....	3
Figure 2. Homeostatic regulation of feeding and energy balance.....	16
Figure 3. Brain circuits involved in feeding encode emotional valence.....	25
Figure 4. <i>Pdx1-Cre</i> expression in hypothalamic brain regions, including LH, which contain segregated GABA and glutamatergic neuron populations.....	38
Figure 5. GABA and glutamate LH neurons send monosynaptic projections to a common subset of PVH neurons.....	40
Figure 6. ChR2 expression in LH ^{<i>Pdx1</i>} neurons.....	41
Figure 7. Optical activation of LH ^{<i>Pdx1</i>} →PVH projections differentially causes feeding and repetitive grooming behaviors, with the former requiring GABA release.....	42
Figure 8. Inhibitory and excitatory post-synaptic currents in PVH elicited by blue light stimulation of LH ^{<i>Pdx1-ChR2</i>} fibers require vesicular GABA transporter (Vgat) and vesicular glutamate transporter 2 (Vglut2), respectively.....	43
Figure 9. Photostimulation of LH ^{<i>Pdx1-GFP</i>} expressing fibers in PVH does not increase feeding or grooming behaviors.....	44
Figure 10. Photostimulation of GABAergic LH→PVH projections causes chewing and licking behavior.....	46
Figure 11. ChR2 expression in LH neurons and PVH projection fibers in <i>Pdx1-Cre</i> and <i>Pdx1-Cre::Vglut2^{flox/flox}</i> mice.....	47

Figure 12. LH^{Pdx1}→PVH evoked grooming requires glutamate release, and activation of non-glutamatergic fibers promotes behavioral approach.....48

Figure 13. Figure 13 Deletion of $\gamma 2$ in *Sim1* neurons does not affect spontaneous firing activity in PVH^{Sim1} neurons.....50

Figure 14. GABA-A and ionotropic glutamate receptor activation in PVH are required for LH^{Pdx1-ChR2}→PVH evoked feeding and grooming, respectively.....51

Figure 15. ChR2 expression in LH neurons and PVH projection fibers in *Pdx1-Cre:: $\gamma 2^{flox/flox}$* and *Pdx1-Cre::Sim1-Cre:: $\gamma 2^{flox/flox}$* mice.....52

Figure 16. Figure 16. LH^{Pdx1} neurons project to PVH^{Sim1} but not to other prominent *Sim1*-positive brain regions.....53

Figure 17. Inhibition of GABAergic LH^{Pdx1}→PVH fibers reduces feeding after a fast, and inhibition of glutamatergic fibers reduces water-spray induced grooming.....55

Figure 18. eArchT3.0-mediated inhibition of GABA and glutamate release in LH^{Pdx1}→PVH terminals.....56

Figure 19. ChR2 expression in LH neurons and PVH projection fibers in *Pdx1-Cre::Vgat^{flox/flox}* used in fast-refeeding competition experiments, and photostimulation of LH→PVH GABAergic terminals strongly promotes feeding.....58

Figure 20. Antagonistic control of feeding and self-grooming by GABAergic and glutamatergic LH^{Pdx1}→PVH fibers.....59

Figure 21. Photostimulation of PVH^{Sim1} neurons induces grooming behavior and competes with fast-refeeding, and inhibition increases feeding and reduces stress-induced grooming.....61

Figure 22. ChR2 or iC++ expression in PVH^{Sim1} neurons of <i>Sim1-Cre</i> and <i>Sim1-Cre::Vglut2^{flox/flox}</i> mice	62
Figure 23. Photostimulation of PVH^{Sim1-GFP} neurons does not increase grooming behavior	63
Figure 24. PVH projecting LH neurons do not send collaterals to lateral habenula or VTA	65
Figure 25. Optogenetic Activation of PVH Neurons Elicits Flight and Escape Behaviors	75
Figure 26. Photoactivation of PVH Neurons Drives Grooming, Escape-Jumping, and Flight	76
Figure 27. Glutamatergic Transmission from PVH to Midbrain Drives Flight and Escape	79
Figure 28. PVH Projections in Downstream Brain Sites	81
Figure 29. Photoactivation of PVH→Midbrain Circuit in Grooming and Locomotion	83
Figure 30. PVH→Midbrain Activation on Fast-Refeeding and Aversive Conditioning	85
Figure 31. PVH and PVH→Midbrain Photostimulation Does Not Impact Approach to Food or Locomotion after Fasting	87
Figure 32. Activation of Glutamatergic-Midbrain Neurons in Escape Behaviors	89

**Figure 33. Activation of Glutamatergic-Midbrain Neurons is Not Required For
PVH→Midbrain-Evoked Hyperlocomotion and Avoidance.....91**

**Figure 34. Population Dynamics of Glutamatergic Midbrain Neurons in Response to
Fear.....94**

List of Tables

Table 1. PVH Outputs	7
Table 2. Effects of manipulating PVH neural activity on feeding	9
Table 3. PVH Inputs	10

Abbreviations

III	Third Ventricle
IV	Fourth Ventricle
4-AP	4-Aminopyridine
AAV	Adeno-associated virus
AGRP	Agouti-related protein
AHA	Anterior hypothalamic area
AHP	Anterior hypothalamic area
APV	Amino-5-phosphonovaleric acid
Aq	Aqueduct
Arc	Arcuate Nucleus
AVP	Vasopressin
BNST	Bed nucleus of the stria terminalis
CBX	Cerebellum
CCK	Cholecystokinin
CeA	Central nucleus of the amygdala
CGRP	Calcitonin gene-related peptide
ChR2	Channelrhodopsin-2

CNO	Clozapine-n-oxide
CNQX	Cyanquixaline
CNS	Central nervous system
Cre	Cre recombinase
CRH	Corticotropin releasing hormone
DA	Dopamine
D-AP5	Amino-5-phosphonovaleric acid
DMH	Dorsomedial hypothalamus
DNQX	6,7-dinitroquinoxaline-2,3-dione
DR	Dorsal raphe
DREADD	Designer receptors exclusively activated by designer drugs
DRN	Dorsal raphe
eArchT _{3.0}	Archaeorhodopsin-T-3.0
f	fornix
fr	fasciculus retroflexus
GLP1	Glucagon-like peptide-1
HPA	Hypothalamic-pituitary-adrenal axis
i.p.	Intraperitoneal

ic	Internal capsule
IPN	Interpeduncular nucleus
KO	Knockout
LC	Locus ceruleus
LepR	Leptin receptor
LH	Lateral hypothalamus
LHb	Lateral habenula
LPBN	Lateral parabrachial nucleus
MC4R	Melanocortin receptor 4
MCH	Melanin-concentrating hormone
Mdbrn	Midbrain
ME	Median eminence
MeA	Medial Amygdala
MM	Medial mammillary nucleus
MSc	Medial septal complex
Mtt	mammillothalamic tract
NAc	Nucleus accumbens
NLOT	Nucleus of the lateral olfactory tract

Nos1	Nitric oxide synthase 1
NPY	Neuropeptide Y
NTS	Nucleus of the solitary tract
oEPSC	Optically-evoked excitatory post-synaptic potential
oIPSC	Optically-evoked inhibitory post-synaptic potential
opt	Optic tract
OXT	Oxytocin
Oxtr	Oxytocin receptor
PACAP	Pituitary adenylate cyclase-activating peptide
PAG	Periaqueductal gray
PBN	Parabrachial nucleus
Pdx1	Pancreatic and duodenal homeobox 1
PH	Posterior hypothalamus
PMd	Dorsal premamillary nucleus
POMC	Pro-opiomelanocortin
PVH	Paraventricular hypothalamus
RTPP	Real-time place preference assay
RTPP/A	Real-time place preference/aversion assay

Scp	superior cerebellar peduncles
SF-1	Steroidogenic factor 1
Sim1	Single-minded homolog 1
SST	Somatostatin
SUM	Supramammillary nucleus
TH	Tyrosine hydroxylase
TN	Tuberal nucleus
TRH	Thyrotropin-releasing hormone
TTX	Tetrodotoxin
TVA	Avian tumor virus receptor A
Vgat	Vesicular GABA transporter
Vglut2	Vesicular glutamate transporter 2
VMH	Ventromedial hypothalamus
VTA	Ventral Tegmental Area

Chapter 1.

Background and Significance

Introduction

“First we eat, then we do everything else.” -M.F.K Fisher, American food writer

The simplest action for all forms of life is the act of consuming food for nourishment. As modern humans, most of us make decisions regarding the timing, choice, and amount of foods we consume on a daily basis. Unfortunately, such modern luxuries, as well as lifestyles permitting less movement in daily activities, have been concomitant with the widespread emergence of obesity, eating disorders, and metabolic dysregulation^{2,3}. The “obesogenic” environment we inhabit today favors alterations in eating behavior and poor food choice^{4,5}. The consequence of repeated overconsumption of cheap, highly palatable foods results in physiological alterations that promote adiposity and continued eating beyond homeostatic need^{6,7}. Recently, much effort has been put into researching how the body responds to over- or under-consumption of food, and it has become increasingly clear that neural mechanisms in the central nervous system (CNS) drive the pathological perturbations in feeding and body weight^{8,9}. It is to our advantage that we have a complete and accurate picture of how the CNS regulates energy homeostasis and feeding, as we can use the basic knowledge as entry points for developing novel strategies targeting brain systems causal to dysregulated feeding behavior and energy metabolism.

Brain circuits involved in feeding are complex and intricately connected to control the homeostatic, emotional, motivational, and cognitive aspects of feeding^{8,10}. These systems have evolved to promote optimal feeding strategies in changing environmental contexts in order to enhance survival¹¹⁻¹³. In the following sections, I will outline key brain circuits and neurotransmitter systems involved in homeostatic and non-homeostatic aspects of feeding, and how they converge to guide feeding decisions based on interoceptive and emotional

processing. Additionally, I will describe the technological framework that has allowed precise dissection of cell types and circuits implicated in feeding-related behaviors.

Homeostatic Feeding

Hypothalamus and Brainstem

Arcuate Nucleus

The hypothalamus occupies a small region at the base of the forebrain, and contains spatially distinct neighboring nuclei that coordinate a variety of homeostatic and autonomic processes essential for survival (Figure 1). First-order energy sensing neurons reside at the

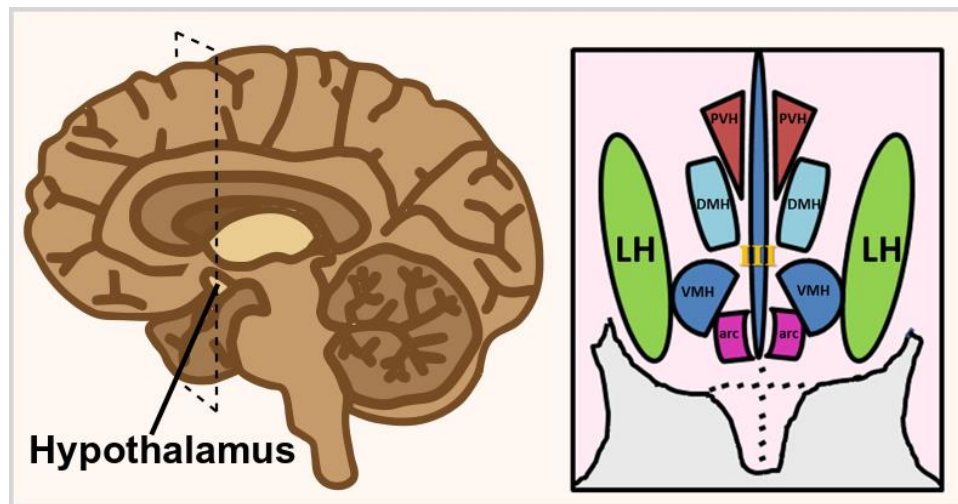


Figure 1. The hypothalamus is composed of several spatially clustered neural populations. (Left) Location of the hypothalamus at the base of the forebrain. Dashed lines indicate a coronally-cut section of the hypothalamus shown on the right. (Right) Simplified diagram of hypothalamic nuclei involved in feeding behavior and energy metabolism. III, third ventricle; arc, arcuate nucleus; DMH, dorsomedial hypothalamus; LH, lateral hypothalamus; PVH, paraventricular hypothalamus; VMH, ventromedial hypothalamus.

base of the third ventricle in a region called the arcuate nucleus (Arc). Arc consists of agouti-related protein (AGRP)/neuropeptide Y (NPY) and pro-opiomelanocortin (POMC) neurons (referred to as Arc^{Agrp} and Arc^{Pomc}, respectively), as well as other populations including glutamatergic, GABAergic, and dopaminergic neurons^{14, 15}. Arc^{Agrp} neurons are well-known

for their ability to stimulate feeding, conserve energy, and promote weight gain¹⁶⁻¹⁸; whereas Arc^{Pomc} neurons exert feeding inhibition, energy wasting, and weight loss^{17, 19, 20}. Genetic and ablation studies support the significance of these populations on feeding and body weight regulation. Targeted ablation of Arc^{Agrp} cells in the postnatal period has been shown to cause anorexia and wasting²¹⁻²³, whereas postnatal Arc^{Pomc} neuron ablation promotes hyperphagia and weight gain²³. Further corroborating evidence for opposing roles of these neurons comes from human studies that show polymorphisms or mutations in AGRP and Arc^{Pomc} genes are associated with anorexia²⁴ and obesity²⁵, respectively.

Arc^{Agrp} and Arc^{Pomc} cells have been described as interoceptive sensory neurons that respond to peripheral signals, adjusting homeostatic processes related to energy balance in accordance to humoral input²⁶. Both populations express receptors for circulating factors reflecting nutrient status; these include hormones and peptides released by adipose tissue and endocrine cells in the gut and pancreas²⁷. Satiety signals, such as insulin via pancreatic secretion and leptin via adipose secretion, inhibit Arc^{Agrp} cells^{28, 29} and activate Arc^{Pomc} cells^{30, 31}, whereas hunger signals, such as the gut-derived hormone, ghrelin, activate Arc^{Agrp}^{29, 32} and inhibit Arc^{Pomc} neurons³². Changes in Arc^{Agrp} and Arc^{Pomc} neural activity via circulating factors are thought to significantly mediate the long-term homeostatic adjustments in feeding behavior and energy expenditure²⁷. At the same time, both Arc populations have been shown to rapidly alter activity during food presentation³³; *in vivo* population recordings³⁴ as well as single cell monitoring^{35, 36} showed that food presentation alone caused a drop in Arc^{Agrp} neural activity³⁴⁻³⁶, which persisted during food consumption³⁴. In contrast, Arc^{Pomc} neurons responded to food presentation by rapidly increasing activity^{34, 36}, and remained elevated as mice approached and ate food³⁴. These findings indicate that not only do Arc neurons respond to long-term energy status, they also acutely drive feeding by rapidly altering neural activity in response to sensory cues.

Supporting the role of Arc neurons in rapidly modulating feeding behavior, direct manipulation of Arc^{Agrp} neurons has shown that excitation of this population acutely drives feeding^{16, 18}, whereas inhibition promotes hypophagia in the calorically-depleted state¹⁸. However, chronic activation of Arc^{Pomc} neurons is required to produce a hypophagic response^{16, 19}, and long-term inhibition is needed to precipitate higher food intake¹⁷. Thus, the evidence suggests that activity dynamics of Arc^{Agrp} and Arc^{Pomc} are intricately linked to coordinate rapid changes in feeding behavior with slower homeostatic processes in response to food intake.³³

One of the mechanisms by which Arc^{Agrp} and Arc^{Pomc} neurons exert their respective actions on feeding is by targeting melanocortin-4 receptors (MC4Rs) in downstream brain sites³⁷. AgRP, a neuropeptide released by Arc^{Agrp} cells, antagonizes MC4Rs³⁸⁻⁴⁰, and promotes neuronal hyperpolarization⁴¹. Oppositely, α -MSH, a cleavage product of POMC, is released by Arc^{Pomc} neurons and acts as an MC4R agonist⁴², leading to neuronal activation⁴¹. AgRP and α -MSH signaling on downstream MC4R-expressing neurons is proposed to underlie protracted adjustments in feeding behavior based on long-term energy status^{16, 17, 37, 43}. By contrast, rapid changes in feeding via Arc neurons require fast-acting neurotransmitter release. For instance, GABA and NPY, fast-acting inhibitory neurotransmitters released by Arc^{Agrp} cells, account for the acute elevation of feeding induced by Arc^{Agrp} neuronal activation^{17, 43}, and the fast-acting excitatory transmitter, glutamate, released from Arc-neurons (Arc^{Vglut2}) co-expressing the oxytocin receptor, attenuates feeding in the short-term⁴⁴. A separate Arc population demarked by neurons co-releasing GABA and dopamine (a slow-acting neuromodulator) has also been shown to acutely drive feeding, presumably by GABA action on downstream sites combined with enhanced inhibitory role of dopamine⁴⁵. Together, these studies have underscored the importance of Arc neuron populations in feeding and energy balance. A unifying

downstream site for their action resides in a nearby hypothalamic site called the paraventricular hypothalamus (PVH).

Paraventricular Hypothalamus

The PVH is a heterogenous region that contains a variety of non-peptidergic and peptidergic-expressing cells, including those that express oxytocin, vasopressin, thyrotropin-releasing hormone (TRH), and corticotropin-releasing hormone (CRH)⁴⁶. Neuropeptide-releasing cells in the PVH have an integral part in neuroendocrine control of certain homeostatic functions, such as reproduction and stress response. Additionally, lesions of the PVH produce hyperphagia and obesity⁴⁷⁻⁴⁹, demonstrating the significance of PVH neurons in metabolism and feeding regulation. It was later discovered that PVH abundantly expresses MC4Rs^{50, 51}, which are critical for body weight regulation, as MC4R insufficiency in both mice and humans leads to early-onset obesity⁵²⁻⁵⁴. Interestingly, genetic deletion of MC4R in PVH neurons causes hyperphagia and weight-gain⁵⁵, whereas restoration of the receptor only in PVH neurons, on an otherwise MC4R deficient background, greatly attenuates the obese phenotype^{50, 55}, suggesting that MC4R expression on PVH neurons is necessary and sufficient for normal feeding behavior. Further, PVH-MC4R neurons (PVH^{MC4R}) have been suggested as a main converging point for Arc^{Agrp} and Arc^{Pomc} action³⁷, as microinjections of Agrp and α -MSH directly into the PVH area was shown to most extensively stimulate and inhibit feeding behavior, respectively, compared to injections in other brain sites⁵⁶. Supporting this, GABAergic and/or NPY transmission from Arc^{Agrp} neurons onto PVH neurons drives feeding¹⁷, and Arc^{Agrp}→PVH-evoked feeding specifically requires inhibition of PVH^{MC4R} neurons⁵¹. In contrast, Arc^{Pomc} regulates PVH^{MC4R} activity via a post-synaptic mechanism, specifically by potentiating glutamatergic transmission across Arc^{Vglut2}→PVH^{MC4R} synapses, and is a proposed mechanism for signaling satiety⁴⁴. Accordingly, direct activation of PVH^{MC4R} neurons confers enhanced satiety and decreases

feeding during hunger, whereas inhibition elevates feeding during caloric sufficiency⁵¹. Given that most PVH neurons use glutamate as a neurotransmitter, it is not surprising that regulation of feeding by PVH^{MC4R} neurons requires glutamate release⁵⁷. In fact, glutamatergic signaling from PVH^{MC4R} onto lateral parabrachial nucleus (LPBN) neurons in the brainstem is the main pathway by which PVH^{MC4R} neurons suppress feeding^{51, 55}. Although PVH may regulate feeding by other neurotransmitters and neuropeptides, glutamatergic signaling may be the most critical manner by which PVH neurons suppress food intake, as genetic deletion of vesicular glutamate transporter (Vglut2, required for pre-synaptic release of glutamate) in PVH neurons promotes weight gain similar to MC4R nullizygosity⁵⁷.

The importance of glutamate release from PVH neurons for feeding regulation has been further bolstered by our recent study, showing that acute feeding suppression by PVH activation is completely abrogated when glutamate machinery is genetically compromised⁶¹. As mentioned above, the LPBN is one of the brain regions receiving glutamatergic input from PVH neurons. In addition to the LPBN, PVH targets many other downstream brain regions poised for feeding regulation and energy metabolism (Table 1). These include areas

Table 1. PVH Outputs	
Downstream excitation: Reduce Feeding	Downstream Excitation: Induce Feeding
<u>PVH^{MC4R} → LPBN</u> 51	<u>PVH^{TRH} → Arc^{Agrp}</u> 58
<u>PVH^{Sim1} → PAG/DR</u> 59	<u>PVH^{PACAP} → Arc^{Agrp}</u> 58
<u>PVH^{Vglut2(non-MC4R)} → NTS</u> (evidence for, but not directly shown for PVH ^{Vglut2} projections) 51, 60	

Table 1. PVH projects to hypothalamic and brain stem sites to control feeding.

of the brainstem and spinal cord, as well as other hypothalamic nuclei and limbic areas. Notably, glutamatergic-PVH projections to the nucleus of the solitary tract (NTS) in the brainstem have been suggested as a mechanism for satiety⁶⁰. Additionally, the periaqueductal gray/dorsal raphe (PAG/DRN) area, also in the brainstem, has also been implicated in the PVH circuitry for feeding suppression, as inhibiting axonal release of neurotransmitters from PVH onto PAG/DR neurons acutely promotes feeding⁵⁹. Given the rapid onset of feeding behavior, it was proposed that PVH→PAG/DR pathway in feeding suppression may involve glutamatergic neurotransmission⁵⁹. In most cases, activation of different PVH neural populations has an inhibitory effect on feeding (Table 2); however, a minority were found to increase feeding, via glutamatergic transmission onto Arc^{Agrp} neurons⁵⁸ (Table 1). Nevertheless, the prevailing view of PVH neural action has been its role in satiety and feeding suppression. Many recent studies support this notion by demonstrating that excitation of PVH neurons via input from upstream sites suppresses feeding (Table 3). In many cases, brain regions relaying excitatory input are bidirectionally connected with PVH neurons^{62, 63}, hinting that these circuits may function in positive feedback loops.

Opposite of excitation, inhibition of various PVH neurons engenders increased feeding behavior (Table 2), suggesting that ongoing PVH neural activity restrains overconsumption. Supporting this, studies have shown that inhibitory inputs (mainly GABAergic) from several brain sites onto PVH elevate feeding (Table 3), and embryonic deletion of the GABA_A receptor in PVH^{Sim1} neurons reduces post-weaning feeding, resulting in stunted growth and lower body weight⁶⁴. Interestingly, neurons of the Arc and lateral hypothalamus (LH) have been shown to bidirectionally control feeding behavior via excitatory and inhibitory

Table 2. Effects of manipulating PVH neural activity on feeding		
PVH population	Activation	Inhibition
PVH ^{Sim1}	Chemogenetic- decrease feeding ⁶⁵ Optogenetic- decrease feeding ⁶¹	Chemogenetic- increase feeding ^{17, 59} Optogenetic- increase feeding ⁶¹
PVH ^{Sim1-Vglut2 KO}	Optogenetic- no effect ⁶¹	Not reported
PVH ^{MC4R}	Chemogenetic- decrease feeding ⁵¹	Chemogenetic- increase feeding ⁵¹
PVH ^{AVP}	Chemogenetic- decrease feeding ⁶⁶	Chemogenetic- partially reverses melanocortin-induced anorexia ⁶⁶
PVH ^{OXT}	Chemogenetic- no effect, though increases energy expenditure ⁶⁵	Chemogenetic- no effect ⁵¹
PVH ^{TRH}	Chemogenetic- increase feeding ⁵⁸	Chemogenetic- decrease feeding ⁵⁸
PVH ^{CRH}	Chemogenetic- decrease feeding ⁶⁷	Chemogenetic- no effect ⁵¹
PVH ^{PACAP}	Chemogenetic- increase feeding ⁵⁸	Not reported
PVH ^{Nos1}	Chemogenetic- decrease feeding ⁶⁵	Not reported

Table 2. Exciting or inhibiting PVH neural activity using different techniques affects feeding behavior. (See Tools section for description of techniques).

projections to PVH neurons^{17, 44, 61}. As mentioned in the previous section, GABAergic-Arc^{AgRP} neurons increase feeding^{17, 43}, and glutamatergic Arc^{Oxtr} neurons suppress feeding⁴⁴; indeed, these opposite actions on feeding by different Arc populations were shown to converge on PVH^{17, 44}. Similarly, inhibitory (GABAergic) and excitatory (glutamatergic) projections from the lateral hypothalamus (LH) onto the PVH promote and abolish acute feeding behavior,

Table 3. PVH Inputs	
PVH excitation: Reduce Feeding	PVH inhibition: Induce Feeding
<u>LH^{Pdx1-Vglut2} → PVH^{Sim1}</u> 61	<u>Pdx1 → PVH^{Sim1}</u> 64
<u>NTS^{CCK} → PVH</u> 68	<u>LH^{Pdx1-Vgat} → PVH^{Sim1}</u> 61, 69
<u>NTS^{GLP1} → PVH^{CRH} (not reliant on glutamate release though)</u> 67	<u>Arc^{AgRP} → PVH^{Sim1, OXT}</u> 17
<u>Arc^{Oxtr} → PVH^{MC4R}</u> 44	<u>Arc^{AgRP} → PVH^{MC4R}</u> 51
<u>MSc^{Vglut2} → PVH</u> 70	<u>TN^{SST} → PVH</u> 71
	<u>DMH^{GABA} → PVH</u> 72

Table 3. Excitation or inhibition of PVH neurons from unique upstream sites oppositely affects feeding behavior.

respectively⁶¹. Like the PVH, the LH is a region composed of heterogenous neural populations, and is also critical in the maintenance of homeostatic aspects of feeding regulation.

Lateral Hypothalamus

Opposite of PVH lesion, early studies showed that lesions of the LH area in rodents leads to anorexia⁷³⁻⁷⁶, indicating the vast importance of LH circuitry in appetitive and/or consummatory properties of feeding behavior⁷⁷. Like the arcuate, LH contains neurons expressing receptors for hormones and factors signaling energy status. For example, leptin receptor (LepR)-expressing LH neurons are implicated in feeding and locomotion^{78, 79}, and administration of exogenous leptin to the LH area decreases feeding and body weight^{80, 81}. Oppositely, the gut-derived hormone ghrelin, which acts as a signal for hunger, activates LH

neurons and stimulates feeding⁸²⁻⁸⁴. Other LH neurons implicated in homeostatic regulation of feeding, namely those expressing the peptides orexin and melanin-concentrating hormone (MCH), also play a role in other homeostatic functions, such as the sleep-wake cycle⁸⁵. Orexin is expressed in a subset of LH neurons^{86, 87}, and direct stimulation of this population causes increased wakefulness⁸⁸, and exogenous orexin administration to the brain increases food intake⁸⁹. In contrast, genetic ablation of orexin neurons causes narcolepsy and no change or decreased food consumption concurrent with weight gain and obesity, due to a reduction in energy expenditure from decreased spontaneous locomotor activity^{90, 91}. However, another study using a different model of genetic ablation attributed weight gain to increased feeding during aberrant periods of the day-light cycle⁹². Opposite of orexin action, increasing the activity of MCH neurons promotes REM sleep⁹³; though similar to orexin, exogenous administration of MCH to the brain produces hyperphagia and weight gain⁹⁴. Confirming the feeding-promoting role of MCH action, genetic studies have shown that over-expressing the peptide induces overfeeding and obesity⁹⁵, whereas genetic neural ablation or deletion of MCH gene promotes chronic underfeeding and leanness^{96, 97}. While MCH and orexin neurons in the LH form separate populations⁹⁸, both groups co-express Vglut2, suggesting they co-release glutamate⁹⁹⁻¹⁰¹. Neuropeptide-producing neurotensin cells are another neuropeptide-expressing population in the LH, which form a separate group from MCH and orexin cells⁸¹. In contrast to the feeding-promoting actions of orexin and MCH, neurotensin has been shown to correlate with decreased feeding¹⁰². In fact, inactivation of neurotensin receptors results in overfeeding and weight gain¹⁰³, which may be due to insufficient signaling of neurotensin by LH neurons¹⁰⁴.

In addition to neuropeptide-producing neurons, LH contains distinct fast-acting neurotransmitter populations, expressing Vglut2 or vesicular GABA transporter (Vgat, required for presynaptic release of GABA) that have been well-studied for their opposing

roles on feeding⁷⁷. As mentioned above, MCH and orexin neurons co-express markers for glutamate (Vglut2), and it has been reported that both release glutamate as a neurotransmitter^{101, 105}. Both cell populations also express markers for GABA synthesis⁹⁹; however, current evidence suggests that GABAergic populations in the LH are separate from orexin/MCH-producing cells^{106, 107}. Moreover, not all glutamatergic-LH neurons are MCH/orexin positive⁹⁹, suggesting that broad manipulation of glutamate-releasing cells in LH target MCH/orexin neurons, as well as separate populations.

GABA and glutamate cells in LH are non-overlapping, and are broadly expressed throughout the LH area^{77, 108}. Analogous to Agrp/POMC neurons in the Arc, Vglut2 and Vgat LH neurons have a yin-yang relationship on feeding, with LH^{Vglut2} neurons having a feeding-inhibiting role^{61, 109, 110}, and LH^{Vgat} neurons promoting food intake^{61, 107, 109}. Genetic ablation of LH^{Vglut2} neurons leads to increased food intake and weight gain¹¹⁰, whereas genetic ablation of LH^{Vgat} neurons¹⁰⁷, or deletion of the Vgat transcript in LH¹⁰⁸, restrains food consumption and weight gain. Supporting the anorexigenic action of LH^{Vglut2} neurons, activation of this population acutely suppresses feeding during hunger, whereas inhibition of LH^{Vglut2} via inhibitory input from the bed nucleus of the stria terminalis (BNST) promotes feeding in well-fed mice¹⁰⁹. Moreover, inhibition of neurotransmission in the LH^{Vglut2}→lateral habenula (LHb) circuit promotes feeding behavior¹¹⁰. As mentioned in the previous section, activation of glutamatergic neurotransmission in the LH^{Pdx1-Vglut2}→PVH circuit suppresses food intake⁶¹. Thus, glutamate release from LH neurons negatively impacts feeding, and does so by acting on at least two different brain sites. Oppositely, activation of LH^{Vgat} neurons¹⁰⁷, or their projections to the ventral tegmental area (VTA)¹¹¹ and PVH^{61, 108}, produces appetitive and/or consummatory feeding behaviors. Monitoring *in vivo* real-time single cell dynamics of LH^{Vgat} neurons showed that distinct clusters of LH^{Vgat} cells become active during food-seeking (appetitive arm), while separate groups were activated in response to eating the food

(consummatory arm)¹⁰⁷, supporting that LH^{Vgat} neurons are heterogeneous in nature and promote different aspects of feeding.

Other hypothalamic sites and connections with the brainstem

Other hypothalamic sites that have been implicated in feeding behavior include the ventromedial hypothalamus (VMH) and the dorsomedial hypothalamus (DMH), both of which are interconnected with various hypothalamic nuclei described above¹¹². The significance of VMH neurons in body weight regulation came from early studies that showed lesions to this area caused marked obesity and overfeeding, suggesting that neurons in this region limit excessive food intake¹¹³. Similar to other hypothalamic nuclei, the VMH is composed of several distinct nuclei, and a representative and well-studied population is demarked by the transcription factor, steroidogenic factor-1 (SF-1)¹¹⁴. VMH^{SF1} neurons hold important functions in energy expenditure, thermogenesis, and glucose homeostasis; however, as demonstrated by conditional knockout studies, their role in food intake is less clear¹¹⁴. Other VMH populations, such as those expressing brain-derived neurotrophic factor¹¹⁵ and estrogen receptor-alpha¹¹⁶, are more likely than SF-1 neurons alone to account for the restraint on feeding by VMH neurons¹¹⁴.

Oppositely, the DMH has been implicated in promoting feeding, as lesions of this area, similar to LH lesions, causes hypophagia¹¹⁷. Further, DMH action on feeding is thought to be important for circadian aspects of food intake¹¹⁸, as lesions caused disruptions in the expression of food-entrainable daily rhythms¹¹⁹. Cell-type specific manipulation in later studies showed that GABAergic DMH neurons may promote or restrain food consumption based on their projection targets; specifically, projections from GABAergic DMH^{LepR} neurons co-expressing prodynorphin onto Arc^{AgRP} neurons were reported to suppress feeding¹²⁰, whereas DMH^{GABA}→PVH circuit is implicated in feeding promotion⁷². Additionally, cholinergic

neurons in the DMH increases feeding by enhancing GABAergic neurotransmission onto Arc^{POMC} neurons¹²¹. Thus, the DMH exerts opposing actions on feeding behavior through unique cell types and circuits.

Various hypothalamic nuclei are bidirectionally connected with brainstem neurons, and these circuits are critical in coordinating the effects of food intake and energy metabolism¹¹². For example, as shown in Tables 1 and 3, PVH sends excitatory input to the NTS, and NTS neurons excite PVH neurons to reduce feeding^{60, 67, 68}. Supporting the role of this projection in feeding regulation, lesion studies showed that damage of PVH fibers in the NTS leads to hyperphagia and obesity¹²². The NTS receives gut signals conveying nutritional state from the adjacent area postrema (an area lacking a blood-brain-barrier), and vagally-derived afferents¹²³. Gastric vagal afferent signaling promotes the action of satiety peptides like glucagon-like-peptide-1 (GLP-1) in the NTS¹²⁴, and adipose-derived hormone leptin acts on NTS^{LepR} neurons to potentiate gastrointestinal signals of satiety and reduce food intake^{123, 125}. In turn, the NTS relays taste information and other signals to the PBN, also located in the brainstem, and signals to the dorsal motor nucleus of the vagus (DMV) to control gut motility and vagal reflexes^{112, 123}. Notably, NTS→PBN circuitry is critical for mediating the anorexigenic response to AGRP neuron ablation¹²⁶. Confirming its feeding-suppressing action, activation of NTS→PBN circuit acutely reduces food intake¹²⁷. NTS excites PBN neurons via glutamatergic transmission¹²⁷, and direct stimulation of PBN neurons expressing calcitonin gene-related peptide (CGRP) results in suppression of feeding and eventual starvation with chronic stimulation¹²⁸. Further, PBN^{CGRP} action on appetite suppression was shown through its projections to the central nucleus of the amygdala (CeA)¹²⁸. Since the PBN inhibits appetite by responding to anorectic hormones as well as chemicals and toxins, this nuclei is thought to be involved in both normal satiety aspects and suppression of food intake due to illness or visceral malaise¹²⁹. Thus, an

NTS→PBN→CeA circuit plays an important role in relaying signals of extreme satiety and visceral discomfort.

In addition to NTS and PBN, neurons in the dorsal raphe (DRN) are also important in feeding regulation^{130, 131}. Interestingly, it was shown that GABAergic and glutamatergic neurons in this region can bidirectionally control food intake; activation of glutamatergic DRN neurons suppressed food intake, whereas GABAergic populations increased feeding¹³². Moreover, GABA/glutamate neurons responded to energy state consistent with their function in promoting and inhibiting feeding, respectively. Inhibiting the GABA population was sufficient in reducing hyperphagia and body weight in leptin deficient obese mice, suggesting that DRN neurons play an important role in preventing chronic overfeeding and obesity¹³².

Undoubtedly, the homeostatic regulation of eating behavior is essential for normal body weight maintenance and adaptive control of energy metabolism (Figure 2). However, the decision to eat relies on additional factors, and it has become increasingly apparent that the same brain circuits guiding homeostatic feeding also play a role in non-homeostatic aspects^{133, 134}. For the following section, I will focus on the relevant hypothalamic nuclei in non-homeostatic feeding and their connections to brain centers that impact feeding-related and emotional behaviors.

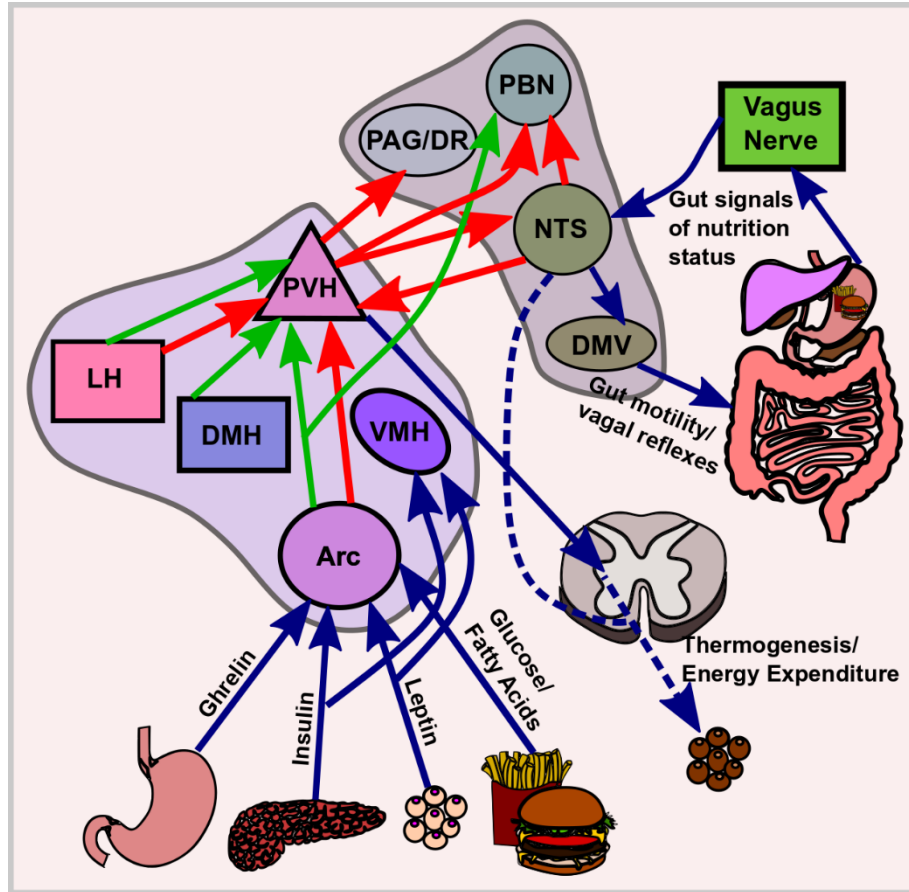


Figure 2. Homeostatic regulation of feeding and energy balance. Simplified schematic showing major pathways in the hypothalamus for feeding and metabolic regulation. Peripheral signals are sensed by hypothalamic neurons, especially in the Arc, and signal energy status. Other hypothalamic sites, like the VMH, express receptors for hormones like insulin and leptin, and have an important role in glucose and energy homeostasis via hormonal signaling pathways. Red arrows signify circuits that inhibit feeding, and green arrows are those that promote feeding. Blue arrows indicate pathways related to peripheral integration with brain circuits for feeding and metabolic regulation.

Non-Homeostatic Feeding and Emotional Regulation

In the section above, I explained how several brain sites and circuits control homeostatic adjustments in feeding behavior, presumably by linking internal signals and metabolic state (via input of peripheral signals). This model presumes a fine-tuned regulation of body weight such that fat stores are maintained at optimal levels for survival and reproduction. However, as evidenced by a modern society where obesity is now considered at epidemic proportions⁴, and where the rate of eating disorders is on the rise¹³⁵⁻¹³⁷, one will have to consider aspects of how the brain may maladaptively alter feeding. To understand the etiology of such conditions, it is imperative to apprehend the underlying brain circuits governing non-homeostatic feeding behavior, and more importantly, to grasp the convergence of the two systems in mediating decisions on whether and how much to eat.

Non-homeostatic feeding can be likened to homeostatically-driven food intake, in that both serve to either increase or decrease food consumption, but differ in the reasons behind changes in feeding behavior. In homeostatic feeding, chronically low body fat stores, or the occurrence of hypoglycemia in disease states, promotes hormonal and neural mechanisms relaying hunger signals that ultimately encourages increased feeding; oppositely, high fat stores enhance satiety signals from food intake, leading to decreased food consumption¹³⁸. In contrast, positive emotional valence signals (e.g., reward, pleasure) and conditioned responses may increase feeding¹³⁹; whereas negative emotional valence, engendered by anxiety/stress and aversive associative learning, can decrease feeding in a non-homeostatic manner¹⁴⁰. A famous example of non-homeostatic feeding in action is demonstrated by Pavlov's dog, which exhibited a feeding response (increased salivation) upon cue activation (the sound of a bell), that was associated with the delivery of palatable food¹⁴¹. Not too unlike Pavlov's dog, humans can also be conditioned to associate food cues with eating

tasty treats, and such cues themselves may eventually cause eating behavior in the absence of hunger^{142, 143}.

Though the terms “homeostatic” and “non-homeostatic” feeding may elicit the idea that the underlying substrates of the two are separable, recent evidence suggests this is not the case, and in fact, both aspects of feeding on a brain circuits level are intricately intertwined^{13, 133, 134, 144}. This concept is in line with the evolutionary perspective that hunger signals drive the pursuit of food, with brain circuits integrating memories of food location and sensory cues to guide adaptive processes of finding food¹³⁴. At the same time, pursuit of food is often dangerous and energetically costly, thus the brain must integrate conflicting messages on hunger and fear to devise the most favorable route for survival. The lateral hypothalamus (LH) is a prominent brain center that lies on the crossroads of homeostatic feeding regulation, reward, and food-seeking behaviors⁷⁷.

The Lateral Hypothalamus in Reward and Other Behaviors

The first clues that the LH was involved in both feeding and emotional behavior came from studies on electrical stimulation of this region in rats⁷⁷. These foundation studies demonstrated that stimulation of the LH area evoked voracious feeding behavior¹⁴⁵, and instrumental lever-pressing for self-stimulation¹⁴⁶, indicating the LH governs feeding and reward behavior^{147, 148}. Later studies using new technologies allowing for cell-type specific manipulation showed that the GABAergic-LH population drives appetitive and consummatory aspects of feeding, as well as reward-related behaviors and positive emotional valence¹⁰⁷. In line with electrical stimulation studies that showed higher intensity stimulation causes aversion, contemporary work demonstrated negative emotional aspects and feeding-suppressing roles of glutamatergic-LH neurons^{109, 110}. Fast-acting neurotransmitter populations in the LH are co-expressed with a variety of neuropeptides and

receptors for hormones implicated in homeostatic feeding regulation^{77, 79}. These populations participate dually in the homeostatic, as well as rewarding aspects of feeding.

Subsets of neurons in the LH that express the leptin receptor (LepR) are GABAergic, and they act to promote appropriate behavioral responses concurrent with their effect on feeding regulation⁷⁹. It was shown that, in line with the anorexigenic role of leptin, leptin action on LH^{LepR} neurons suppresses feeding and body weight⁸⁰. At the same time, leptin signaling in LH-neurotensin neurons is required for regulating the mesolimbic dopamine system, in part through direct projections to the ventral tegmental area (VTA) and indirectly by modulating intra-LH orexin function^{78, 149}. The consequence of diminished leptin signaling in LH neurons may result in increased hedonic feeding and obesity, in part by downregulation of natural reward perception^{80, 149}. Similarly, ghrelin action on ghrelin receptor-LH neurons has been implicated in reward processing concurrent with its action on feeding^{150, 151}. Specifically, it was shown that ghrelin signaling in the LH promotes regular food intake, as well as reward-driven food seeking behavior in a sex-specific manner¹⁵¹. Orexin and MCH neurons also have important roles in reward-seeking and palatable food consumption¹⁵². Orexin neurons promote reward-seeking and reward-learning, especially for attaining food reward^{153, 154}, whereas MCH neurons respond to sensory content of food, enhancing the rewarding value based on caloric content or palatability^{152, 155}. Both systems converge on the mesolimbic dopamine system to mediate behavioral effects¹⁵². These studies underscore the importance of LH-neural circuitry modulation of VTA-dopamine system, and recent studies have further unpacked the nature of LH→VTA circuits in feeding and reward.

The LH sends excitatory and inhibitory input to dopamine (DA) and GABA neurons in the VTA, and activation of LH→VTA circuit in live animals produces feeding and compulsive procurement of sucrose reward, despite application of an aversive stimulus (foot shock)¹¹¹. It

was shown that GABAergic LH projections to the VTA mediated increased feeding, and also elicited aberrant feeding-related behaviors like gnawing and licking¹¹¹. A subsequent study showed that the GABAergic-LH→VTA pathway promoted behavioral approach, exploratory behavior, and self-stimulation, whereas glutamatergic projections had the opposite effect¹⁵⁶. Functionally, it was shown that GABA transmission from LH onto VTA neurons caused disinhibition of VTA-DA neurons, leading to increased flux of DA in the nucleus accumbens¹⁵⁶ (a known mechanism underlying reward-seeking¹⁵⁷). Another study elaborated that feeding vs. reward-driven behavior in the GABAergic-LH→VTA circuit is differentially imposed by low vs. high frequency stimulation, respectively¹⁵⁸. Further, it was shown that dopamine receptor type 1 neurons of the nucleus accumbens (NAc) inhibit GABAergic-LH neurons to suppress feeding¹⁵⁹. Thus, a LH-GABA→VTA circuit promotes feeding and DA release, which feeds back on LH-GABA cells through VTA-DA→NAc-GABA→LH-GABA to terminate food consumption following sufficient levels of DA-signaling. Collectively, these studies link the mechanisms by which LH drives feeding, reward, and emotional valence.

GABAergic and glutamatergic LH projections to other parts of the brain have also been shown to influence feeding, emotion, stress-related behaviors, and defense. Unexpectedly, it was shown that intrahypothalamic connections between LH and PVH could drive feeding and repetitive self-grooming, which are two inherently opposing behavioral states⁶¹. While GABAergic LH→PVH circuit engendered voracious feeding and positive emotional valence, the glutamatergic arm promoted self-grooming, which was shown to be stress-related⁶¹. Supporting the negative emotional effects of LH^{Vglut2} neurons, activation of LH^{Vglut2} to lateral habenula (LHb) circuit is aversive and promotes escape behaviors^{110, 160}, whereas silencing LH^{Vglut2} neural activity via inhibitory inputs from the bed nucleus of the stria terminalis (BNST) causes feeding and positive valence. Interestingly,

GABAergic/glutamatergic LH projections to the periaqueductal gray area (PAG), a region involved in defensive behaviors and feeding regulation^{59, 161}, were shown to differentially drive predatory attack and evasion, respectively, whereas both projection components elicited avoidance behaviors¹⁶². Thus, beyond its role in homeostatic regulation, the LH is strategically poised for modulating multiple survival behaviors and associated emotional states through common cell types and diverse circuit connections in the brain. The PVH and Arc nuclei are additional centers that have been shown to modulate fear, stress/anxiety, and emotional behaviors that interact with feeding.

Arc^{Agrp} Neurons in Feeding-Related Behaviors and Emotion

Agrp neurons in the Arc, as explained in the previous section, are critical for producing feeding behavior during energy deficit and starvation. Intuitively, we know that intense hunger is usually an unpleasant sensation, and can be accompanied by feelings of frustration and annoyance (hence the term, “hangry”). In line with this instinct, recent studies have shown that mice conditioned to associate Arc^{Agrp} stimulation to a specific location or type of food will learn to avoid future encounters with those foods and locations³⁵. Conversely, paired inhibition of Arc^{Agrp} neurons to specific foods and locations during hunger causes a preference for those foods and places³⁵. Interestingly, another study demonstrated that foods paired with *pre*stimulation of Arc^{Agrp} neurons (stimulation occurring for a 30 minutes to an hour prior to conditioning experiments) caused an increased preference for that specific food¹⁶³. Indeed, presentation of food paired with pre-stimulation of Arc^{Agrp} neurons caused eating of the particular food in the absence of hunger, suggesting that Arc^{Agrp} encode enhanced incentive value to the rewarding sensory aspects of foods¹⁶³. Based on *in vivo* recordings of Arc^{Agrp} neurons, which demonstrated an increase in activity during hunger, but a dramatic fall in neural activity during presentation of food and during subsequent eating³³, one could speculate that the act of finding food and then eating after

prolonged, involuntary fasting (during times of food scarcity, for example) would correlate with emotional valence concurrent with Arc^{Agrp} neural properties (i.e., negative valence during hunger/food-seeking (high Arc^{Agrp} neural activity), and positive valence once food was found and consumed (low Arc^{Agrp} activity)). Thus, these important studies show how Arc^{Agrp} neurons integrate emotional aspects with hunger and satiety.

Other studies have further explored the role of Arc^{Agrp} neurons in feeding-related behaviors, and how these neurons navigate hunger drive and competing behavioral and emotional states. In the absence of food, food deprivation or stimulation of Arc^{Agrp} neurons in the fed state similarly causes foraging behaviors such as increased activity and digging, and stereotypical repetitive behaviors (grooming, marble burying)¹⁶⁴. Additionally, evidence was provided to support the hypothesis that different Arc^{Agrp} neural populations encode separable aspects of consummatory feeding, foraging, and stereotypic behaviors¹⁶⁴. Interestingly, Arc^{Agrp} neural activation has an anxiolytic effect, such that mice are more willing to approach fearful and aversive locations in a testing arena¹⁶⁴⁻¹⁶⁶. In fact, fasted mice or fed mice with Arc^{Agrp} neural stimulation causes increased approach to food placed in an anxiety-provoking location, and suppresses social interaction¹⁶⁵, including aggression¹⁶⁶, in favor of eating^{165, 166}. Other hypothalamic nuclei, like the PVH and VMH, have also been implicated in repetitive behaviors and aggression, respectively.

The PVH, VMH, and Brainstem Neurons Produce Diverse Behaviors and Emotional States

The PVH is a well-known neuroendocrine center, playing a key role in the stress response via hypothalamic-pituitary-adrenal (HPA) cascade¹⁶⁷. In addition to its role in the hormonal aspects of stress, corticotropin-releasing hormone (CRH) cells of the PVH also drive the repertoire of behavioral responses following stress, independent of hormonal action¹⁶⁸. This includes repetitive grooming, a behavior linked to increased anxiety¹⁶⁹.

Interestingly, increased self-grooming is induced by stimulating PVH^{CRH}→LH and LH→PVH circuits^{61, 168}, suggesting this behavior is promoted by feedforward hypothalamic loops. Inhibition of PVH^{CRH} or bulk PVH neurons reduces stress-induced repetitive grooming^{61, 168}, suggesting the necessity for PVH in eliciting a behavior associated with negative valence. As mentioned previously, PVH inhibition also causes increased feeding (see Table 2). Interestingly, PVH can bidirectionally modulate stress-like behavior and feeding antagonistically; activation of PVH neurons halts ongoing fast-refeeding, and in turn promotes repetitive grooming, an effect that can switch rapidly depending upon stimulation state⁶¹. Thus, it appears that PVH circuitry functions dually in homeostatic control and emotional behaviors.

The VMH, an important center for energy metabolism, also plays a role in negatively-valenced emotional behaviors, such as fear and defense^{170, 171}. VMH^{SF1} neurons were shown to generate both the negative emotional aspects of a defensive state (aversion and anxiety)¹⁷⁰ concurrent with defensive expression (freezing and flight) via collateral projections to the PAG and anterior hypothalamic nucleus^{171, 172}. Similar to the amygdala, a brain center previously thought to be the seat of emotion, VMH^{SF1} neurons were shown to be crucial in fear-learning¹⁷¹, suggesting the VMH, like the LH, is capable of producing emotional states concurrent with their role in energy metabolism and feeding¹⁷⁰. Other VMH cell populations distinct from SF1 positive neurons play roles in social behaviors, such as mating and aggression^{173, 174}.

Brainstem neurons serve crucial roles in autonomic regulation and energy balance, and also encode emotional states concurrent with their roles in feeding behavior. For example, leptin or GLP-1 action on NTS neurons reduces food consumption, and engenders decreased motivation for food reward^{175, 176}, suggesting that GLP-1 and leptin responsive NTS neurons inhibit food consumption by altering motivational salience for obtaining food.

This emotional reaction would be in line with the homeostatic regulation aspects of feeding constraint during energy surfeit. Recently, it was shown that different NTS^{CCK} circuits suppress feeding while encoding either positive (NTS^{CCK}→PVH) or negative valence (NTS^{CCK}→PBN)¹⁷⁷. Thus, specific NTS pathways may serve to decrease food intake through inclusive emotional states. The PBN and PAG are additional sites that have dual roles in feeding, emotions, and other behaviors. PBN neural activity is important for signaling satiety and the sensory and emotional aspects of visceral malaise and pain¹²⁹. It does this in part by communicating with forebrain structures that regulate emotional behaviors¹²⁹. PBN^{CGRP} neurons, which function in satiety and sensory relay, were also shown to facilitate fear-learning¹⁷⁸. Similar to PBN, the PAG is involved in feeding suppression⁵⁹, and also promotes fear-related behaviors, including freezing, flight, and avoidance^{179, 180}. Taken together, brainstem neurons are important for satiety regulation and eliciting appropriate emotional and behavioral action in response to internal and external stimuli. In summary, hypothalamic and brainstem sites implicated in homeostatic regulation of feeding play dual roles in emotional behavior, and are thus strategically positioned for controlling a diverse repertoire of adaptive behaviors aimed at survival (Figure 3).

The majority of studies described in this background have taken advantage of vastly progressive technological advances of the 21st century. In the following section, I will describe the tools and methods used to deeply probe neural function and behavior.

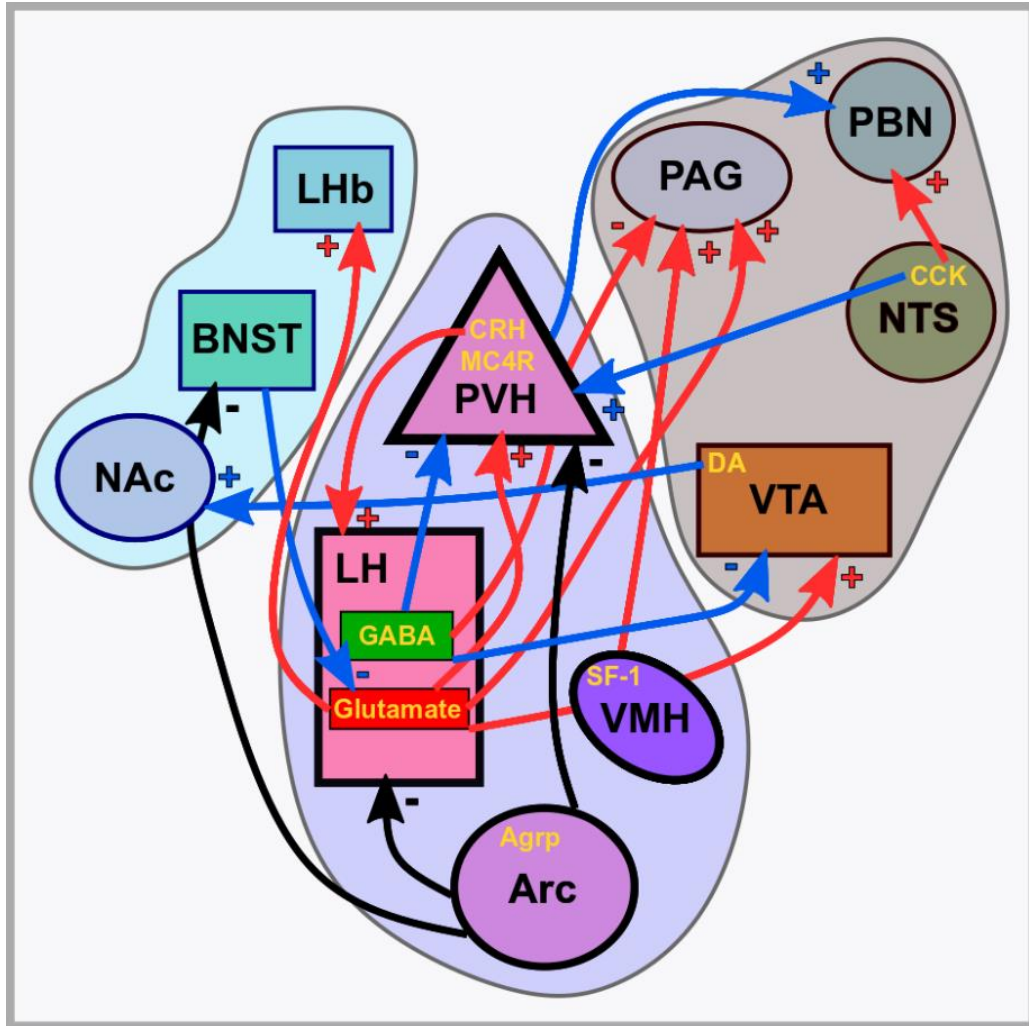


Figure 3. Brain circuits involved in feeding encode emotional valence. Summary schematic showing various brain centers and circuit connections that dually regulate feeding and emotion. Red arrows indicate projections that promote negative emotional behaviors, and blue arrows indicate circuits that engender positive valence and/or reward-related behaviors. Black arrows signify Arc^{Agrp} projections to various sites that enhance feeding, though their role in emotional behaviors evoked by Arc^{Agrp} stimulation is unknown at this point. (+) sign indicates excitatory (glutamatergic) transmission and (-) sign indicates inhibitory (GABAergic) transmission. Purple region designates hypothalamic nuclei, and gray and blue regions indicate brainstem and extra-hypothalamic forebrain regions, respectively.

Tools for Interrogating Neural Circuits Underlying Behavior

The use of rodent models in neuroscience research has been critical for advancing the understanding of the brain. Rats have historically supplied the bulk of behavioral research in the previous century, however, since the 1990s, the use of mice has risen dramatically, and currently represents the organism of choice in neuroscience research¹⁸¹. The reason for the shift in model organism was primarily due to the development and wide implementation of genetic tools designed for mouse genome manipulation¹⁸¹. The availability of human genetic research, paired with mouse models that aim to replicate human disorders with a genetic cause, aid in development of novel therapeutics for disease^{182, 183}. Further, genetically modified rodents help us access specified neuronal cell types in the brain, allowing for precise manipulation that can causally link neural mechanism and behavior¹⁸⁴.

Cre-LoxP Technology

Traditional transgenic and knock-in/knockout mice are important tools for investigating the effects of genetic modification on a whole-body basis beginning in embryonic development¹⁸³. However, the advancement of new tools allowing for conditional genetic and cell-type specific manipulation, has allowed spatial and temporal control over gene expression, allowing for greater flexibility and degree of precision for understanding biological pathways on the cellular level¹⁸⁴. Cre recombinase (Cre), an enzyme derived from bacteriophage, can be genetically engineered in mice to express under specified promotor elements. Thus, cell-type specific promoters will drive Cre expression in only the cell population of interest¹⁸⁵. Cre recognizes specific sequences in the genome, called LoxP sites, and catalyzes a recombination event that can excise or invert the genetic material flanked by the LoxP sites, depending on the orientation of the LoxP sequences¹⁸⁶. Cre-expressing genetically modified mice, combined with knock-in mice engineered with LoxP

sites flanking specific genes, allows for genetically-defined knockout or re-expression of gene(s) of interest^{185, 187}. The use of Cre-LoxP technology has been integral in furthering the understanding of how specific hypothalamic neurons function in feeding regulation and energy metabolism¹⁸⁴. For example, the use of Sim1-Cre combined with Vglut2^{loxp/loxp} mice produces glutamate transporter deletion in Sim1-expressing neurons (which include neurons of the PVH and a few other brain sites)⁵⁷. The Sim1-Cre::Vglut2^{loxp/loxp} mouse bred with loxp-[transcription blocker]-loxp-MC4R mice, in which MC4R can only be expressed with Cre recombination, showed that glutamate release is required for the rescue effect of MC4R re-expression in Sim1 neurons on body weight regulation⁵⁷. The beauty of this study shows the elegance of Cre-LoxP technology for deep interrogation of cell types and mechanisms for energy homeostasis.

Cre-LoxP technology in neuroscience is often combined with intersectional approaches for probing neural function¹⁸⁴. A prominent method uses stereotaxic injection of recombinant adeno-associated viral vectors (AAV) that package a transgene of interest under a strong promoter. By flanking the transgene with “FLEX” sequences, which Cre recognizes, expression of the transgene can be limited to spatially-targeted cre-expressing cells¹⁸⁸. The techniques described below take advantage of Cre-LoxP systems and AAV viruses for expression of genes that aid in manipulating and interrogating neural cell types and circuits¹⁸⁴.

Optogenetics

Classic studies using electrical stimulation were pioneering for their ability to causally link specific brain site to behavior. However, these early studies lacked cell-type specificity despite spatial precision. Further, blunt application of electrical current can not only stimulate cell bodies, but also fibers of passage, precluding the attribution of effects solely to

neural cell types in the location of interest¹⁸⁹. In recent years, a new technology called optogenetics has been shown to circumvent the downsides of electrical stimulation, while maintaining high fidelity of neuronal activation¹⁸⁹. The premise of this technology relies upon light-gated features of membrane proteins derived from certain microbial organisms, such as algae. These proteins are activated by specific wavelengths of light, and respond to light by channel opening or pump activation, which permits the flow of electrically charged ions across the membrane. This action causes a change in membrane potential, which leads to activation or inhibition of neural activity. For example, shining blue wavelength light on channelrhodopsin-2, a widely used neural activator, causes a conformational change in the protein, allow channel opening and flow of positively charged ions across the membrane, leading to neuronal depolarization¹⁸⁹. Some neural silencers, such as halorhodopsin, allow the passive flow of negatively charged ions across the membrane upon light activation, whereas others, like archaerhodopsin, hyperpolarize cells by acting as a proton pump¹⁹⁰. Importantly, activation of optogenetic proteins occurs on a millisecond timescale, allowing for precise temporal manipulation of neural activity. Genetic material encoding for these proteins are often packaged into viral vectors and delivered in the brain for neural expression in live animals¹⁸⁴. By attaching optic fiber implants for delivery of light over the brain region of interest, scientists have been able to directly control the activity of specified neural cell types and circuits *in vivo*¹⁸⁹. The first application of optogenetics in feeding circuits was reported in 2011, in which researchers demonstrated that activation of Arc^{Agrp} neurons via ChR2 promotes voracious appetitive and consummatory feeding behaviors¹⁶. Notably, the magnitude of the observed response was positively correlated with the density of ChR2 expression in Arc^{Agrp} neurons¹⁶. A downside of the optogenetic technique is the requirement to use head-affixed optic implants, which must be tethered to an optic fiber cord for light delivery. Additionally, repeated or prolonged stimulation of light-gated channel proteins could lead to phenomena like depolarization block and reversal of intended

activity^{191, 192}. Another method described below circumvents physical barriers and channel desensitization, but sacrifices fast temporal control over neural activity.

Designer Receptors Exclusively Activated by Designer Drugs (DREADDs)

The DREADD system belongs to a class of tools called chemogenetics, characterized by genetically engineered receptors that uniquely respond to exogenously administered small-molecule ligands¹⁹³. DREADD proteins are genetically mutated muscarinic G-protein-coupled receptors that bind the drug clozapine N-oxide (CNO), but not endogenous acetylcholine. The DREADD receptors can be coupled to Gαq or Gαi-signaling pathways, which serve to increase or inhibit neural activity, respectively¹⁹³. DREADDs are often expressed in neural tissue in a cre-dependent manner by AAV delivery, where they can exert action on specified neural cell types of interest. The advantage of using DREADDs include cell-type specific manipulation that is minimally invasive, allowing a greater degree of freedom for experimental setup that is not precluded by optic fiber tethering to mouse head¹⁸⁴. Activation or inhibition of neural activity is achieved by delivering the ligand, CNO, intraperitoneally (i.p.), or in drinking water, or centrally in a region-specific fashion via drug-delivery cannula¹⁸⁴. The action of DREADDs on neural activity following delivery of CNO is relatively prolonged, and can last for hours. However, onset to alter neural activity takes significantly longer in DREADD systems vs. optogenetics, which constrains temporal control over neural perturbations¹⁹³. Nevertheless, the use of DREADD tools has proven vastly useful for the study of the neural cell types and circuits governing feeding behavior. Early work on Arc^{Agrp} neural manipulation showed that activating or inhibiting Arc^{Agrp} neurons via DREADD technology increased and decreased feeding, respectively¹⁸. Additionally, silencing PVH^{Sim1} neurons, which receive inhibitory input from Arc^{Agrp} neurons, confirmed that silencing this nucleus with inhibitory DREADDs engenders increased feeding behavior¹⁷. While DREADD and optogenetic tools are outstanding for probing the gain of

function and loss of function phenotypes of manipulated neural activity, these tools do not capture or mimic natural endogenous activity of neural networks. Fortunately, novel *in vivo* tools for monitoring real-time neural activity dynamics has helped shed light on correlations between neural activity and behavior.

Deep Brain Imaging in vivo

Recent advances in deep brain imaging have taken advantage of genetically encoded fluorescent calcium indicators for probing neural activity *in vivo*¹⁸⁴. These molecular probes produce fluorescent changes depending upon calcium flux inside the cell¹⁹⁴. Because intracellular free calcium changes rapidly with neural activity, fluorescence emission from calcium indicators can be used as a proxy for dynamic changes in neural activity over time¹⁹⁴. Ultra-sensitive calcium sensors, termed GCaMP6, exhibit high temporal precision in detecting alterations in neural activity, and have been gaining popularity in neuroscience research¹⁹⁵. Taking advantage of good signal-to-noise ratio, researchers can employ this helpful tool in deep brain structures to image the activity of neurons while animals perform tasks or are engaged in behavior^{184, 196}. This technique can be used in imaging bulk neural population activity, or fine-tuned to the single-cell level, depending upon the imaging device used¹⁹⁶. By collecting fluorescent emissions with an implanted optic fiber, data on the population dynamics of neurons genetically targeted with GCaMP6 can be gathered and analyzed, and synced to changes to behavioral state. Another method utilizes head-mounted miniature microscopes to resolve single-cell activity changes in fluorescence, though drawbacks include movement artifacts and displacement of brain tissue that prevents optimal lens focus and resolution^{184, 196}.

Landmark studies in the neural control of feeding regulation have utilized GCaMP6 indicators to monitor Arc^{AgRP}, Arc^{Pomc}, and LH^{Vgat} populations *in vivo*. Interestingly, and

contrary to logical derivation based on stimulation studies, *in vivo* recordings showed that calcium activity was elevated in Arc^{Agrp} during hunger, but declined rapidly upon presentation of food and the feeding behavior that followed^{34, 35}. In contrast, optogenetic or chemogenetic activation of Arc^{Agrp} neurons was shown to promote feeding, while inhibition decreased feeding in the hunger state^{16, 18}. Oppositely, Arc^{Pomc} cells showed an increase in activity during feeding behavior³⁴, whereas optogenetic or chemogenetic stimulation of this population was shown to decrease food intake, albeit in the long-term^{16, 19}. These findings suggest that Arc neurons may be able to anticipate homeostatic changes and adjust activity accordingly based on food availability³³. Using single-cell recording techniques, monitoring of LH^{Vgat} cells showed that separate subpopulations within this nucleus respond differently to appetitive versus consummatory aspects of feeding¹⁰⁷. In contrast, despite evidence for different neural subtypes with differing projection targets^{164, 197}, Arc^{Agrp} neurons respond homogeneously to feeding by decreasing their activity³⁵. In summary, genetic tools allowing for precise control and observation of neural dynamics in discrete cell populations have potentiated the ability to deeply probe the neurobiology behind feeding and related behaviors.

Significance

As evidence accumulates on how energy systems controlled by the brain are intricately connected to neural processes underpinning emotional behaviors^{13, 133}, a emergent framework for novel approaches in treating obesity and eating-related disorders will be necessary to tackle otherwise difficult and intractable cases. Relatedly, given the link on mood dysregulation and changes in eating behavior^{144, 198, 199}, new therapeutics that target brain systems involved in feeding regulation may prove useful for concurrent treatment of mood disorders and vice versa. For example, a new combination drug for obesity treatment combines bupropion, a drug classically used for depressive disorders, and naltrexone, a

drug used for opioid dependence²⁰⁰. The first clues on the power of food intake on mood and behavior came from classic human semi-starvation experiments conducted in the mid 1940s, that showed subjects who were subject to severe caloric restriction displayed alterations in temperament, with most developing melancholy and compulsive behaviors²⁰¹. These observations are reminiscent of food-restricting disorders such as anorexia nervosa (AN)²⁰². However, the current literature suggests that the maladaptive behaviors in AN is not solely due to the physical effects of eating restriction, as weight-restored patients do not have complete resolution of psychopathology²⁰³⁻²⁰⁵. Nevertheless, as suggested by some of the subjects in the semi-starvation studies who suffered from emergent psychiatric symptoms for months to years²⁰⁶, it is unclear the extent to which the indelible effects of malnutrition have on cognitive and emotional function. Notably, patients with eating disorders often have co-occurring psychiatric conditions, such as obsessive-compulsive disorder, suggesting shared neural processes between disorders^{202, 207}. Anxiety and fear-related disorders also commonly co-occur with feeding disorders^{208, 209}, and in severe cases, can result in severe malnutrition and stunted growth²¹⁰. Conversely, over-eating disorders like binge eating disorder contributes to severe obesity and metabolic derangement^{211, 212}. Disorders of over-eating and obesity have been linked to pathological changes in the dopamine (DA) mesolimbic system^{139, 213}, suggesting a feasible entry point for interrogating shared mechanisms contributing to eating and mood dysregulation. In fact, recent studies have shown that homeostatic circuits bidirectionally affect motivation and reward via direct or indirect connections to mesolimbic DA circuitry¹³³, suggesting a neural basis for homeostatic control of feeding and its link to mood regulation. Fear-based disorders that oppositely result in food restriction behavior are based in neural systems that are also affected by homeostatic feeding circuits¹³³, and when experimentally isolated can produce alterations in feeding behavior independent of homeostatic input^{133, 214}. Given the burden of rising economic costs associated with mental health and obesity, it is quite disappointing

that current therapies fail in substantially alleviating societal impacts of these conditions^{4, 215}. Thus, scientific understanding of neural circuits concurrently involved in feeding and emotional valence is of utmost importance for unraveling the perplexities of complex mood disorders and obesity, and for designing new methods for successful treatment.

Chapter 2.

A Neural Basis for Antagonistic Control of Feeding and Compulsive Behaviors

This chapter is based upon:

Mangieri LR, Lu Y, Xu Y, Cassidy RM, Xu Y, Arenkiel BR, Tong Q. A neural basis for antagonistic control of feeding and compulsive behaviors. *Nature Communications* 9, Article number: 52 (2018).

Permission policy of Springer Nature content: Ownership of copyright in original research articles remains with the Author, and provided that, when reproducing the contribution or extracts from it or from the Supplementary Information, the Author acknowledges first and reference publication in the Journal, the Author retains the following non-exclusive rights:

To reproduce the contribution in whole or in part in any printed volume (book or thesis) of which they are the author(s).

Summary

Abnormal feeding often co-exists with compulsive behaviors, but the underlying neural basis remains unknown. Excessive self-grooming in rodents is associated with compulsivity. Here, we show that optogenetically manipulating the activity of lateral hypothalamus (LH) projections targeting the paraventricular hypothalamus (PVH) differentially promotes either feeding or repetitive self-grooming. Whereas selective activation of GABAergic LH→PVH inputs induces feeding, activation of glutamatergic inputs promotes self-grooming. Strikingly, targeted stimulation of GABAergic LH→PVH leads to rapid and reversible transitions to feeding from induced intense self-grooming, while activating glutamatergic LH→PVH or PVH neurons causes rapid and reversible transitions to self-grooming from voracious feeding induced by fasting. Further, specific inhibition of either LH→PVH GABAergic action or PVH neurons reduces self-grooming induced by stress. Thus, we have uncovered a parallel LH→PVH projection circuit for antagonistic control of feeding and self-grooming through dynamic modulation of PVH neuron activity, revealing a common neural pathway that underlies feeding and compulsive behaviors.

Introduction

Feeding is essential for survival, and abnormal eating habits can manifest in the form of either uncontrolled hyperphagia or anorexia, leading to obesity or life-threatening nutrient insufficiency^{202, 216}. Although it is well known that such feeding abnormalities severely impact the quality of life, the neural basis that underlies uncontrolled over-feeding or restrictive dieting remains elusive. Accumulating evidence supports the notion that feeding behavior reciprocally interacts with affective behaviors^{144, 202, 216}. Overeating and obesity are often associated with an emotional state of increased impulsivity and positive reinforcement, similar to drug addiction^{217, 218}. Anorexia nervosa has several diagnostic subtypes

associated with compulsive restriction, compulsive bingeing with purging, and compulsive hoarding^{202, 219}. Interestingly, it has been suggested that compulsive behaviors associated with anorexia nervosa may manifest as a way to relieve stress and anxiety^{202, 220}. In rodents, asocial repetitive self-grooming is a typical behavior that models compulsivity in neuropsychiatric diseases²²¹. Recent observations²²² suggest a provocative link between feeding disturbances and psychological dysregulation related to compulsivity, supporting a common neural pathway underlying maladaptive feeding and compulsive behaviors. However, despite extensive research on both feeding and psychiatric compulsivity, it is unclear whether a shared neural pathway regulates both behaviors.

The hypothalamus has been well established to regulate feeding behaviors. Discrete groups of neurons within the hypothalamus have been identified to be capable of sensing changes in various hormones or neuronal inputs in order to gauge nutritional status, and adjust food intake to maintain proper energy homeostasis²²³. The lateral hypothalamus (LH) functions as a hunger center, and modulates feeding and other homeostatic processes²²⁴. Current studies demonstrate that the LH contains two distinct groups of neurons that exert opposite actions on feeding regulation. GABAergic neurons have been implicated in driving feeding^{69, 107}, in part via local LH GABAergic projections to the ventral tegmental area or paraventricular hypothalamus (PVH)^{69, 111}. In contrast, LH glutamatergic neurons were shown to suppress feeding¹⁰⁹, at least in part by their projections to the lateral habenula¹¹⁰. The physiologic implication of the contrasting effects on feeding behavior by LH GABAergic and glutamatergic neurons has remained unexplored.

The PVH, an important integration site, receives massive synaptic inputs from multiple brain areas, and plays an important role in feeding regulation⁴⁶. The PVH receives melanocortin inputs from arcuate peptidergic POMC and AgRP neurons, which have been well characterized in their roles towards feeding regulation³⁷. Recent studies demonstrated

that the PVH also receives both GABAergic and glutamatergic inputs from the arcuate nucleus, thereby potentially promoting and inhibiting food intake respectively^{17, 225}. Our previous work supports a role for GABAergic inputs from LH to PVH in feeding promotion⁶⁹. However, a role for glutamatergic projections from LH to PVH has not been characterized. Importantly, whether LH and PVH, the well-established brain regions for feeding regulation, directly modulate affective states such as compulsivity is unknown.

Here, we utilize transgenic mice that express cre recombinase from the pancreas-duodenum homeobox 1 promoter (*Pdx1-Cre*) to access mixed GABAergic and glutamatergic LH neurons⁶⁹. We find that LH→PVH GABAergic projections promote feeding and suppress self-grooming, whereas glutamatergic projections promote excessive self-grooming and suppress feeding. Direct modulation of these behaviors is achieved through antagonistic control of PVH neuron activity. These findings provide a novel framework for understanding circuit-level mechanisms that link feeding and compulsive behaviors.

Results

LH→PVH projections directly synapse on a common subset of PVH neurons

To selectively mark and manipulate LH neurons, we employed transgenic *Pdx1-Cre* mice. In this line, Cre is abundantly expressed in the LH, the dorsal medial hypothalamus (DMH), the Arc, and preoptic areas, but not in the PVH²²⁶. Within the LH, *Pdx1-Cre* neurons reside in medial-caudal regions, and are not present in rostral domains (**Figure 4a-h**). Regions of the LH known to express *Pdx1-Cre* were shown to contain GABAergic and glutamatergic neuron populations, which were largely segregated (**Figure 4i-k**). To investigate how LH neurons modulate PVH neurons, we first monitored monosynaptic projections from LH *Pdx1-Cre* (LH^{*Pdx1*}) neurons to PVH neurons using channelrhodopsin 2 (ChR2)-assisted circuit mapping¹⁸⁸. Towards this, we bilaterally

Pdx1-Cre::Ai9

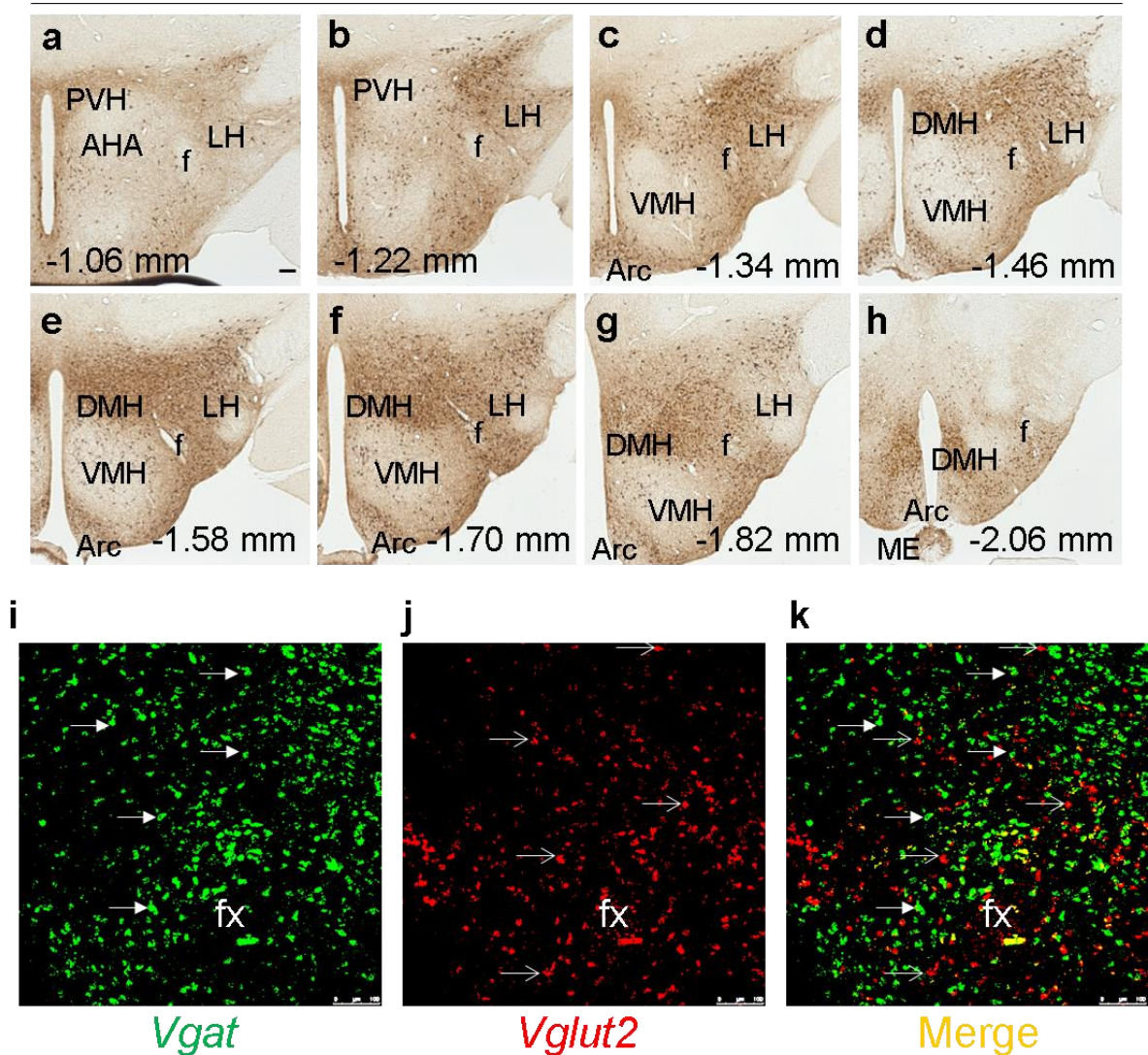


Figure 4. *Pdx1-Cre* expression in hypothalamic brain regions, including LH, which contain segregated GABA and glutamatergic neuron populations. *Pdx1-Cre* mice were bred to Gt(ROSA)26Sortm9(CAG-tdTomato)Hze, also known as Ai9 reporter mice, to allow red-fluorescent protein (RFP) visualization in cre-positive neurons and fibers. In a rostral to caudal fashion, (a-h) show RFP expression in hypothalamic neurons, including those in the LH, and projection fibers located in the PVH. Prominent *Pdx1-Cre* expression in LH is noted in the medial to caudal portions of the LH (-1.22 to -1.82 mm Bregma, b-g), but is not seen in LH area anterior to Bregma -1.22 mm. Other prominent *Pdx1-Cre* positive neurons are seen in the DMH and Arc. Measurements indicate millimeter anterior-posterior distance relative to Bregma. Arc, arcuate nucleus; DMH, dorsomedial hypothalamus; f, fornix; LH, lateral hypothalamus; VMH, ventromedial hypothalamus. (i-k) Double in situ hybridization of *Vgat* (i) and *Vglut2* (j) in the LH area of a wild-type mouse. Merged image (k) shows most *Vgat* and *Vglut2* expressing neurons in LH do not overlap. fx, fornix

delivered **AAV-FLEX-ChR2-EYFP** viral vectors to the LH in *Pdx1-Cre* mice (LH^{*Pdx1-ChR2*}; **Figure 5a**). Three weeks post-injection, we identified ChR2-EYFP expressing neurons in the LH (**Figure 5c and Figure 6**), and observed their associated projections in the PVH (**Figure 5b**). Targeted photostimulation of LH fibers revealed both excitatory post-synaptic currents (oEPSCs) and inhibitory post-synaptic currents (oIPSCs) in PVH neurons in acute brain slices from LH^{*Pdx1-ChR2*} mice. To ensure that recorded responses were comparable between animals, we targeted neurons in the dorsal medial part of the PVH (spanning anterior-posterior Bregma coordinates, -1.06 mm to -1.22 mm), since this region contained abundant ChR2 expressing projections from LH^{*Pdx1-ChR2*} neurons (**Figure 5b**). We found that more than 91% of the recorded cells (110 out of 120) showed inhibitory responses, while less than 33% (39 out of 120) showed excitatory responses (**Figure 5d**). These photo-induced postsynaptic currents were blocked by bath-applied ionotropic GABA and glutamate receptor antagonists, respectively (**Figure 5d**). Interestingly, the majority of neurons that showed light-evoked EPSCs also exhibited IPSCs (**Figure 5f**). Both oEPSCs and oIPSCs in the PVH were resistant to bath-applied tetrodotoxin (TTX) and 4-aminopyridine (4-AP), known to block action potentials and inhibit network activity⁵¹, suggesting monosynaptic

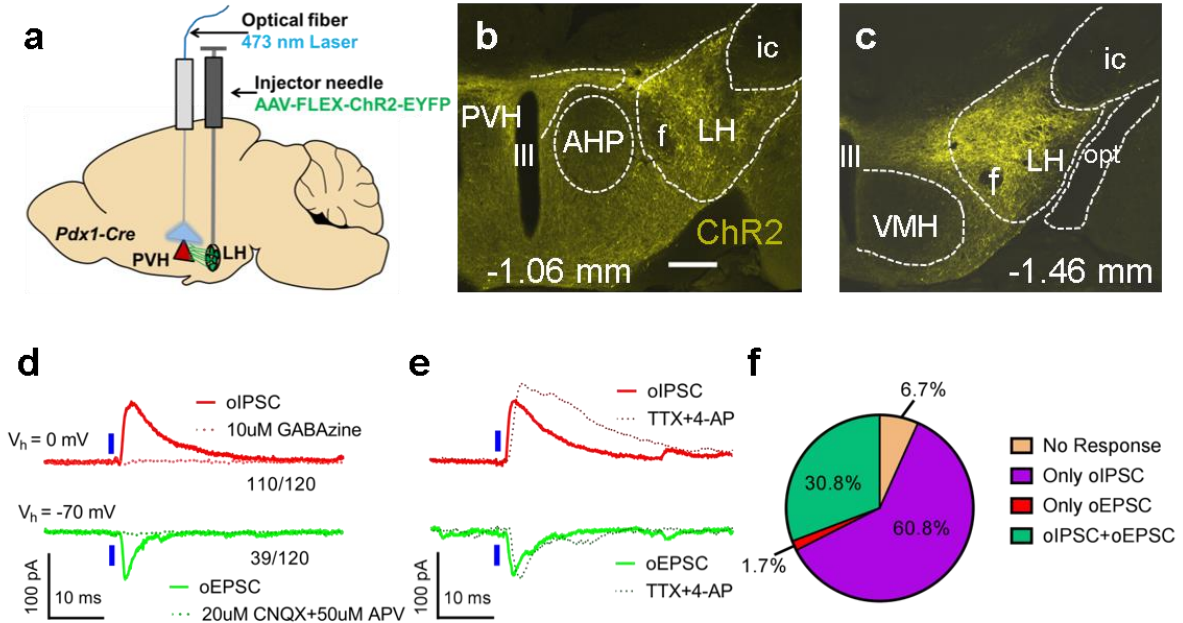


Figure 5. GABA and glutamate LH neurons send monosynaptic projections to a common subset of PVH neurons. (a) Experimental schematic. (b) Representative image showing ChR2-EYFP LH^{Pdx1} fibers in PVH. (c) ChR2 expression in LH^{Pdx1} neurons. Coordinates in (a-b) are anterior-posterior (AP) measurements relative to Bregma. III, 3rd ventricle; AHP, anterior hypothalamic area, posterior; f, fornix; ic, internal capsule; LH, lateral hypothalamus; opt, optic tract; PVH, paraventricular nucleus of the hypothalamus; Scale bar = 300 μ m. (d) Electrophysiology traces from patch-clamp recordings showing optical-evoked inhibitory post-synaptic currents (oIPSCs, top) and optical-evoked excitatory post-synaptic currents (oEPSCs, bottom) in a PVH neuron held at the indicated potentials (V_h) following 1-ms blue light pulse to LH^{Pdx1-ChR2} fibers. Currents can be blocked by ionotropic GABA or glutamate receptor blockers, GABA_A and CNQX+APV, respectively. (e) Effect of co-application of TTX and 4-AP in oIPSCs (top) and oEPSCs (bottom). (f) Pie chart showing percentage of PVH neurons receiving excitatory and/or inhibitory inputs from LH^{Pdx1-ChR2} neurons, as suggested by electrophysiology current responses to blue light. Electrophysiology data used with permission from Yungang Lu.

connectivity (**Figure 5e**). Thus, LH→PVH glutamatergic and GABAergic inputs target a common subset of PVH neurons.

Activation of LH→PVH fibers induces feeding and self-grooming

Similar to our previous study⁶⁹, we activated LH^{Pdx1-ChR2}→PVH terminal fibers using optic fibers implanted above the PVH (**Figure 5a** and **Figure 6a-b**). A stimulation protocol of blue 473 nm light pulsed at constant 5 Hz and 100ms pulse-width duration caused voracious feeding in *Pdx1-Cre* mice (**Figure 7a and 7e**). However, conditional knockout mice lacking

the vesicular GABA transporter (*Vgat*, which is required for presynaptic GABA release) and expressing ChR2 in LH (*Pdx1-Cre::Vgat^{flox/flox}* mice)

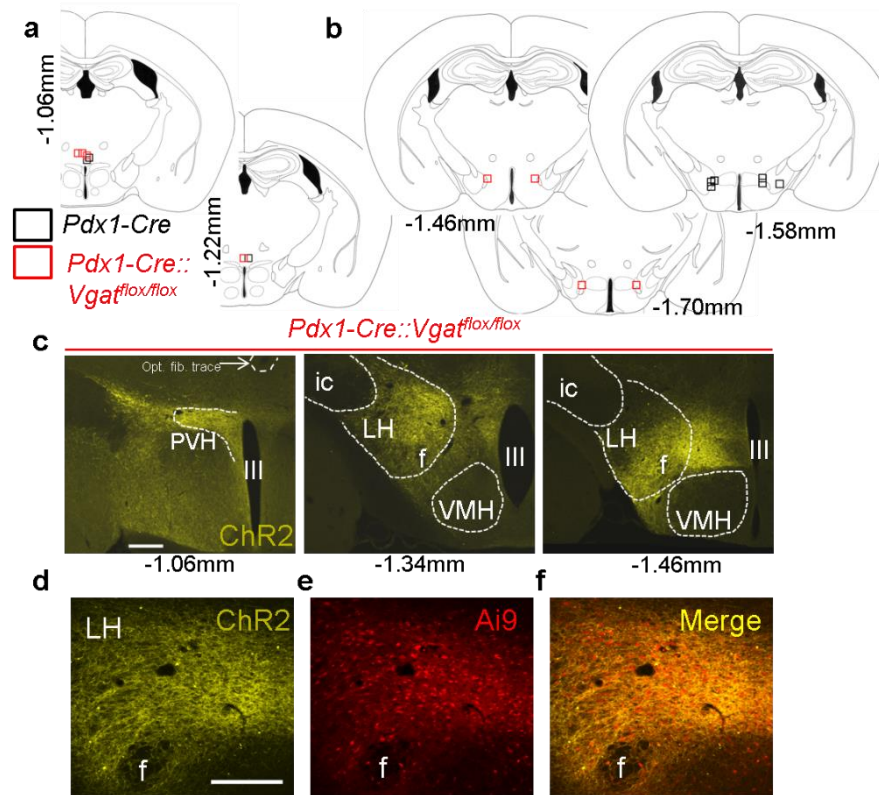


Figure 6. ChR2 expression in LH^{Pdx1} neurons. (a) Post-hoc analysis in coronal brain sections revealed optic fiber traces over caudal portions of the PVH in *Pdx1-Cre* mice (black outlined boxes) and *Pdx1-Cre::Vgat^{flox/flox}* mice (red outlined boxes) used for experiments in **Figure 7**. (b) Shows approximate ChR2 injection sites, as determined by dense eYFP expression, in the same mice. (c) Representative images taken from brain slices of a *Pdx1-Cre::Vgat^{flox/flox}* mouse used in experiments for **Figure 7** reveal ChR2 expression in PVH projection fibers and optical fiber implantation above PVH (opt. fib. trace, arrow) (left image) and ChR2 expression in LH^{Pdx1} neurons (middle and right images). (a-c): millimeter measurements indicate anterior-posterior distance relative to Bregma. III, third ventricle; f, fornix; ic, internal capsule; LH, lateral hypothalamus; PVH, paraventricular hypothalamus; VMH, ventromedial hypothalamus. Scale bar = 300µm. (d-f) Representative coronal brain slice images from a *Pdx1-Cre::Ai9* reporter mouse used in **Figure 7** experiments show ChR2 (d) and Ai9 (e) expression overlapping in the LH region (f). Scale bar = 250 µm.

showed no alteration in feeding behavior during light stimulation (**Figure 7a** and **Figure 6c**).

Electrophysiological recordings in PVH brain slices of *Pdx1-Cre::Vgat^{flox/flox}* mice confirmed selective disruption of GABA release from LH^{Pdx1-ChR2} fibers to PVH neurons (**Figure 8a-b**).

These results are consistent with our previous findings that GABA release from LH→PVH

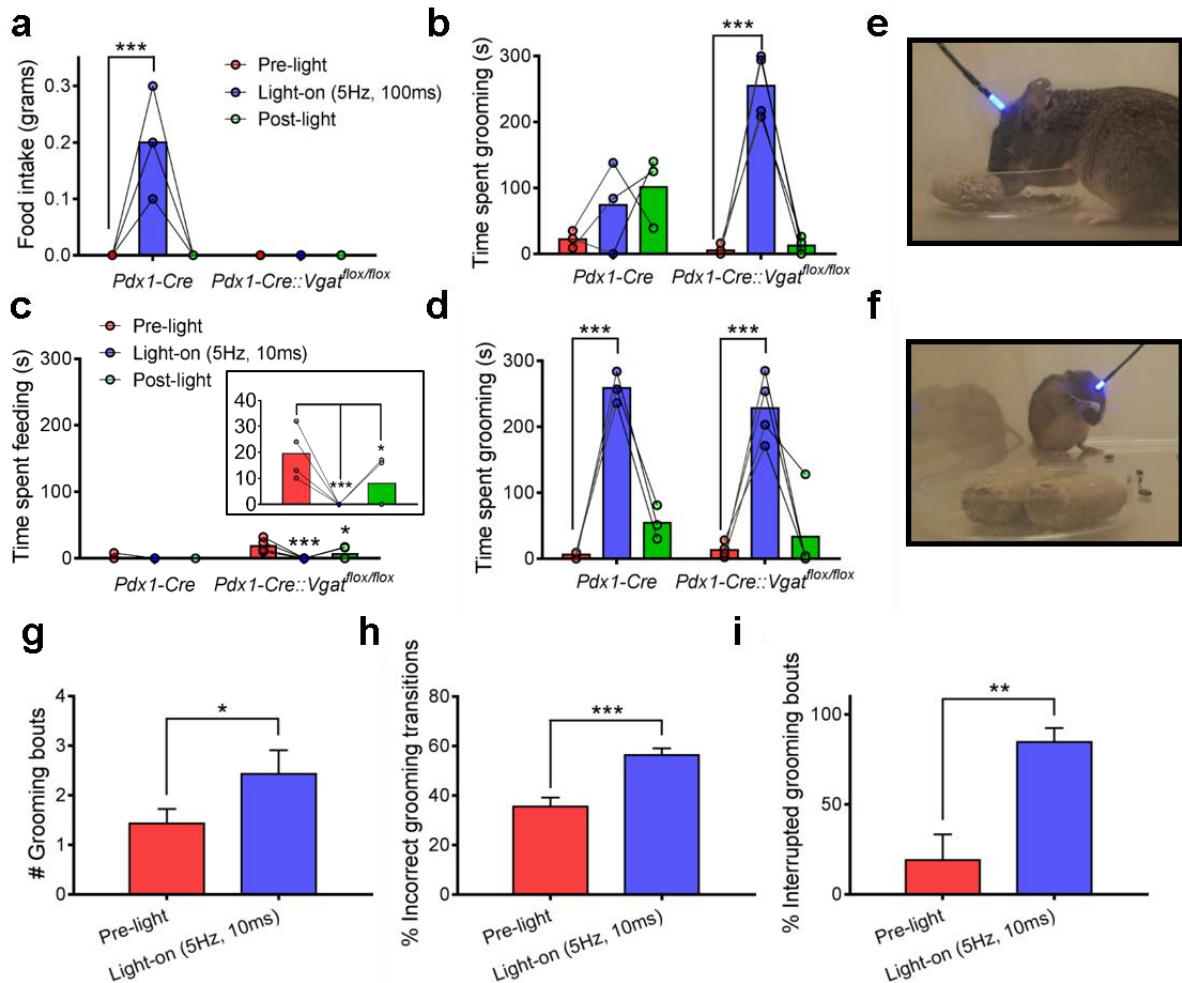


Figure 7. Optical activation of LH^{Pdx1}→PVH projections differentially causes feeding and repetitive grooming behaviors, with the former requiring GABA release. Food intake (a) and grooming time (b) before (pre-light), during (light-on), and after (post-light) 5 Hz, 100 ms photostimulation of LH^{Pdx1-ChR2}→PVH fibers in *Pdx1-Cre* and *Pdx1-Cre::Vgat^{flox/flox}* mice. Feeding time (c) and grooming time (d) before, during, and after 5 Hz, 10 ms photostimulation of LH^{Pdx1-ChR2}→PVH fibers in the same mice. Inset in (c) is expanded from *Pdx1-Cre::Vgat^{flox/flox}* grooming data in the same figure. Snapshots taken from videos of *Pdx1-Cre* (e) and *Pdx1-Cre::Vgat^{flox/flox}* (f) engaged in feeding and grooming behaviors, respectively, during light-on epoch (5 Hz, 100ms). (g-i) Grooming microstructure characterization during pre-light and light-on (5 Hz, 10ms) epochs. (a-d and g-i) Pre-light, light-on, and post-light epochs occurred consecutively and lasted 5 mins each; *Pdx1-Cre*, n = 3 animals; *Pdx1-Cre::Vgat^{flox/flox}*, n = 4 animals.

terminals promotes feeding behavior⁶⁹. Using these models, we also assayed behavioral responses during photostimulation of LH→PVH terminals when food was removed, and observed that most of *Pdx1-Cre* mice tested exhibited aberrant licking behavior, which was never observed in *Pdx1-Cre::Vgat^{flox/flox}* mice. LH→PVH evoked behavioral responses were

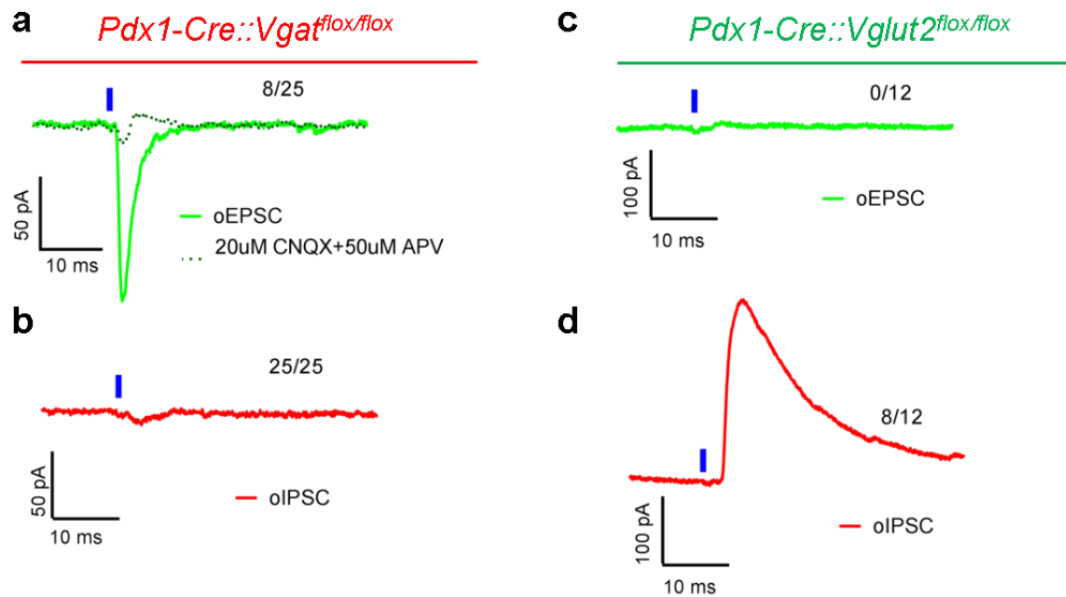


Figure 8. Inhibitory and excitatory post-synaptic currents in PVH elicited by blue light stimulation of LH^{Pdx1-ChR2} fibers require vesicular GABA transporter (Vgat) and vesicular glutamate transporter 2 (Vglut2), respectively. (a) Voltage clamp recordings in PVH brain slices of *Pdx1-Cre::Vgat^{flox/flox}* mice reveal optically-evoked excitatory post-synaptic currents (oEPSCs, which can be blocked by ionotropic glutamate receptor blockers CNQX+APV), but not optically-evoked inhibitory post-synaptic currents (oIPSCs) (b). Conversely, PVH recordings in *Pdx1-Cre::Vglut2^{flox/flox}* brain slices show light can elicit IPSCs (d) but not EPSCs (c). Blue ticks indicate 1-ms blue light pulse. Figure used with permission from Yungang Lu.

comparable between unilaterally and bilaterally injected mice with ChR2; thus, data from these two groups were combined and presented herein.

Interestingly, we noted that in a five minute period following 5 Hz, 100 ms light stimulation, *Pdx1-Cre* mice tended to exhibit self-grooming behavior (**Figure 7b**). Strikingly, during the 5 min light-on period, *Pdx1-Cre::Vgat^{flox/flox}* mice exhibited extensive repetitive self-grooming behavior (**Figure 7b and 7f**). These data suggest that GABA release in LH→PVH suppresses evoked grooming behavior. To gauge the activation threshold of LH→PVH fibers in driving feeding behavior, we evaluated multiple stimulation protocols for the ability to elicit grooming vs. feeding behavior. We found that, in *Pdx1-Cre* mice, photostimulation with 5 Hz, 10 ms pulses failed to induce any feeding (**Figure 7c**), and instead induced intense self-grooming (**Figure 7d**). Similarly, the same stimulation regime did not elicit

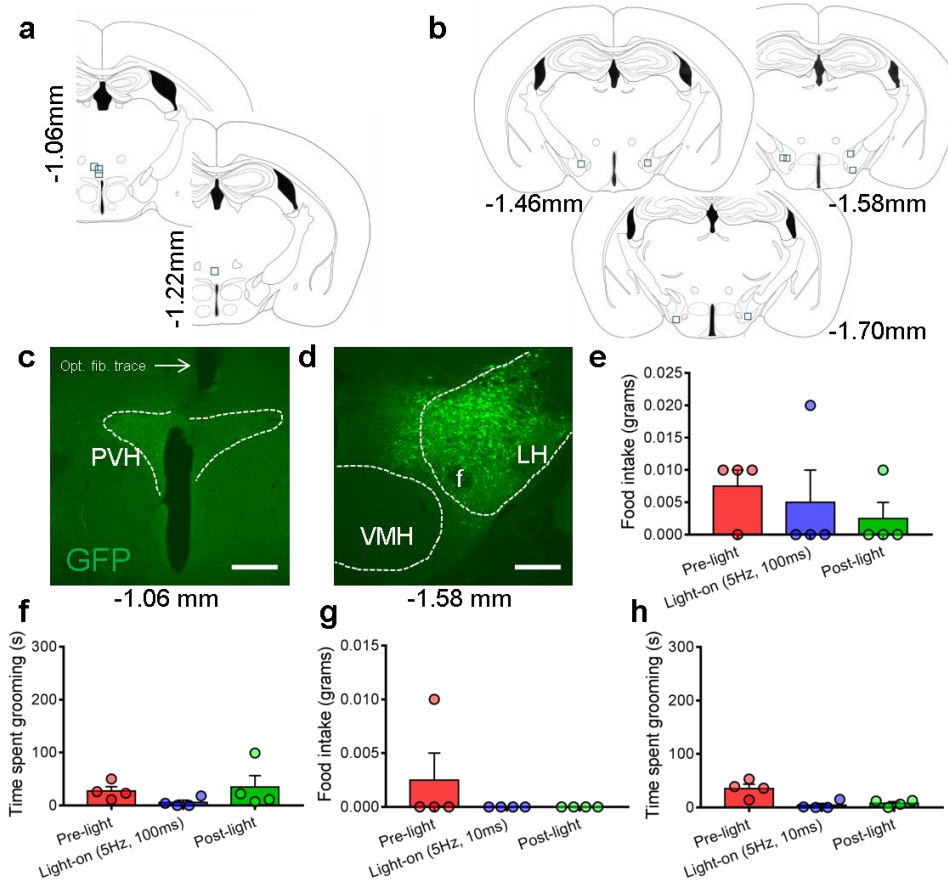


Figure 9. Photostimulation of LH^{Pdx1-GFP} expressing fibers in PVH does not increase feeding or grooming behaviors. (a) Post-hoc analysis of brain slices show optic fiber placements (blue outlined boxes) above caudal PVH regions in *Pdx1-Cre* mice injected with cre-dependent GFP virus in LH. (b) Shows approximate injection locations of GFP (blue outlined boxes) in the same mice. Representative images from a *Pdx1-Cre::GFP* mice (n=4) showing GFP-expressing fibers in PVH and optical fiber implantation above PVH (opt. fib. trace, arrow) (c) and injection site in LH (d). Scale bar = 300 μ m. *In vivo* photostimulation of LH^{Pdx1-GFP}→PVH fibers does not cause significant increases in either feeding (e, g) or grooming behaviors (f, h), irrespective of light stimulation protocol (5Hz, 10 vs. 100 ms). Repeated measures ANOVA: (e) Light epoch F (2, 6) = 0.4286, P=0.6699; (f) Light epoch F (2, 6) = 1.644, P=0.2696; (g) Light epoch F (2, 6) = 1, P=0.4219 (h) Light epoch F (2, 6) = 7.057, P=0.0265). Data presented as \pm s.e.m.

feeding in the *Pdx1-Cre::Vgat^{flx/flx}* mice, but instead suppressed the time spent feeding (Figure 7c), and led to repetitive self-grooming that was indistinguishable from that in *Pdx1-Cre* mice (Figure 7d). Multiple trials revealed that 5 Hz, 100 ms light pulses consistently induced feeding responses, whereas 5 Hz, 10 ms pulses consistently induced self-grooming in *Pdx1-Cre* animals. Thus, we used these two protocols to differentially induce feeding and self-grooming in this study. As a control, *Pdx1-Cre* mice that received cre-dependent GFP

virus (opsin-negative vectors) to LH did not exhibit elevated feeding or grooming behaviors upon PVH illumination (**Figure 9**).

Stressful and anxiety-provoking situations increase self-grooming behavior and alter the natural progression of grooming transitions, which normally proceed in an uninterrupted cephalocaudal direction¹⁶⁹. With this in mind, we investigated whether light-evoked self-grooming resulted in changes in stress-related grooming “microstructure.” Using a grooming analysis algorithm²²⁷ we analyzed the number of grooming bouts, incorrect grooming transitions, and interrupted grooming bouts, and found that all these components of grooming behavior were significantly increased (**Figure 7g-i**), suggesting that LH→PVH stimulation induced grooming is stress-related in nature.

Glutamate release from LH→PVH fibers in self-grooming behavior

The rapid onset of self-grooming behavior by LH→PVH activation is independent of GABA release, suggesting that glutamate may mediate this effect. To explore this, we used *Pdx1-Cre::Vglut2^{fllox/fllox}* mice (*Vglut2*, also named *Slc17a6*, is required for presynaptic glutamate release in most hypothalamic neurons). *In situ* hybridization data showed that the number of *Vglut2*-expressing neurons in the LH was dramatically reduced in *Pdx1-Cre::Vglut2^{fllox/fllox}* mice compared to controls (**Figure 10a-b**), suggesting that a significant portion of LH^{*Pdx1*} neurons are glutamatergic. To evaluate glutamate release from LH^{*Pdx1*} neurons via *Vglut2* deletion, we recorded oIPSCs and oEPSCs in PVH neurons following blue light stimulation of LH^{*Pdx1-ChR2*} fibers in *Pdx1-Cre::Vglut2^{fllox/fllox}* mice. 0/12 PVH neurons exhibited oEPSCs in response to blue light (**Figure 8c**). Concurrently, 8/12 PVH neurons showed oIPSCs

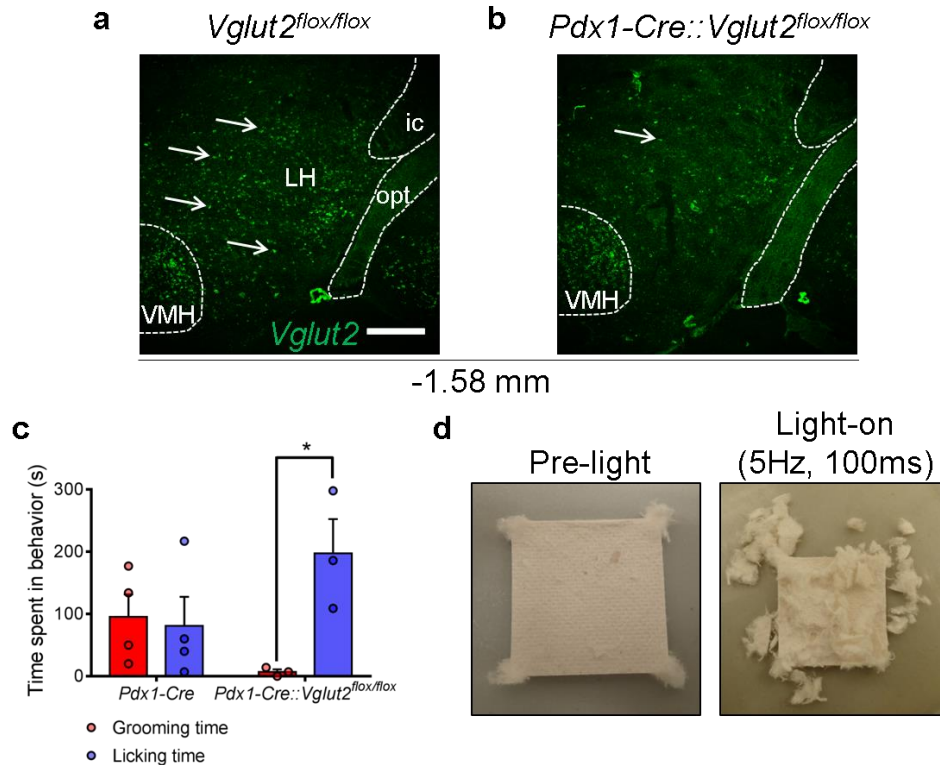


Figure 10. Photostimulation of GABAergic LH→PVH projections causes chewing and licking behavior. (a-b) *In situ* hybridization for *Vglut2* mRNA in fresh frozen coronal brain slices shows numerous neurons with *in situ* fluorescent signal (arrows) in the LH region of *Vglut2^{flox/flox}* mice (a). In contrast, in *Pdx1-Cre::Vglut2^{flox/flox}* mice, the number of neurons with *in situ* fluorescent signal in a matching LH-containing section is dramatically reduced while it is not changed in neighboring VMH area (b). Scale bar = 300µm. Millimeter measurement indicates anterior-posterior distance from Bregma. ic, internal capsule; LH, lateral hypothalamus; opt, optic tract; VMH, ventromedial hypothalamus. (c) When mice were placed in a bare cage (no food or bedding), *Pdx1-Cre* mice spent approximately equal amounts of time grooming and aimlessly licking the floors and sides of the cage upon LH^{*Pdx1-ChR2*}→PVH photostimulation (5Hz, 100ms); however, *Pdx1-Cre::Vglut2^{flox/flox}* spent significantly more time licking the cage than grooming upon the same light stimulation (two-way ANOVA; Interaction $F(1, 10) = 5.984$, $P = 0.0345$; Sidak's multiple comparisons test: Grooming time vs. Licking time (*Pdx1-Cre::Vglut2^{flox/flox}*) * $p < 0.05$). Data presented as \pm s.e.m. (d) A portion of the *Pdx1-Cre* and *Pdx1-Cre::Vglut2^{flox/flox}* mice violently chewed on a square piece of bedding upon light stimulation of LH^{*Pdx1-ChR2*}→PVH circuit when food was absent. Pictures are of the same piece of bedding following 5 minutes pre-light and 5 minutes light-on stimulation.

(Figure 8d), demonstrating that deletion of *Vglut2* in *Pdx1-Cre* neurons leads to selective loss of glutamate release from LH→PVH terminals while GABAergic neurotransmission remains intact.

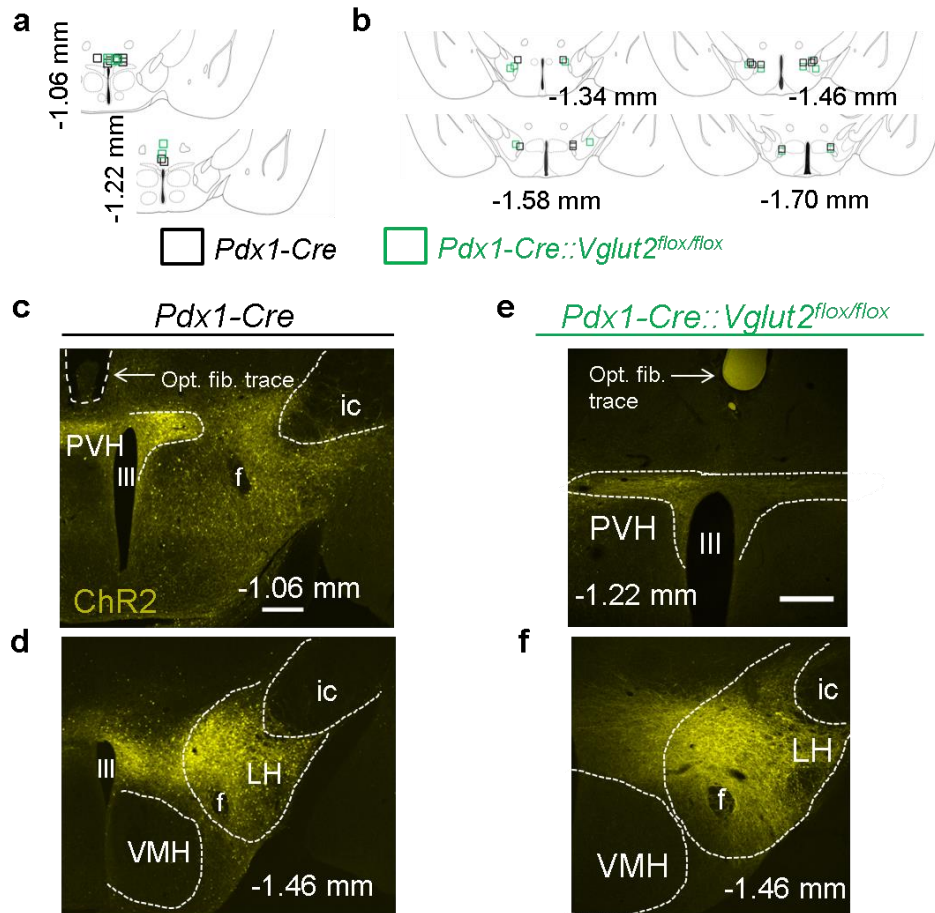


Figure 11. ChR2 expression in LH neurons and PVH projection fibers in *Pdx1-Cre* and *Pdx1-Cre::Vglut2^{flox/flox}* mice. (a) Post-hoc analysis in brains of mice used for **Figure 12** experiments shows optic fiber placements above caudal PVH region (indicated by black and green outlined boxes). (b) The same mice received ChR2 injections consistently targeted in the LH region (black and green outlined boxes). Representative PVH brain slice image of a *Pdx1-Cre* mouse showing ChR2-expressing fibers in rostral PVH and optical fiber implantation above PVH (opt. fib. trace, arrow) (c) and ChR2 injection site in LH (d). Representative brain slice images from a *Pdx1-Cre::Vglut2^{flox/flox}* mouse reveals ChR2 fibers in caudal PVH and optical fiber implantation above PVH (left image) (e) and ChR2 injection site in LH (f). Scale bar = 300µm. III, third ventricle; f, fornix; ic, internal capsule; LH, lateral hypothalamus; PVH, paraventricular hypothalamus; VMH, ventromedial hypothalamus.

To test the behavioral effects of LH→PVH terminal stimulation, *Pdx1-Cre* and *Pdx1-Cre::Vglut2^{flox/flox}* mice received LH injections of **AAV-FLEX-ChR2-EYFP** vectors and optic fiber implants over PVH (**Figure 11**). *In vivo* 5 Hz, 100 ms light stimulation of LH^{*Pdx1-ChR2*} fibers in the PVH led to comparable ravenous feeding in both *Pdx1-Cre* and *Pdx1-Cre::Vglut2^{flox/flox}* mice (**Figure 12a**). Similar to the previous findings (**Figure 7b**), light

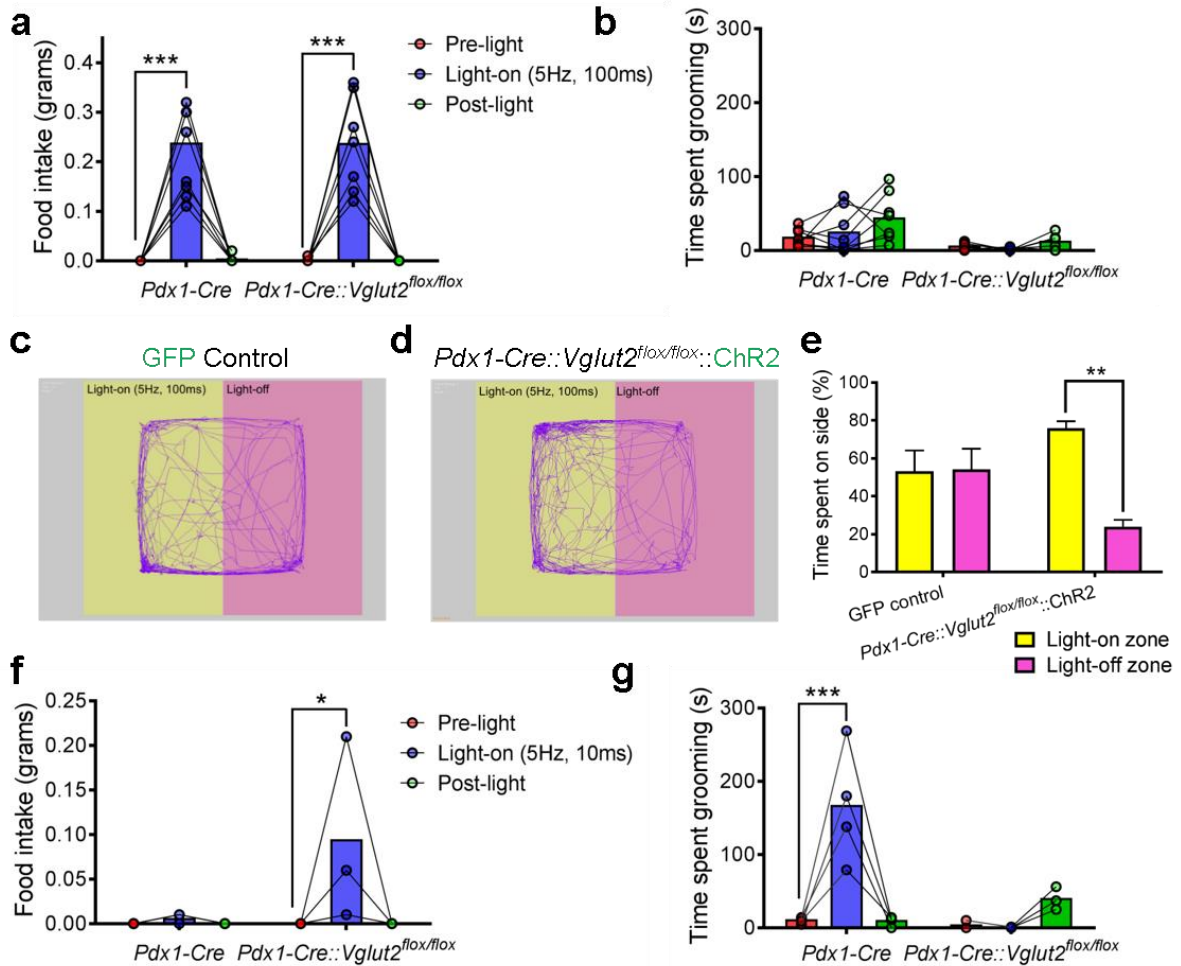


Figure 12. LH^{Pdx1}→PVH evoked grooming requires glutamate release, and activation of non-glutamatergic fibers promotes behavioral approach. Food intake (a) and grooming time (b) before (pre-light), during (light-on), and after (post-light) 5 Hz, 100 ms photostimulation of LH^{Pdx1-ChR2}→PVH fibers in *Pdx1-Cre* (n = 8) and *Pdx1-Cre::Vglut2^{flox/flox}* (n = 7) mice. Real-time place preference assay (RTPP) during optical stimulation of LH^{Pdx1}→PVH in GFP control (n = 6) and *Pdx1-Cre::Vglut2^{flox/flox}::ChR2* mice (n = 4). (c-d) Representative tracks tracing locomotion; (e) Percentage time spent on each side. Food intake (f) and grooming time (g) for 5 Hz, 10 ms photostimulation test.

stimulation elicited mild self-grooming in some *Pdx1-Cre* mice, but no grooming in *Pdx1-Cre::Vglut2^{flox/flox}* mice (Figure 12b). When stimulated with 5 Hz, 10 ms, *Pdx1-Cre* mice showed no changes in feeding (Figure 12f), but exhibited intense self-grooming (Figure 12g). On the other hand, *Pdx1-Cre::Vglut2^{flox/flox}* mice exhibited feeding (Figure 12f), but no grooming behavior (Figure 12g). In the absence of food, 5 Hz, 100 ms light stimulation elicited extensive licking behavior in *Pdx1-Cre::Vglut2^{flox/flox}* mice, which differed from the

combined licking and grooming behavior seen in *Pdx1-Cre* mice (**Figure 10c**). When presented with a piece of square bedding in the absence of food, some *Pdx1-Cre::Vglut2^{fllox/fllox}* mice violently chewed and ripped the bedding (**Figure 10d**). These findings support our conclusion that LH→PVH GABAergic activity strongly promotes the drive to feed and suppresses grooming, while LH→PVH glutamatergic activity promotes self-grooming.

We next probed the valence of LH→PVH activity in *Pdx1-Cre::Vglut2^{fllox/fllox}* mice using a real-time place preference assay (RTPP)¹¹⁰. Mice previously unexposed to the test were placed in a large test chamber with two equal zones: a light-off zone paired with no light stimulation, and a light-on zone paired with 5 Hz, 100 ms blue light stimulation. Control mice that received **AAV-FLEX-GFP** injections into the LH and optic fibers implants above PVH did not display significant preference for either the light-paired or light-unpaired side of the chamber (**Figures 12c and 12e**). In contrast, *Pdx1-Cre::Vglut2^{fllox/fllox}* mice expressing ChR2 in LH^{*Pdx1*} and with optic fibers implanted above PVH, significantly preferred the light-paired side of the chamber over the light-off zone (**Figures 12d and 12e**). Together, these data suggest that activation of GABAergic LH→PVH circuit produces positive valence.

PVH neurons mediate feeding and self-grooming behavior

Activation of remote sites through collateral fiber activation remains a caveat of targeting projections for stimulation with optogenetics²⁶. Thus, to determine if photostimulation of LH^{*Pdx1-ChR2*} fibers in the PVH activated additional LH collaterals in non-PVH sites through antidromic action, we crossed *Pdx1-Cre* mice with *Sim1-Cre::γ2^{fllox/fllox}* mice⁶⁴, in which the GABA-A receptor γ2 subunit, an essential subunit for GABA-A receptor function, is deleted in *Sim1*-expressing PVH neurons. The resulting *Pdx1-Cre::Sim1-Cre::γ2^{fllox/fllox}* mice lacked γ2 subunit in both *Pdx1-Cre* and *Sim1-Cre* neurons⁶⁹. We used *Pdx1-Cre::γ2^{fllox/fllox}* mice as a control group. Surprisingly, spike firing rates of PVH neurons between *Sim1-Cre* and *Sim1-*

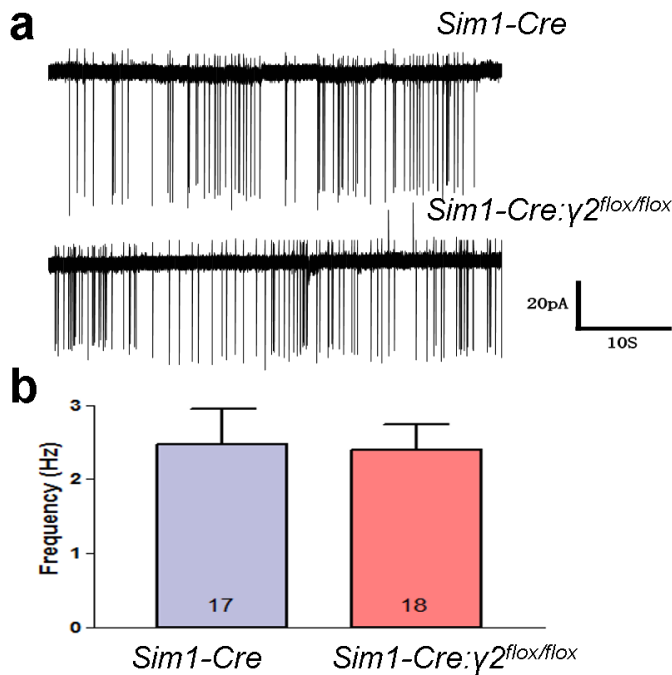


Figure 13. Deletion of $\gamma 2$ in *Sim1* neurons does not affect spontaneous firing activity in PVH^{Sim1} neurons. (a) Loose-patch recordings (voltage-clamp mode) of spontaneous spike discharge in PVH^{Sim1} neurons of *Sim1-Cre* (top) and *Sim1-Cre:: $\gamma 2^{flox/flox}$* (bottom) mice. (b) Quantification of firing frequency in PVH^{Sim1} neurons between the indicated two groups of mice does not reveal changes in overall neuron activity between genotypes. Figures used with permission from Yungang Lu.

Cre:: $\gamma 2^{flox/flox}$ mice were similar (**Figure 13**). Further whole cell recordings showed that $\gamma 2$ deletion in *Sim1-Cre* PVH (PVH^{Sim1}) neurons led to a reduction in evoked IPSCs as well as evoked EPSCs (data not shown), suggesting that the lack of change in PVH^{Sim1} neuron activity with $\gamma 2$ deletion is due to a compensatory reduction of glutamatergic inputs. We then performed whole-cell recordings on PVH neurons following photostimulation of LH^{Pdx1-ChR2} fibers. Whereas light evoked comparable monosynaptic EPSCs in both *Pdx1-Cre:: $\gamma 2^{flox/flox}$* mice and *Sim1-Cre::Pdx1-Cre:: $\gamma 2^{flox/flox}$* mice (**Figure 14**), oIPSCs displayed significantly reduced amplitudes in *Sim1-Cre::Pdx1-Cre:: $\gamma 2^{flox/flox}$* mice compared to that of *Pdx1-Cre:: $\gamma 2^{flox/flox}$* mice (**Figure 14b-c**). Additionally, a smaller fraction of neurons displayed oIPSCs in *Sim1-Cre::Pdx1-Cre:: $\gamma 2^{flox/flox}$* compared to *Pdx1-Cre:: $\gamma 2^{flox/flox}$* mice (**Figure 14c**). However, the fraction of neurons that displayed oEPSCs was similar between groups (**Figure 14c**). Behaviorally, light stimulation of LH^{Pdx1-ChR2}→PVH fibers in control *Pdx1-Cre:: $\gamma 2^{flox/flox}$* mice induced voracious feeding (**Figure 14d and Figure 15**) similar to that observed in *Pdx1-Cre* mice. In contrast, the same photostimulation paradigm failed to

induce any feeding behavior in *Sim1-Cre::Pdx1-Cre::γ2^{flox/flox}* mice (**Figure 14d and Figure 15**).

It is possible that non-PVH, *Sim1-Cre* positive brain regions expressing $\gamma 2$ mediated the light-evoked feeding behavior via collateral activation and consequent release of GABA

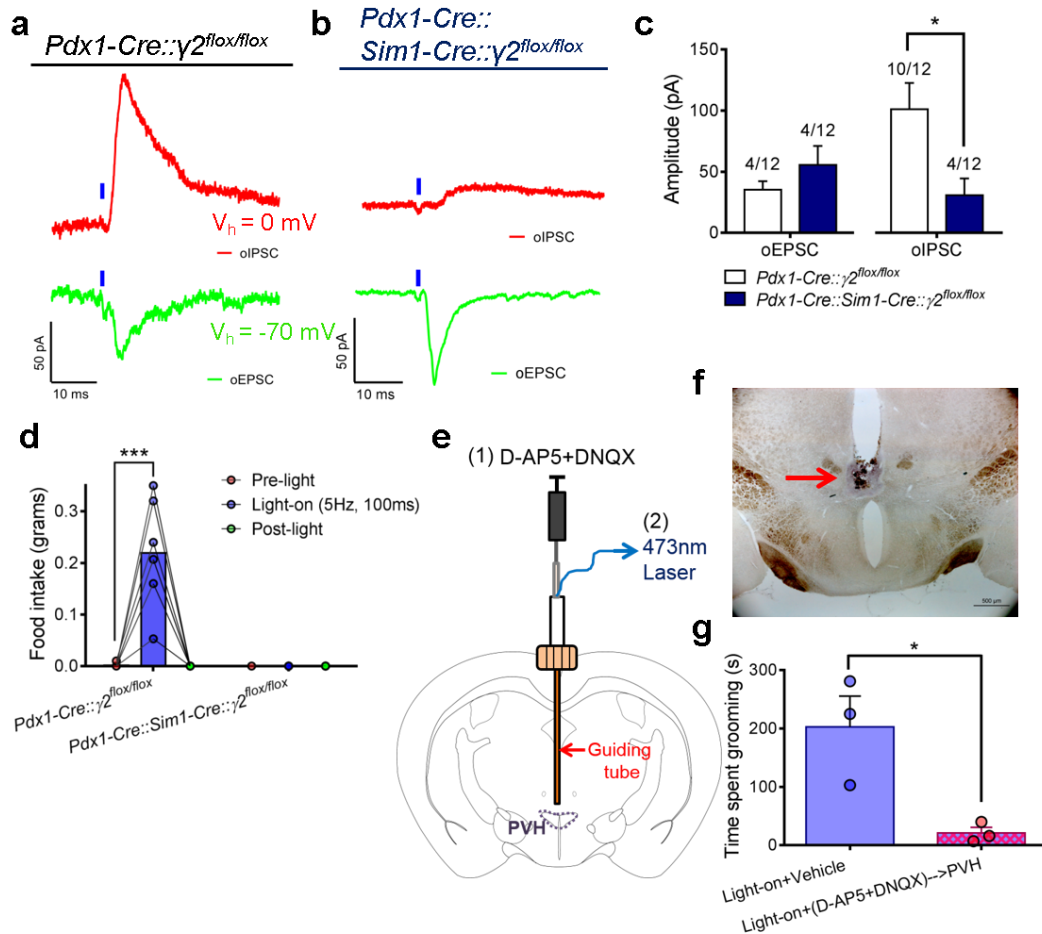


Figure 14. GABA-A and ionotropic glutamate receptor activation in PVH are required for LH^{*Pdx1-ChR2*}→PVH evoked feeding and grooming, respectively. (a) Inhibitory (oIPSC, top) and excitatory (oEPSC, bottom) post-synaptic current responses evoked by 1-ms blue light pulse (blue tick) in a PVH neuron of a *Pdx1-Cre::γ2^{flox/flox}* mouse (control). (b) oIPSC (top) and oEPSC (bottom) responses to 1-ms blue light pulse in a PVH neuron of a *Pdx1-Cre::Sim1-Cre::γ2^{flox/flox}* mouse (double-cre knockout). (c) Quantification of current amplitude in control and double-cre knockout mice. Number of cells showing current response out of total number of cells recorded is shown above bars. (e) Schematic illustrating custom-made guide cannula allowing for interchangeable fluid and optical delivery to PVH. (f) Approximate fluid injection location in PVH area is shown by microinjection of blue ink before sacrifice. Scale bar=500 μm. (g) Time spent grooming during 5 mins of 5 Hz, 10-50 ms photostimulation of LH^{*Pdx1-ChR2*}→PVH following vehicle or D-AP5+DNQX microinjection to PVH. Figures a-c used with permission from Yungang Lu.

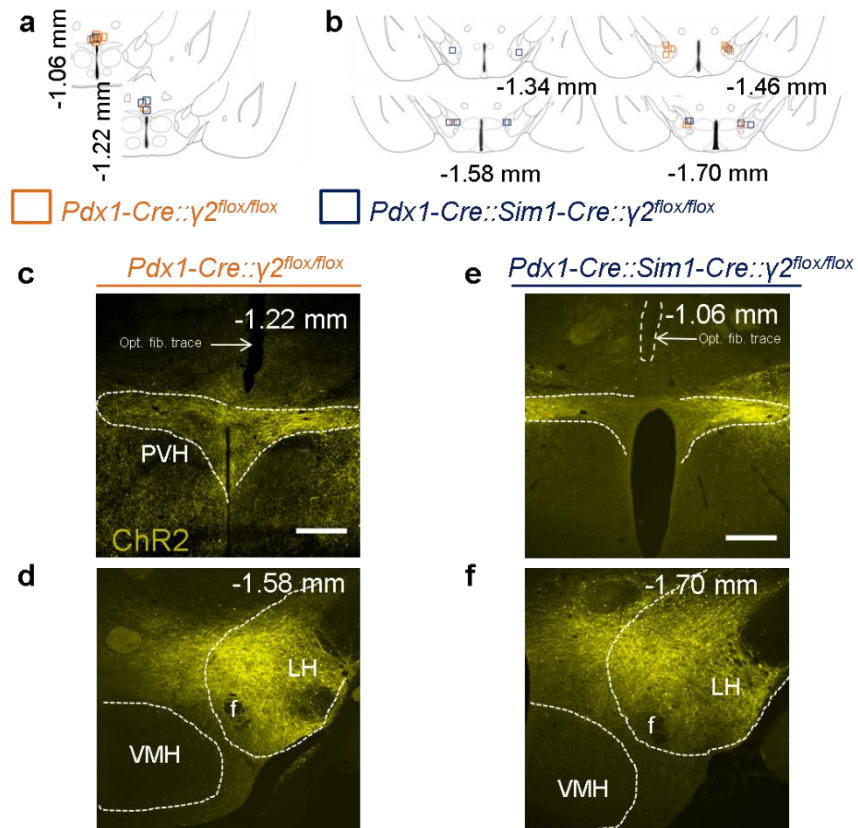


Figure 15. ChR2 expression in LH neurons and PVH projection fibers in *Pdx1-Cre::γ2^{flox/flox}* and *Pdx1-Cre::Sim1-Cre::γ2^{flox/flox}* mice. (a-b) Post-hoc analysis in brains of mice used for **Figure 14d** experiments confirmed optic fiber placements above caudal PVH region (a) (orange and blue outlined boxes) and successful targeting of ChR2 to the LH region (b) (orange and blue outlined boxes). Representative coronal brain slice images from a *Pdx1-Cre::γ2^{flox/flox}* mouse showing ChR2 expression in caudal PVH fibers and optical fiber implantation above PVH (opt. fib. trace) (c) and ChR2 expression in LH injection site (d). Representative coronal brain slice images from a *Pdx1-Cre::Sim1-Cre::γ2^{flox/flox}* mouse showing ChR2-expressing fibers in caudal PVH and optical fiber implantation above PVH (opt. fib. trace, arrow) (e) and ChR2 expression in LH injection site (f). Millimeter measurements indicate anterior-posterior distance relative to Bregma. LH, lateral hypothalamus; VMH, ventromedial hypothalamus.

to these regions. Thus, we examined if LH *Pdx1-Cre* fibers project to *Sim1* neurons in non-PVH brain sites by implementing conditional viral vectors that contained a cre-dependent synaptophysin-EGFP reporter²²⁸ injected into the LH of *Pdx1-Cre::Sim1-Cre::Ai9* mice (**Figures 16a and 16c**). Synaptophysin-EGFP fluorescence localizes in presynaptic terminals, thus serving as an effective anterograde tracer. In these animals, abundant EGFP expression was noted in the caudal portions of the PVH, as expected (**Figure 16b**).

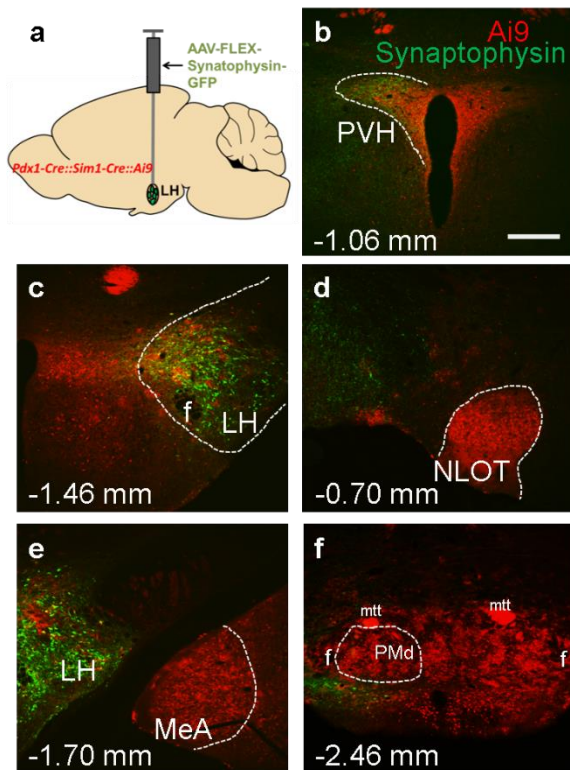


Figure 16. LH^{Pdx1} neurons project to PVH^{Sim1} but not to other prominent Sim1-positive brain regions. (a) Schematic illustrates cre-dependent delivery of synaptophysin-GFP to LH neurons (unilateral injection) in a *Pdx1-Cre::Sim1-Cre::Ai9* mouse for anterograde tracing studies. (b) As expected, prominent synaptophysin-GFP contacts were made with Ai9 neurons in the PVH, suggesting LH^{Pdx1}→PVH^{Sim1} synaptic connections. (c) Shows successful viral delivery of synaptophysin-GFP to the LH region. (d-f) Prominent *Sim1*-positive sites include NLOT (d), MeA (e), and preammillary nucleus (f), all of which show little to no GFP overlap in the respective regions. Millimeter measurements indicate anterior-posterior distance relative to Bregma. f, fornix; LH, lateral hypothalamus; MeA, Medial Amygdala nucleus; mtt, mammillothalamic tract; NLOT, nucleus of the lateral olfactory tract; PMd, dorsal preammillary nucleus. Scale bar = 300 μm.

None of the dense, non-PVH *Sim1-Cre* expressing brain regions, including the

nucleus of lateral olfactory tract, medial amygdala, and preammillary nucleus, showed obvious EGFP expression (**Figure 16d-f**), suggesting that non-PVH, *Sim1-Cre*-expressing brain regions do not contribute to the evoked feeding behavior. Together, these data show that PVH neurons mediate the avid feeding response observed with local stimulation of LH→PVH fibers.

To test whether PVH neurons mediate self-grooming induced by photostimulation of LH^{Pdx1-ChR2}→PVH fibers, we employed a custom-made guide cannula that allowed simultaneous delivery of light and local drug infusion to targeted PVH areas (**Figure 14e**). Since glutamate release contributes significantly to the evoked self-grooming behaviors (**Figure 12g**), we examined the effect of local infusion of glutamate receptor antagonists (D-AP5 + DNQX) to the PVH preceding photostimulation (**Figure 14f**). Drug infusion significantly reduced self-grooming behavior induced by photostimulation of LH^{Pdx1-}

ChR2→PVH fibers, compared to the saline infused condition (**Figure 14g**). Collectively, these studies demonstrate that PVH neurons mediate light-evoked self-grooming behavior by receiving LH→PVH glutamatergic input.

LH→PVH projections in physiologic feeding and grooming

To examine the physiological relevance of LH→PVH projections in feeding, we next tested whether increased LH→PVH GABAergic action contributes to fast-refeeding. Towards this, we delivered conditional viral vectors encoding the light-driven outward proton pump eArchT3.0 bilaterally into LH of *Pdx1-Cre::Vglut2^{flox/flox}* mice and implanted optic fibers above the PVH (**Figure 17a**). This allowed silencing of neurotransmitter release from LH presynaptic terminals upon yellow light illumination in the PVH area¹⁰⁷. Strong GFP fluorescence was observed in both LH neurons and LH→PVH fibers in mice that received **AAV-FLEX-eArchT3.0-GFP** injections to LH (LH^{*Pdx1-eArchT3.0*}; **Figure 18a**). To verify that illumination of LH^{*Pdx1-eArchT3.0*} fibers reduced GABA release, we recorded oIPSCs in PVH neurons of *Pdx1-Cre* mice following photostimulation of LH^{*Pdx1-ChR2-eArchT3.0*} fibers that simultaneously expressed eArchT3.0 and ChR2 (see methods). Whereas blue light (473 nm) reliably evoked oIPSCs in PVH neurons, yellow light (556 nm) greatly diminished blue-light evoked oIPSCs (**Figure 18b**). This effect was reversed after removal of yellow light (**Figure 18b**). These data showed that eArchT3.0 activation effectively inhibited presynaptic release of GABA from LH→PVH terminals. To examine the feeding effects of light-mediated inhibition of GABAergic LH→PVH terminals, we fasted *Pdx1-Cre::Vglut2^{flox/flox}* expressing eArchT3.0 in LH^{*Pdx1*} and tested them the following day with the protocol described in **Figure 17b**. Mice continuously engaged in food consumption during ten minutes of fast-refeeding during mock inhibition trials (**Figures 17c and 17e**). During +Light trials, where yellow light illuminated above PVH every other minute (constant 556 nm), the cumulative time spent

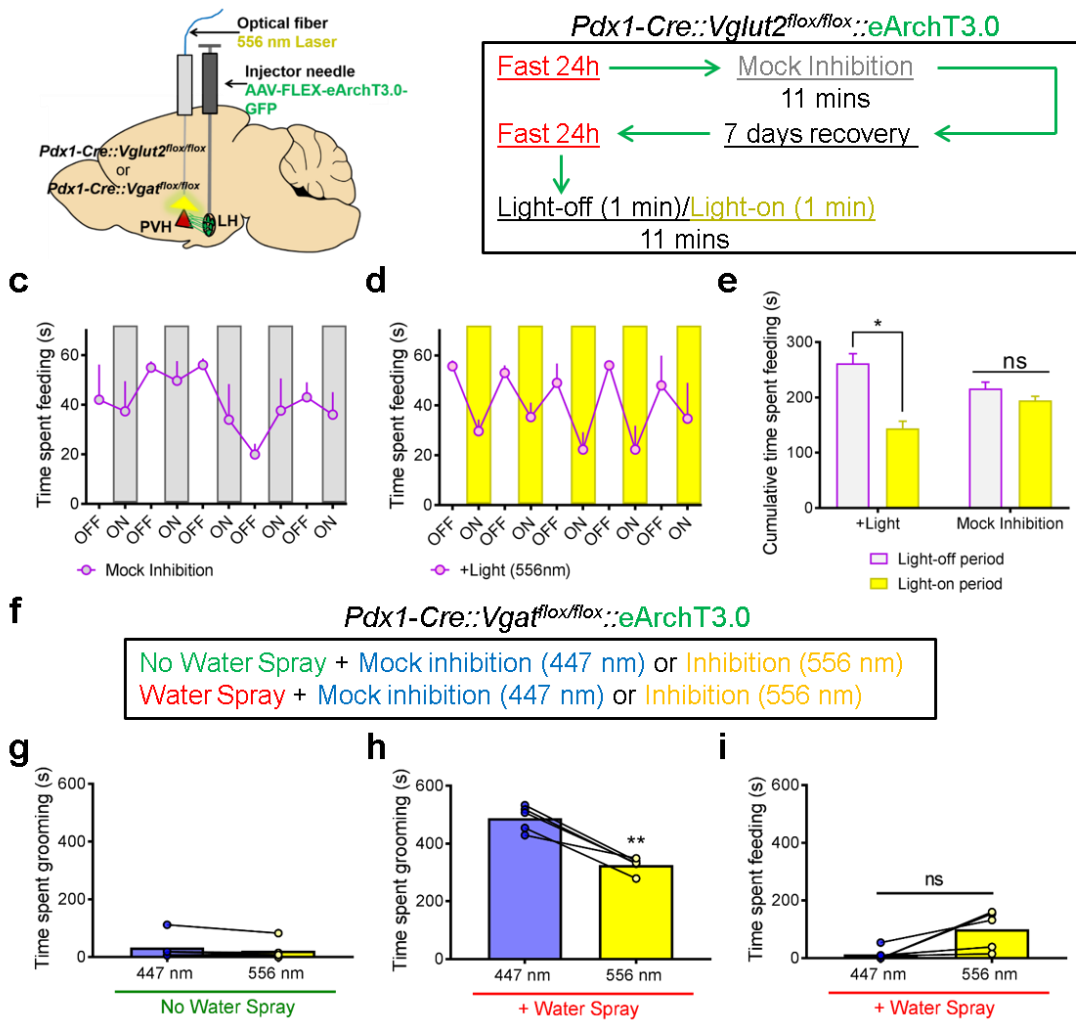
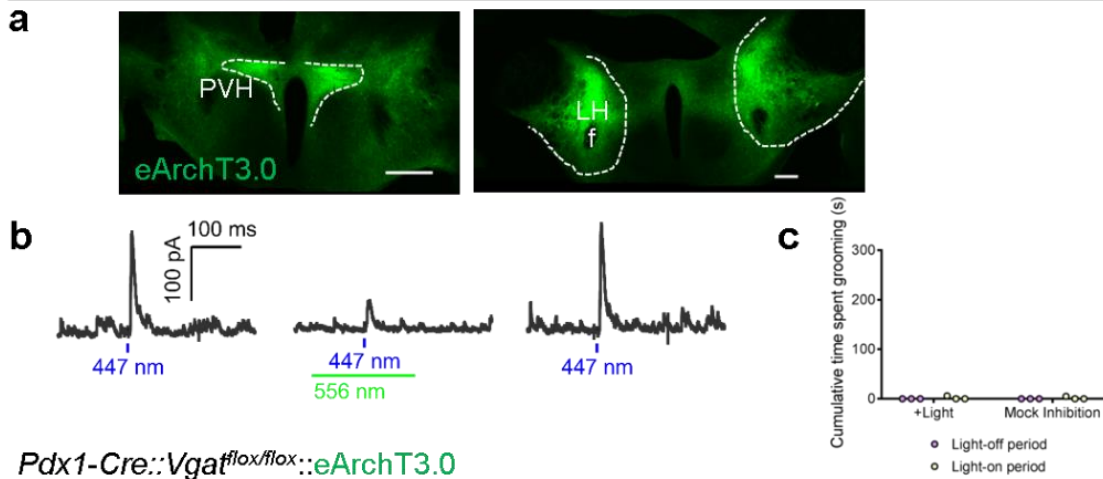


Figure 17. Inhibition of GABAergic LH^{Pdx1}→PVH fibers reduces feeding after a fast, and inhibition of glutamatergic fibers reduces water-spray induced grooming. (a) Experimental schematic. (b) Experimental protocol used to test fast-refeeding in $Pdx1-Cre::Vglut2^{flox/flox}::eArchT3.0$ mice under mock or 556 nm light inhibition. (c) Time spent refeeding after a fast during mock inhibition trial. (d) Time spent re-feeding after a fast under +Light trial, whereby 556nm constant light was applied every other minute during 10 consecutive minutes. (e) Comparison of cumulative time spent feeding during light-off vs. light-on periods during +Light and Mock inhibition trials. n = 3 animals. (f) Experimental protocol used to test water spray induced grooming in $Pdx1-Cre::Vgat^{flox/flox}::eArchT3.0$ mice under mock (447 nm) or 556 nm light inhibition. (g) Time spent grooming during mock and 556 nm inhibition when no water spray was delivered. (h) Time spent grooming during mock and 556 nm inhibition when water spray was delivered to induce grooming. (i) Simultaneous time spent feeding during water spray trials.

Pdx1-Cre::Vglut2^{flx/flx}::eArchT3.0



Pdx1-Cre::Vgat^{flx/flx}::eArchT3.0

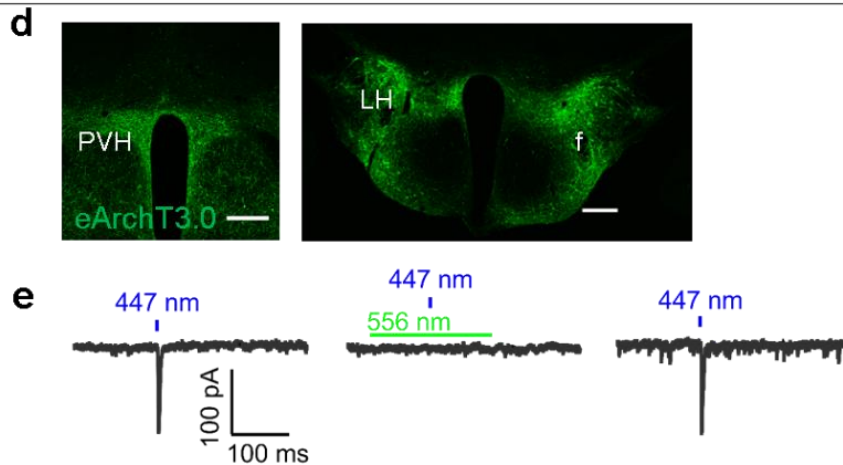


Figure 18. eArchT3.0-mediated inhibition of GABA and glutamate release in $LH^{Pdx1} \rightarrow PVH$ terminals. (a) Representative images from a *Pdx1-Cre::Vglut2^{flx/flx}::eArchT3.0* mouse (used in **Figure 17** for behavioral experiments) showing eArchT3.0-GFP projection fibers from LH to PVH (left image) and injection sites in LH (right). f, fornix; LH; lateral hypothalamus; PVH, paraventricular nucleus of the hypothalamus. Scale bar = 500 μ m. (b) Voltage clamp recordings in PVH brain slices of *Pdx1-Cre* mice receiving LH injections of 50:50 cre-dependent ChR2+eArchT3.0 viruses. Photostimulation-evoked IPSC with a single 2 ms pulse of blue light (left) was reversibly inhibited by illumination with 556nm light (middle, right). Traces shown were averaged responses of 5-6 sweeps. (c) Light (556nm) or mock inhibition of GABAergic $LH^{Pdx1} \rightarrow PVH$ terminals in *Pdx1-Cre::Vglut2^{flx/flx}::eArchT3.0* mice does not significantly impact grooming time during light-off vs. light-on periods. (d) Representative images from a *Pdx1-Cre::Vgat^{flx/flx}::eArchT3.0* mouse (used in **Figure 17** for behavioral experiments) showing eArchT3.0-GFP projection fibers from LH to PVH (left image) and injection sites in LH (right). Scale bar = 300 μ m. (e) Voltage clamp recordings in PVH brain slices of *Pdx1-Cre* mice receiving LH injections of 50:50 cre-dependent ChR2+eArchT3.0 viruses. Photostimulation-evoked EPSC with a single 1 ms pulse of blue light (left) was reversibly inhibited by illumination with 556nm light (middle, right). Traces shown were averaged responses of 5-6 sweeps. Electrophysiology experiments used with permission from Yungang Lu.

eating was significantly reduced during light-on, compared to the light-off period (**Figures 17d and 17e**). At the same time, grooming behavior was unaltered by light condition (**Figure 18c**). These results showed that ongoing GABA transmission in LH→PVH circuit contributes significantly to physiological feeding behavior. To test whether ongoing glutamatergic transmission from LH→PVH is required for stress-induced grooming, we used *Pdx1-Cre::Vgat^{flox/flox}* mice expressing eArchT3.0 in LH^{*Pdx1*} for photoinhibition experiments outlined in **Figure 17f** (also see **Figure 18d-e**). Baseline grooming levels during 556nm light inhibition was unaltered compared to mock inhibition trials with blue light (**Figure 17g**). In contrast, elevated grooming caused by water spraying the mice, a procedure known to elevate stress-related grooming²²⁹, was significantly attenuated with 556 nm vs. mock inhibition (**Figure 17h**). At the same time, feeding behavior was not significantly affected by light condition following water spray (**Figure 17i**).

Antagonistic control of feeding and grooming by LH→PVH projections

We next sought to determine if activity level of GABAergic or glutamatergic action in this circuit could drive competition between the two behaviors. To probe whether activation of the grooming component (i.e., glutamatergic transmission) competes with fast-refeeding, we fasted *Pdx1-Cre::Vgat^{flox/flox}* mice expressing ChR2 in LH^{*Pdx1*} neurons (**Figure 19a-d**), and re-fed them for 30 minutes under either mock or blue light stimulation of LH^{*Pdx1-ChR2*}→PVH fibers (**Figure 20**). Fasted mice with mock stimulation (Fasted + Mock stim) showed a significant increase in food intake compared to that in the Fed + Mock stimulation condition (**Figure 20c**). However, the time spent grooming between these two conditions were similar, and constituted less than 7% of the total testing time (**Figure 20b**). On the other hand, activation of LH^{*Pdx1-ChR2*}→PVH fibers with 5 Hz, 100 ms blue light pulses during the fasted state (Fasted + Light-on) led to a significant increase in time spent grooming (56.6 ± 6.58 percent time spent grooming \pm s.e.m.; **Figure 20a**), and was accompanied by a

corresponding decrease in food consumption (0.02 ± 0.01 grams \pm s.e.m.) compared to the Fasted + Mock stim condition (0.26 ± 0.05 grams \pm s.e.m.; **Figure 20c**). These data suggest

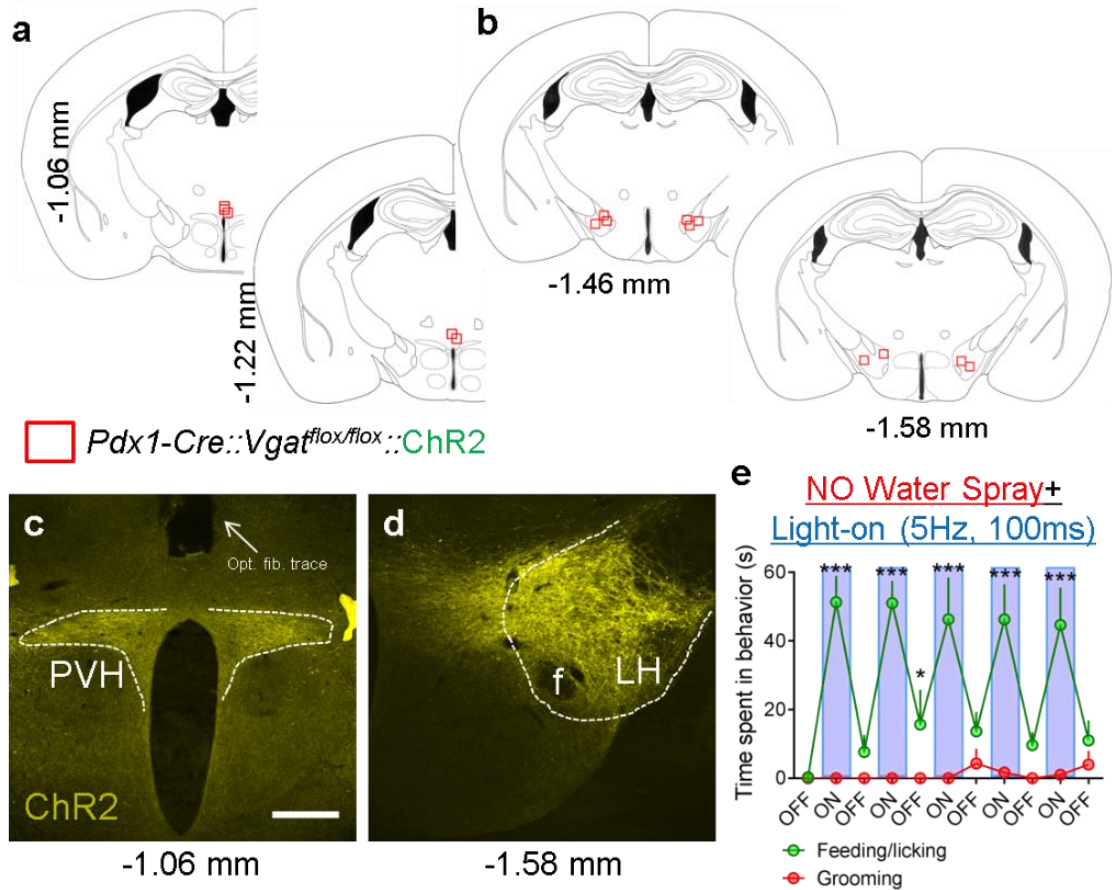


Figure 19. ChR2 expression in LH neurons and PVH projection fibers in *Pdx1-Cre::Vgat^{flox/flox}* used in fast-refeeding competition experiments, and photostimulation of LH→PVH GABAergic terminals strongly promotes feeding. (a-d) Post-hoc analysis of optic fiber placements and LH injection sites for *Pdx1-Cre::Vgat^{flox/flox}::ChR2* mice used for competition experiment in Figure 20a-c. Verification of optic fiber placements above PVH (a) and successful targeting of ChR2 to LH (b). Representative images show ChR2 expression in fibers projecting to PVH and optic fiber trace above PVH (c) and approximate injection site of ChR2 to LH region (d). f, fornix; LH, lateral hypothalamus; PVH, paraventricular hypothalamus. Scale bar = 300 μ m. (e) *Pdx1-Cre::Vgat^{flox/flox}::ChR2* mice (related to Figure 20d-f) consistently spend most of a one-minute block feeding when laser is turned on (473nm; 5Hz, 100ms), while showing little to no increase in grooming behavior regardless of light epoch. Each Off-On epoch lasted one minute each for eleven consecutive minutes.

that fast-refeeding can be antagonized by self-grooming behavior induced by activation of LH→PVH glutamatergic inputs.

To genetically dissect the effects of grooming during GABAergic LH→PVH stimulation, we used *Pdx1-Cre::Vglut2^{flox/flox}* mice that received ChR2 injections to LH and optic fibers implanted above PVH. We water sprayed the mice to evoke extensive self-grooming. After water spray, mice were placed in a bare cage for eleven minutes under mock stimulation

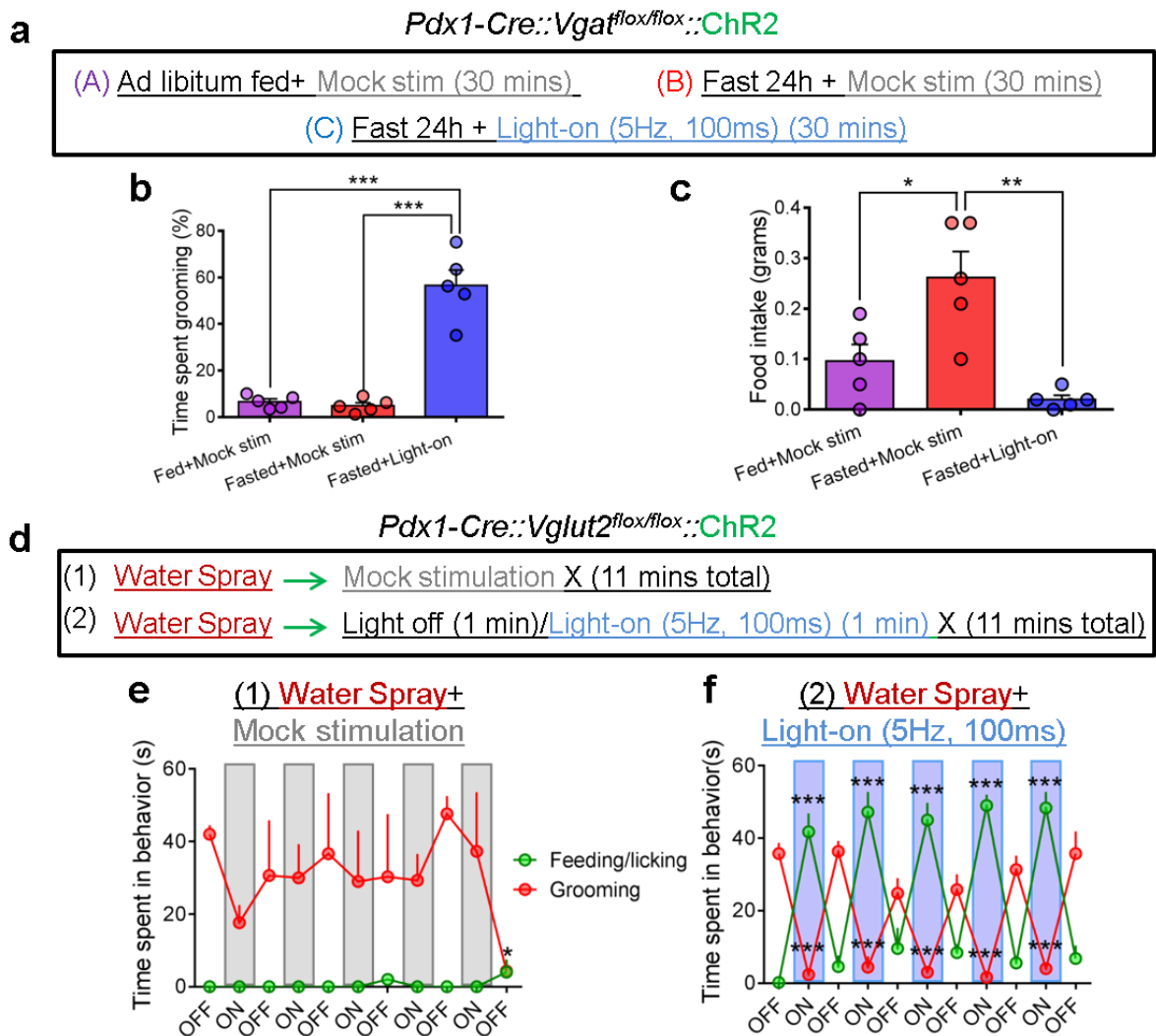


Figure 20. Antagonistic control of feeding and self-grooming by GABAergic and glutamatergic LH^{Pdx1}→PVH fibers. (a) Experimental design for testing effects of glutamatergic LHPdx1-ChR2→PVH fiber photostimulation on grooming and refeeding after a fast. (b) The percentage of time spent grooming during three 30 min trials. (c) Food intake during the same three trials. (d) Experimental protocol to test whether photostimulation of GABAergic LHPdx1-ChR2 →PVH fibers interferes with grooming induced by water spray. (e) Time spent engaged in grooming or feeding/licking behaviors during mock stimulation (n = 3). (f) Time spent grooming or feeding/licking during light-on condition, where 5 Hz, 100ms light pulses were applied every other minute (n = 5).

conditions (**Figure 20d**). Water spray reliably induced approximately ten minutes of continuous grooming behavior, and had no effect on feeding related behaviors (**Figure 20e**). In a separate trial where mice were water sprayed and then paired with photostimulation of LH^{Pdx1-ChR2}→PVH (continuous 5 Hz, 100 ms, 473 nm applied every other minute), grooming behavior was dramatically suppressed, and was accompanied with a concomitant elevation in feeding behavior (**Figure 20f**). Strikingly, the light effect on grooming and feeding behaviors was rapidly reversed during the light-off epochs, such that mice immediately stopped eating, and reverted back to grooming (**Figure 20f**). Of note, the rapid elevation in grooming during the light-off periods was not due to post-light effects (**Figure 19e**). Together, these data show that activation of GABAergic LH→PVH fibers antagonizes stress-related grooming and promotes feeding behavior.

Activation of PVH neurons on self-grooming versus feeding

The above data suggested that the activity level of PVH neurons determines feeding versus self-grooming behaviors. To directly test this, we bilaterally delivered **AAV-FLEX-ChR2-EYFP** to PVH of *Sim1-Cre* mice (PVH^{Sim1-ChR2}; **Figure 21a, 21b, and Figure 22**). Whole cell electrophysiological recordings in acute brain slices showed that blue light pulses reliably excited PVH^{Sim1-ChR2} neurons (**Figure 22f**). Our previous studies showed that glutamate release from PVH was essential in mediating PVH function in body weight regulation⁵⁷. As such, we also included *Sim1-Cre::Vglut2^{flox/flox}* mice in the following optogenetic studies. Recapitulating results from LH^{Pdx1-ChR2}→PVH fiber photostimulation, 5 Hz, 10 ms blue light stimulation in PVH^{Sim1-ChR2} neurons evoked repetitive self-grooming behavior in *Sim1-Cre* mice (**Figure 21c**). However, *Sim1-Cre::Vglut2^{flox/flox}* mice exhibited significant blunting of grooming behavior with the same light stimulation (**Figure 21c**). The elevation in grooming behavior induced by photostimulation was absent in *Sim1-Cre* mice receiving **AAV-FLEX-GFP** viral injections to PVH (**Figure 23**). To examine the effect of PVH neuron activation on

feeding and grooming behaviors, both groups of mice were fasted for 24 hours, then re-fed for eleven minutes with blue light stimulation (5 Hz, 10 ms, 473 nm, every other minute).

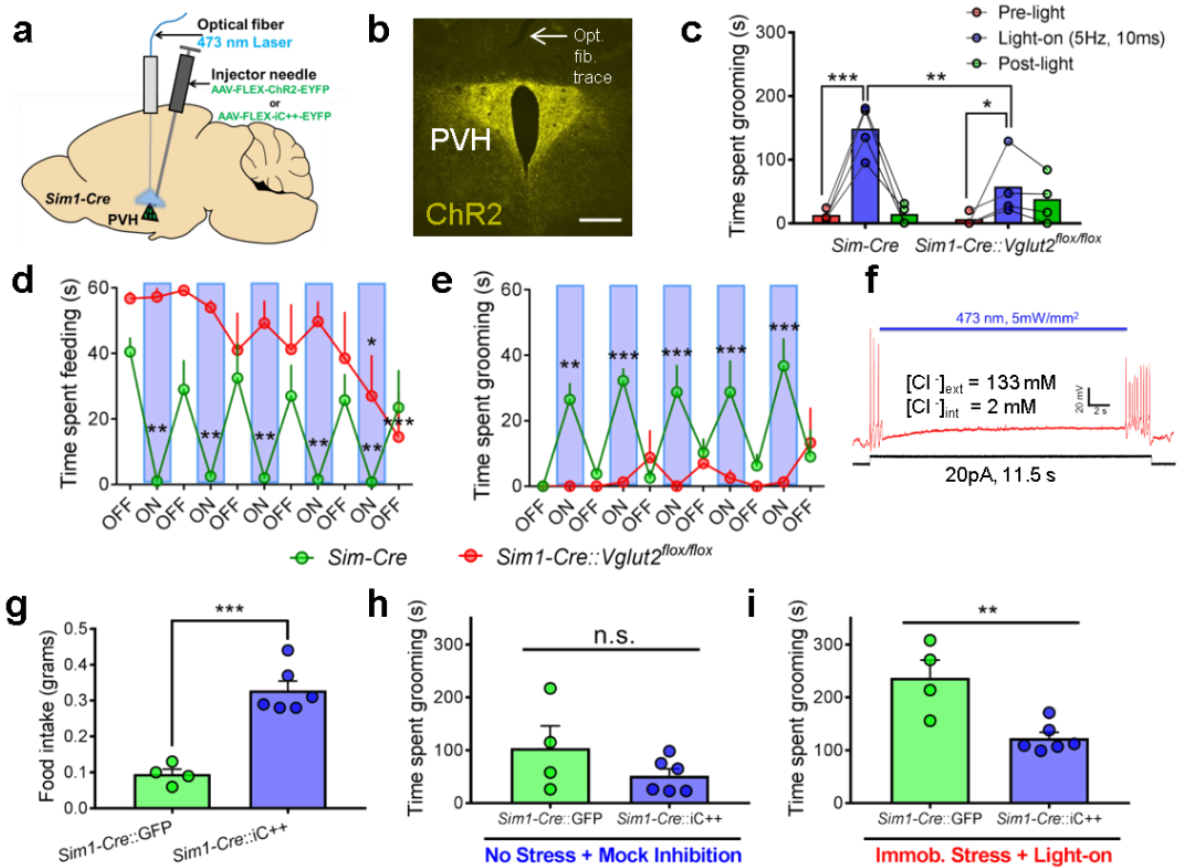


Figure 21. Photostimulation of PVH^{Sim1} neurons induces grooming behavior and competes with fast-refeeding, and inhibition increases feeding and reduces stress-induced grooming. (a) Experimental schematic. (b) ChR2-EYFP expression in PVH^{Sim1} neurons and optical fiber implantation (opt. fib. trace, arrow) above PVH. Scale bar = 300 μ m. (c) Grooming time before (pre-light), during (light-on), and after (post-light) 5 Hz, 10 ms photostimulation of PVH^{Sim1}-ChR2 neurons in Sim1-Cre (n=4) and Sim1-Cre::Vglut2^{flox/flox} (n=4) mice. (d) Time spent feeding after a fast during alternating, 1 minute-light off/on events in Sim1-Cre (n=4) and Sim1-Cre::Vglut2^{flox/flox} (n=4) mice (light-on = 5Hz, 10ms). (e) Time spent grooming in the same experiment. (f) Silencing PVH^{Sim1}-iC++ neurons with blue light blocks action potentials induced by depolarizing current injection. Figure used with permission from Yungang Lu. (g) 30 min food intake during optical inhibition of PVH with blue light in Sim1-Cre::GFP control and iC++ mice. (h) Time spent grooming during 15 mins of mock inhibition following no acute stress in the same mice. (i) Time spent grooming during 15 mins of blue-light inhibition following 10 mins of immobilization stress in the same mice.

Sim1-Cre mice showed persistent repetitive self-grooming and suppressed feeding during light-on periods. During light-off periods, the mice rapidly switched to feeding and displayed

minimal grooming (**Figure 21d-e**). In contrast, *Sim1-Cre::Vglut2^{flox/flox}* mice did not have light-associated grooming behavior and fed regardless of light condition (**Figure 21d-e**). These results suggest that an increased level of PVH neuron activity promotes self-grooming and

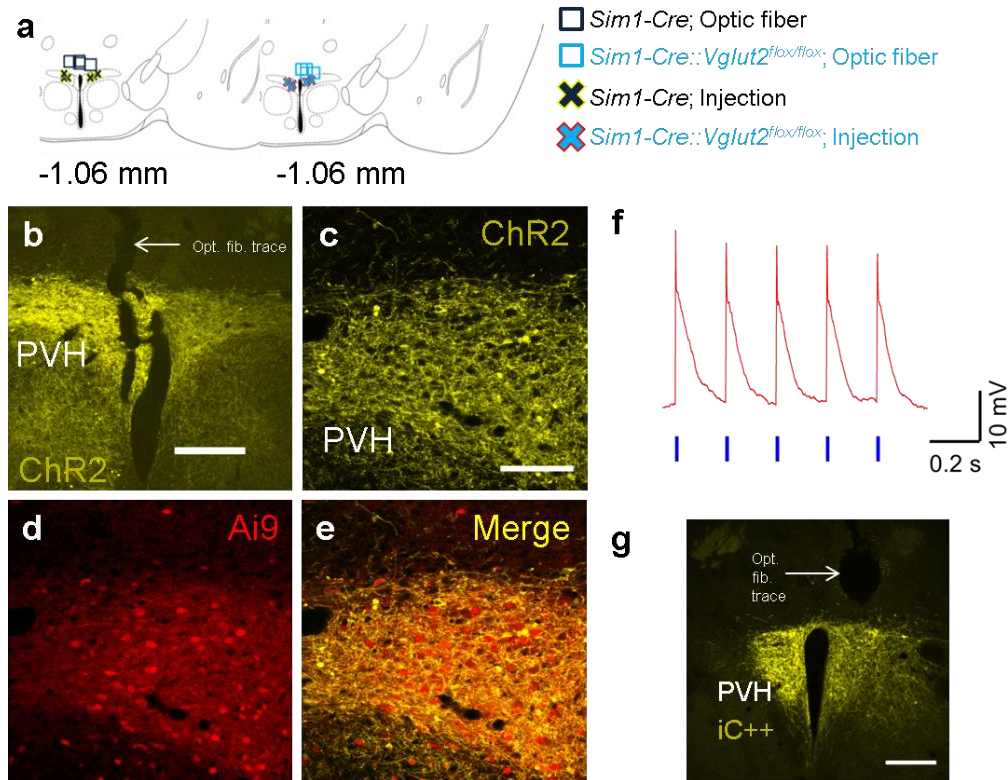


Figure 22. ChR2 and iC++ expression in PVH^{Sim1} neurons of *Sim1-Cre* and *Sim1-Cre::Vglut2^{flox/flox}* mice. (a) Post-hoc analysis in brains of mice used in **Figure 21b-e** shows approximate injection locations of ChR2 in PVH and optical fiber implantation above PVH. Dark blue box and light blue box indicate optical fiber placements in *Sim1-Cre* and *Sim1-Cre::Vglut2^{flox/flox}* mice, respectively; dark blue X and light blue X indicate approximate ChR2 injection sites in *Sim1-Cre* and *Sim1-Cre::Vglut2^{flox/flox}* mice, respectively. (b) Representative image from a *Sim1-Cre::Vglut2^{flox/flox}* mouse showing ChR2 expression in caudal PVH and optical fiber placement above the same region. Scale bar = 300 μ m. (c-e) Representative image from a *Sim1-Cre::Ai9* reporter mouse with ChR2 expression in PVH region. Close-up of PVH showing ChR2-eYFP fluorescence (c) and Ai9-RFP fluorescence (d). Merged image (e) shows ChR2 expression encircles the membranes of Ai9-positive cells. Scale bar = 100 μ m. (f) Whole-cell current clamp traces in ChR2-positive PVH^{Sim1} cells in response to 5 Hz, 10ms blue light pulses (blue ticks = 10ms light pulse). Figure used with permission from Yungang Lu. (g) iC++-EYFP expression in PVH^{Sim1} neurons and optical fiber implantation above PVH. Scale bar = 300 μ m.

inhibits feeding in a glutamate release-dependent manner. We next probed whether optogenetically inhibiting PVH^{Sim1} neurons would affect feeding and grooming. To this end,

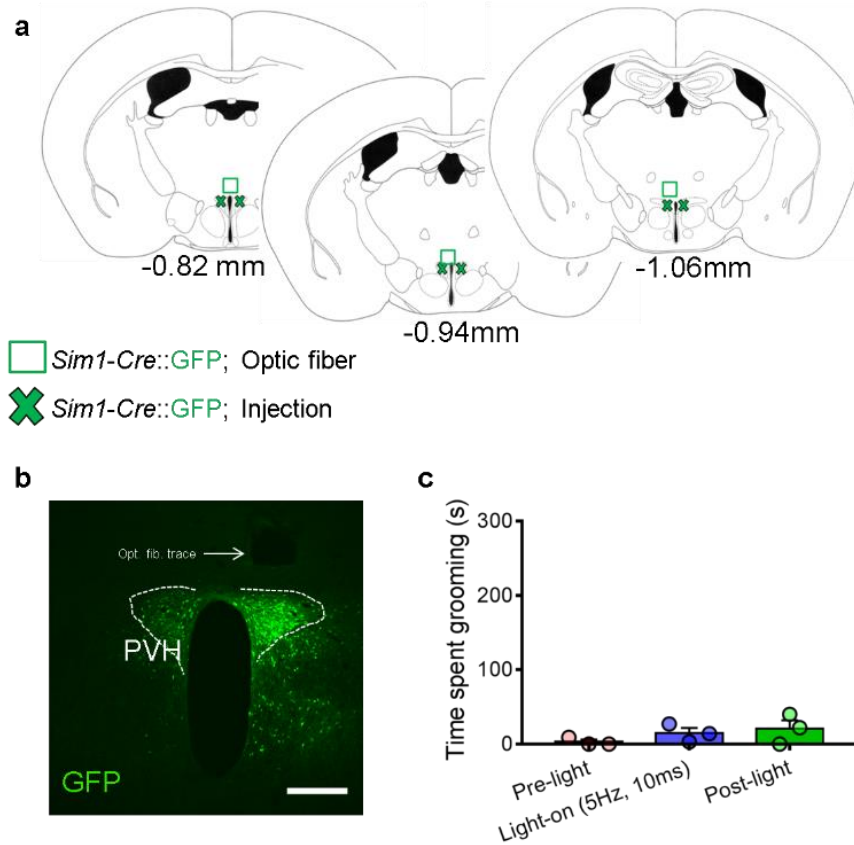


Figure 23. Photostimulation of PVH^{Sim1-GFP} neurons does not increase grooming behavior. (a) Shows approximate optic fiber placements (green outlined boxes) and cre-dependent GFP injection sites (green X's) in *Sim1-Cre* mice used for behavioral experiments in (c). (b) Representative image of a *Sim1-Cre* mouse showing GFP expression in PVH and optic fiber placement above the same region. Scale bar = 300 μm. (c) *In vivo* optical stimulation (5Hz, 10ms) of PVH^{Sim1-GFP} neurons does not lead to increased grooming behavior compared to pre- and post-light epochs (repeated measures ANOVA; light epoch $F(2, 4) = 2.329, P = 0.2134$). Each epoch lasted 5 mins for a total of 15 consecutive minutes. Data are presented as \pm s.e.m.

Sim1-Cre mice were injected with **AAV-FLEX-iC++-EYFP** vectors to allow expression of the inhibitory channel iC++²³⁰ in PVH neurons (Figure 22g). Patch clamp experiments showed that blue light inhibited firing of PVH neurons in *Sim1-Cre::iC++* mice (**Figure 21f**). Acute inhibition of PVH^{Sim1} caused a significant increase in food intake compared with GFP-injected controls (**Figure 21g**). Furthermore, elevated grooming induced by immobilization stress was significantly attenuated in *Sim1-Cre::iC++*, compared to GFP controls during blue-light inhibition (**Figure 21i**). The shortened grooming response in iC++ mice was not due to differences in baseline levels of grooming compared to GFP controls (**Figure 21h**).

These data support that overall activity of PVH neurons significantly participates in normal feeding and stress-related grooming behaviors, and further reinforce the idea that LH→PVH projections regulate both feeding and self-grooming behaviors by modulating PVH neuron activity.

In addition to PVH, LH neurons are known to project to lateral habenula and ventral tegmental area (VTA)^{110, 111}. To examine whether PVH-projecting LH neurons also send collaterals to these brain regions, we used a previously established pseudorabies viral tracing method¹⁹⁷ to label PVH-projecting LH neurons with GFP. While we observed some GFP-labeled fibers in the dorsomedial hypothalamus and LH, none was found in lateral habenula or VTA (**Figure 24**), suggesting that PVH-projecting LH neurons do not send significant collaterals to lateral habenula or VTA.

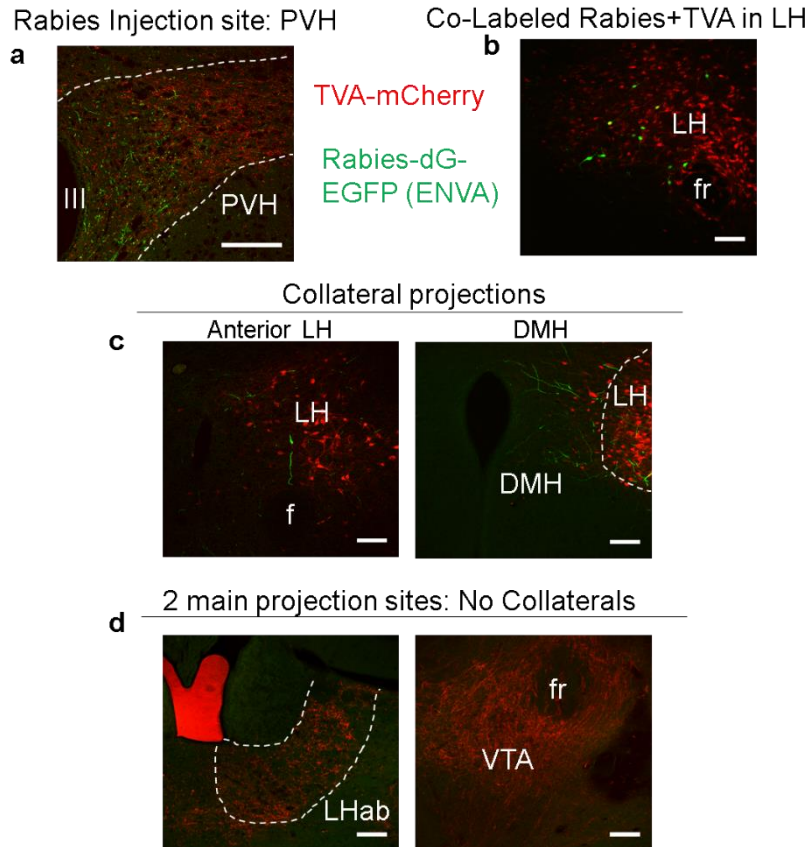


Figure 24. PVH projecting LH neurons do not send collaterals to lateral habenula or VTA. Using *Pdx1-Cre* mice, we performed rabies terminal mapping study to assess the degree of collateralization of LH→PVH to other structures. Using the same protocol as described in previous studies (Betley et. al. Cell 2013 and Garfield et. al. Nat. Neurosci. 2015), we first delivered AAV-FLEX-TVA-mCherry to the LH of *Pdx1-Cre* mice, and 4 weeks later, delivered pseudotyped rabies virus deltaG to the PVH. As shown in panels **a** and **d**, TVA-expressing fibers were found in all known LH projection sites including PVH, lateral habenula and VTA. Importantly, abundant GFP-expressing fibers were also found in the PVH (panel **a**), confirming successful delivery of rabies virus in the PVH. As expected, a subset of LH neurons expressed GFP (panel **b**). However, no apparent GFP-expressing fibers were found in either lateral habenula or VTA (panel **d**). Interestingly, rare GFP-expressing fibers were found in the DMH and LH (panel **c**). These results suggest that the PVH-projecting LH neurons send an insignificant amount of collaterals to other projection sites. fr: fornix; III: 3rd ventricle; PVH:paraventricular hypothalamus; LH: lateral hypothalamus; DMH: dorsomedial hypothalamus; Lhab: lateral habenula; VTA: ventral tegmental area.

Discussion

The etiology of compulsive behaviors and their association with feeding abnormalities remains poorly understood^{202, 221}. Previous studies on the pathophysiology of compulsivity and related disorders mainly focus on forebrain regions^{202, 221, 222, 231}. Our results showed that parallel GABAergic and glutamatergic LH→PVH projections can differentially promote feeding versus repetitive self-grooming by modulating PVH neuron activity. While simultaneous activation of both projections induced mixed feeding and self-grooming, selective activation of one blocked the behavior mediated by the other, demonstrating an antagonistic regulation of these two behaviors by LH→PVH projections. Thus, our study defines previously unknown hypothalamic circuit capable of promoting two competing behaviors, i.e. feeding and self-grooming behavior, and provides a framework for the LH→PVH pathway as a potentially important brain mechanism underlying eating disorders associated with compulsivity.

The use of *Pdx1-Cre* mouse line in our study offers a number of advantages over *Vglut2-Cre* and *Vgat-Cre*. This unique model allowed us to gain access to both LH glutamate and GABA neurons, thus allowing simultaneous activation of LH→PVH GABAergic and glutamatergic terminals. With this dual activation, we identified a common subset of PVH neurons that receive monosynaptic glutamatergic and GABA inputs from LH neurons. The model also allowed the ability to show differential behavioral outcomes with optogenetic activation of the mixed glutamatergic and GABAergic LH→PVH terminals using differing strengths of light stimulation, suggesting neurotransmitter competition for behavior within the LH→PVH circuit. The combinational use of *Pdx1-Cre* with floxed *Vglut2* and *Vgat* alleles also allows specific disruption of glutamate and GABA release and demonstration of the role of the individual neurotransmitters without competing effects from the other. Furthermore, use of *Pdx1-Cre* facilitated genetic confirmation of functional PVH contribution, via *Sim1-Cre*

mediated $\gamma 2$ deletion, in mediating LH→PVH in feeding. Notably, the baseline readings of feeding and self-grooming, two major behaviors that were monitored in this study, were not altered in these knockout mice. Thus, the impact of potential developmental alterations associated with gene knockouts, if it exists, minimally affects our data interpretation.

We discovered that activation of glutamatergic LH→PVH terminals caused extensive, repetitive self-grooming, suggesting a high level of compulsivity. The induced self-grooming behavior was shown to be stress-related, which is consistent with previous observations on the role of LH orexin and leptin responsive neurons in increasing stress levels²³². Remarkably, the evoked repetitive self-grooming behavior consistently overrode extreme hunger-induced feeding following 24 hour fasting. Thus, LH→PVH glutamatergic projection activation produced a phenotype analogous to the maladaptive behaviors often described in human anorexia nervosa, which consist of obsessive thoughts surrounding body weight, compulsive exercise, and extreme eating aversion associated with long-term self-induced starvation²³³⁻²³⁶. Importantly, inhibition of both glutamatergic transmission from LH to PVH and PVH neurons reduced extensive self-grooming behavior induced by stress, suggesting an involvement of activation of PVH neurons by increased glutamate release from the LH in the etiology of stress-related self-grooming. In humans, many forms of compulsive behaviors, including eating disorders, co-exist with higher levels of stress^{169, 237}. Thus, chronic activation of LH→PVH glutamatergic projections may potentially serve as a model for compulsive anorexia in humans.

In addition to feeding behavior, LH→PVH GABAergic projections also promoted feeding-related behaviors in the absence of food, such as licking and chewing up bedding, suggesting an increased level of impulsivity and an uncontrolled drive to eat. Similar aberrant feeding-associated behaviors were also observed during activation of LH→VTA GABAergic projections and LH GABAergic neurons^{111, 238}. This feeding behavior is distinct

from that mediated by AgRP neuron activation, which shows a specific effect toward foraging and feeding, and is not associated with aggressive licking or chewing^{164, 165, 239}. Our data revealed that mice displayed behavioral approach to a side of a test chamber paired with GABAergic LH→PVH activation. In line with this, recent results show that AgRP GABAergic inputs to both LH and PVH are also associated with positive reinforcement¹⁶³. The positive valence associated with LH→PVH-induced feeding may escalate the drive for feeding and its related behaviors. Thus, chronic activation of LH→PVH GABAergic projections may contribute to conditions characterized by uncontrolled overeating.

One striking finding in this study is that LH→PVH glutamatergic projections were in parallel with LH→PVH GABAergic projections. Our findings suggest that short duration stimulation of mixed glutamatergic and GABAergic LH→PVH projections may preferentially activate glutamatergic components and increase PVH neuron excitability, leading to self-grooming, while long duration stimulation may cause a net GABAergic action and reduce PVH neuron activity, leading to feeding. Importantly, we found that the net effect of changing PVH neuron activity swiftly changed behavioral outcomes. Elevating PVH neuron activity by photostimulating PVH^{Sim1-ChR2} neurons caused repetitive self-grooming and inhibited feeding within seconds even during extreme hunger induced by fasting. Similarly, photostimulation of glutamatergic LH→PVH projections abruptly suppressed feeding after a fast, and induced self-grooming. In contrast, inhibiting PVH neuron activity caused the opposite effect, causing increased feeding and attenuation of stress-induced grooming. Consistently, activation of GABAergic projections in LH→PVH circuit potently disrupted repetitive grooming induced by water spray, and promoted feeding, an effect that was rapidly reversed upon photostimulation termination. Thus, acute changes in PVH neuron activity in response to dynamic GABAergic and glutamatergic inputs give rise to self-grooming or feeding. Unbalanced glutamatergic and GABAergic transmission to PVH may

underlie feeding disturbances associated with compulsivity. As LH→PVH-evoked feeding behavior is associated with positive reinforcement, and the evoked grooming is associated with stress, a typical negative reinforcement, these results suggest a scalable regulation of PVH neuron activity on emotional states.

Given the rapid switch between feeding and self-grooming by changing LH→PVH GABAergic and glutamatergic activity, or by acutely activating or inhibiting PVH neurons, it is likely that a shared PVH neuron population mediates the two behaviors. Supporting this, our data suggest that LH^{Pdx1} neurons send monosynaptic GABAergic and glutamatergic projections to a common subset of PVH neurons. Provided the established role of PVH melanocortin receptor 4 (MC4R)-expressing neurons in feeding regulation^{37, 51} these neurons present themselves as a candidate. Notably, MC4R and SAPAP3 double deletion rescues both hyperphagia from MC4R deficiency, and excessive self-grooming from SAPAP3 deficiency²²², raising a possibility that PVH MC4R-neurons contribute to this effect. Activation of PVH thyroxine releasing hormone (TRH) neurons promotes feeding but does not lead to self-grooming⁵⁸, an opposite effect that would be expected from LH→PVH glutamatergic activation. Thus, TRH neurons are an unlikely candidate. Notably, PVH neurons expressing corticotropin releasing hormones (CRH) might contribute to self-grooming behavior¹⁶⁸. Further studies are required to identify the exact subset(s) of PVH neurons that dynamically regulate feeding and self-grooming.

Feeding is essential for survival, and animals respond to fasting by consuming a large amount of food immediately when it becomes available to offset the energy deficit occurred during fasting periods. Despite the key importance of fast-refeeding responses, the neural pathway essential for this life-preserving behavior remains unclear. Thus far, AgRP neurons represent the prevailing group of neurons established in mediating fast-refeeding responses^{18, 21}. Our results showed that optogenetic inhibition of LH→PVH GABAergic

terminals strongly inhibited fast-refeeding and was robust and repeatable, suggesting that an active release of GABA in PVH mediates ongoing fast-refeeding. Thus, we identified LH GABAergic neurons as a novel population of neurons, alongside AgRP neurons, that are capable of governing fast-refeeding behavior. Supporting this, our previous studies showed that loss of GABA release from *Pdx1-Cre* neurons reduced fast-refeeding⁶⁴.

In summary, using a combination of optogenetics, mouse genetics, behavioral assays, and pharmacology, we identified a single LH→PVH projection with GABAergic and glutamatergic components that promote feeding and self-grooming behaviors, respectively. Importantly, dynamic PVH neuron activity changes regulated by glutamatergic and GABAergic inputs induced rapid and reversible transitions between feeding and self-grooming, raising an interesting possibility that defective LH→PVH activity may contribute to eating disorders associated with compulsive behaviors.

Chapter 3.
Defensive Behaviors Driven by a Hypothalamic-Midbrain Circuit

Summary

The paraventricular hypothalamus (PVH) regulates stress, feeding behaviors and other homeostatic processes, but whether PVH also drives defensive states remains unknown. We mapped PVH outputs that densely terminate in the midbrain-ventral tegmental area, and found that activation of the PVH→midbrain circuit produced profound defensive behavioral changes, including escape-jumping, hiding, hyperlocomotion, and learned aversion. Electrophysiological recordings showed excitatory post-synaptic input onto midbrain neurons via PVH fiber activation, and *in vivo* studies demonstrated that glutamate transmission from PVH→midbrain was required for the evoked behavioral responses. Using a dual optogenetic-chemogenetic strategy, we further revealed that escape-jumping and hiding required downstream activation of glutamatergic neurons in the midbrain. Population recordings using fiber photometry provided evidence that glutamatergic-midbrain neurons respond to fear-inducing situations by increasing activity. Taken together, our work unveils a novel hypothalamic-midbrain circuit that encodes defensive properties and may represent an essential component underlying stress-induced defensive responses.

Introduction

Defensive behaviors encompass a repertoire of hard-wired responses critical for survival in the animal kingdom²⁴⁰. Perceived threats prompt expression of fear, and result in escape behaviors, such as fleeing or freezing²⁴¹. Such behaviors are orchestrated by intricate neural networks, comprising multiple brain sites and likely redundant pathways²⁴². The hypothalamus is a complex structure that contains spatially distinct groups of neurons with diverse functions. The vast majority of research on the hypothalamus has historically focused on its role in homeostatic processes via endocrine or autonomic control. However, a growing body of literature suggests that specific hypothalamic sites not only generate innate defensive responses¹⁷², but also drive associated emotional states and learned responses to threat^{171, 243}. Thus, it is plausible that hypothalamic neural subsets that drive physiological adaptations also generate unique behavioral responses, allowing animals to effectively adjust to ever-changing circumstances in their environment.

The PVH has been classically described as a central hub for an array of autonomic and neuroendocrine functions essential for homeostasis²⁴⁴, and as a key output node for adapting internal metabolic activity to energy status⁴⁶. We have recently shown that the activity level of PVH neurons dictates feeding versus stress-related self-grooming, providing evidence that PVH may integrate information across several modalities to adjust emotional and behavioral output⁶¹. PVH neurons, especially those expressing corticotropin-releasing hormone (CRH), are critical in initiating hormonal and behavioral aspects of the stress response¹⁶⁸. Given that encountering various stressors is an integral part of ensuing changes in emotional states and behavior, it is possible that PVH neurons are involved in these processes. Supporting this, prior studies describe motivational and behavioral changes, including elicitation of defensive behaviors, following electrical stimulation of PVH area²⁴⁵⁻²⁴⁷. Notably, PVH neurons project to mesolimbic structures such as midbrain regions within and surrounding the ventral tegmental area (VTA)^{62, 248}, and recent studies showed

that PVH oxytocin-expressing neurons that project to the VTA play a role in pro-social behavior²⁴⁹. However, whether PVH neurons directly drive defensive behaviors is unknown.

The VTA and nearby regions, like the PVH, are composed of heterogeneously expressing neuron populations, including dopaminergic, GABAergic and glutamatergic neurons²⁵⁰. Dopamine neurons are well known for driving reward and a positive emotional state, while glutamatergic neurons have recently been shown to drive aversion²⁵⁰, a negative emotion state associated with fear and anxiety. Here, we uncover a pathway from PVH to the midbrain/VTA region that drives innate defensive behaviors, including escape, learned avoidance, and feeding suppression. Collectively, these findings represent a novel component of defensive neurocircuitry, and provide a potential link between negative emotions (stress and fear) and alterations in feeding behavior.

Results

Activation of PVH neurons elicits escape behavior associated with increased flight and negative valence

Through targeted manipulation of PVH neurons, we recently uncovered a novel hypothalamic site that bidirectionally controls feeding and repetitive, stress-like self-grooming⁶¹. Here, we aimed to explore and characterize other behavioral responses by manipulating PVH neural activity. To this end, we injected cre-dependent channelrhodopsin-2 (ChR2) viral constructs into the PVH of Sim1-Cre mice (Sim1-Cre::ChR2^{PVH}), allowing optogenetic manipulation of the majority of PVH neurons⁵⁰ (Figure 25A). Photostimulation with long pulses of blue light (100 ms) at 5 Hz reliably elicited time-locked activation of PVH neurons (Figure 25B). Similar to our previous findings, *in vivo* photostimulation of PVH neurons produced repetitive self-grooming in the majority of ChR2-expressing mice (Figure 25C), but not in GFP-injected controls (Sim1-Cre::GFP^{PVH}) (Figure 26A). The same

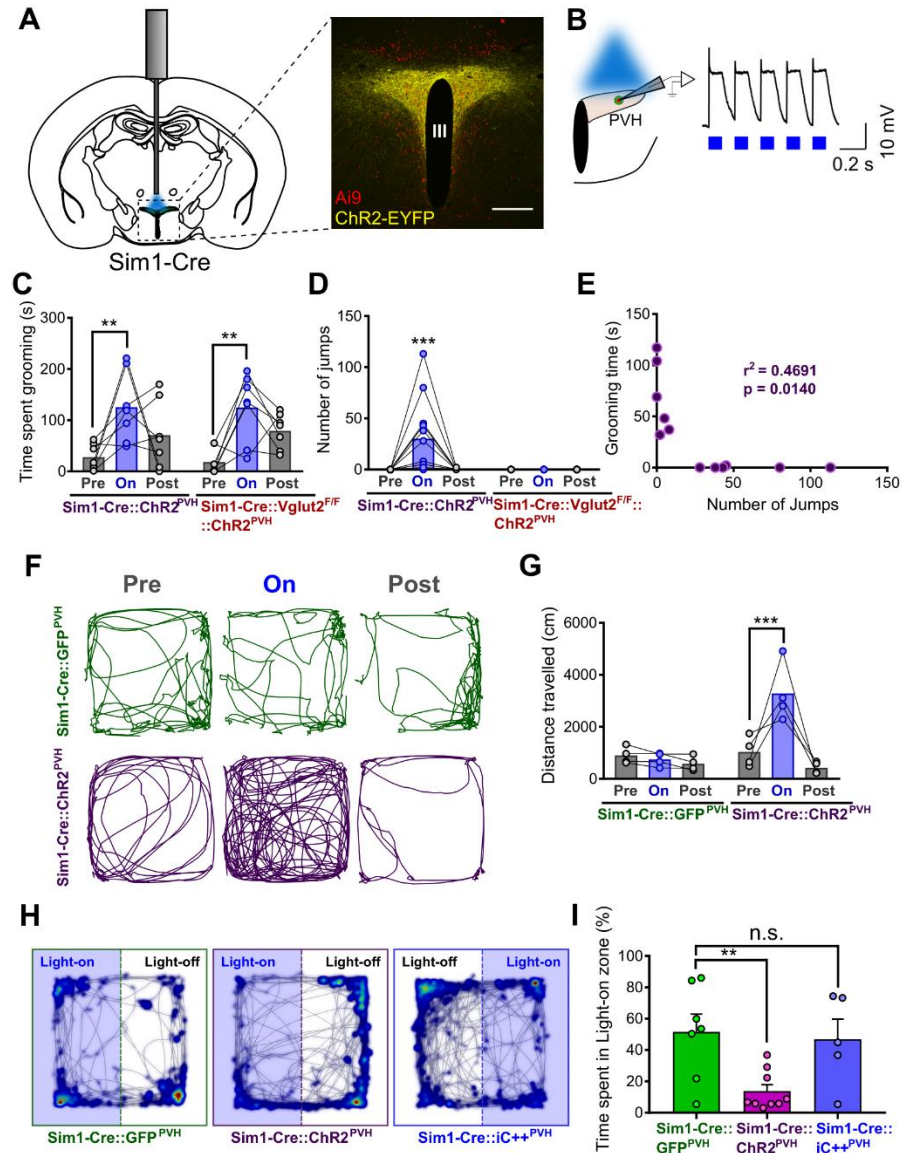


Figure 25. Optogenetic Activation of PVH Neurons Elicits Flight and Escape Behaviors. (A) Experimental schematic and ChR2-EYFP expression in Sim1-Cre::Ai9 cells in PVH. III, third ventricle. Scale bar, 300 μ m. (B) Whole-cell recordings in PVH-ChR2 neurons responding to 5 Hz-100 ms light pulses. Used with permission from Yungang Lu. (C) Quantification of time spent grooming in live animals during 5 Hz-100 ms photostimulation of PVH. (D) Number of jumps elicited by 5 Hz-100 ms photostimulation of PVH. (E) Correlation between grooming time and number of jumps in Sim1-Cre animals during 5 Hz-100 ms PVH photostimulation. (F) Representative locomotion traces before, during, and after 5 Hz-10 ms photostimulation of PVH. (G) Quantification of distance travelled during locomotion test (F). (H) Representative heatmaps of time spent in arena location overlaying activity tracks during Real Time Place Preference/Avoidance Assay (RTPP/A), where one side of the chamber was paired with PVH-photostimulation or inhibition. (I) Quantification of time spent in light-on zone during RTPP/A. Repeated measures 2-way ANOVA and 1-way ANOVA for statistical comparisons, ** $p < 0.005$, *** $p < 0.0005$. Error bars represent SEM.

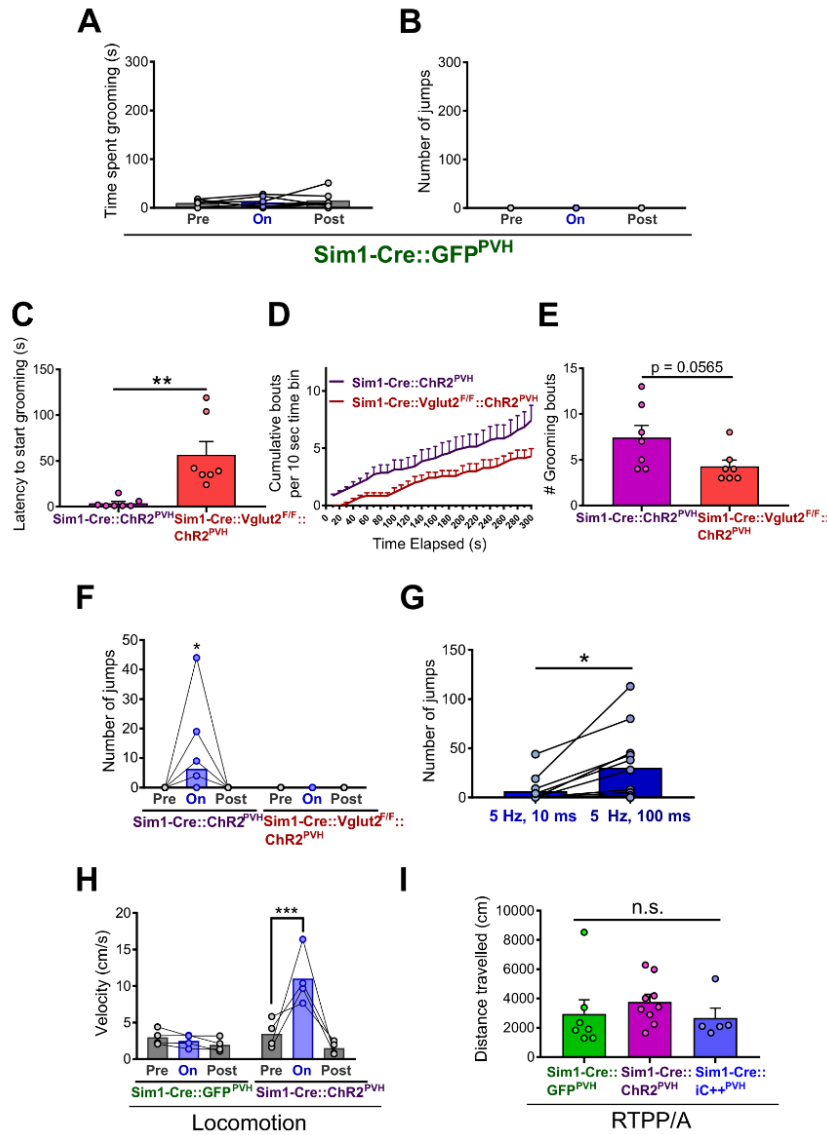


Figure 26. Photoactivation of PVH Neurons Drives Grooming, Escape-Jumping, and Flight. Related to Figure 25. (A) Time spent grooming before, during, and after 5 Hz-100 ms photostimulation of PVH in Sim1-Cre::GFP^{PVH} control mice. (B) Number of jumps counted before, during, and after 5 Hz-100 ms of PVH in control mice. (C) Latency to initiate grooming following the first pulse of light during a 5 minute PVH-photostimulation session. (D) Temporal representation of cumulative grooming bouts, calculated every 10 seconds, during 5 minutes of photostimulation. (E) Comparison of total number of grooming bouts between Sim1-Cre and Sim1-Cre::Vglut2^{F/F} animals during the 5 minutes of photostimulation. (F) Number of jumps counted during 5 minutes of PVH photostimulation with 5 Hz-10 ms pulses of light. (G) Comparison of the number of jumps evoked by 5 minutes of 5 Hz- 10 or 100 ms photostimulation in Sim1-Cre mice. (H) Average velocity during the locomotion assay in Figures 25F-G. (I) Comparison of distance travelled during the Real Time Place Preference/Avoidance Assay in Figures 25H-I. Unpaired or paired t-tests, repeated measures 2-way ANOVA, and 1-way ANOVA for statistical comparisons, *p<0.05, **p<0.005, ***p<0.0005. Error bars represent SEM.

photostimulation in Sim1-Cre::Vglut2^{F/F}::ChR2^{PVH} mice (also known as knockouts, KOs), which lacked vesicular glutamate transporter 2 (Vglut2, required for presynaptic glutamate release) in Sim1-neurons, showed a robust increase in repetitive grooming during light-on periods that was not significantly different than that seen in Sim1-Cre::ChR2^{PVH} mice (Figure 25C). However, self-grooming in Sim1-Cre::ChR2^{PVH} mice was notably more fragmented than in Sim1-Cre::Vglut2^{F/F}::ChR2^{PVH} mice. Notably, latency to initiate grooming after light illumination was significantly longer in KOs (Figure 26C), suggesting a potential role for slower-acting neuropeptides. We also noted a trend towards fewer grooming bouts in KOs (Figures 26D-E). These results suggest that glutamate release is not required for, but contributes significantly to the light-induced self-grooming⁶¹. Interestingly, however, we noted that 5 Hz-100 ms photostimulation elicited frantic escape-like jumping in the majority of Sim1-Cre::ChR2^{PVH} mice, but not in KO or GFP control animals (Figures 25D and 26B), whereas a shorter pulse duration (10 ms, 5Hz) elicited jumping responses in less than half of Sim1-Cre::ChR2^{PVH} mice tested (Figure 26F). Notably, jumping behavior increased in response to the longer length of light-pulses (Figure 26G), indicating scalability of the behavior via strength of neural activation. We also observed that some Sim1-Cre::ChR2^{PVH} mice displayed only grooming or jumping to the exclusion of the other, while others showed a mix of behaviors during the photostimulation session. In fact, we noted a negative correlation between the two behaviors (Figure 25E), consistent with the mutually exclusive nature of such behaviors. We also found that photostimulation in Sim1-Cre::ChR2^{PVH} mice dramatically increased overall locomotion compared to controls, affecting both total distance travelled (Figures 25F-G) and average velocity (Figure 26H), suggesting an elevated state of arousal and agitation. We next probed the emotional valence of PVH activation using a real-time place preference/avoidance assay (RTPP/A)²⁵¹. Compared to GFP controls, Sim1-Cre::ChR2^{PVH} mice avoided the light-paired side of the testing chamber, though total distance travelled was unchanged (Figures 25H-I and Figure 26I). As an additional

comparison, we tested the valence of inhibiting PVH neurons in the RTPP/A assay by using Sim1-Cre mice injected with cre-dependent inhibitory opsin, iC++ (Sim1-Cre::iC++^{PVH})^{61, 230}. Surprisingly, inhibition of PVH neurons did not elicit significant preference or avoidance to the light-paired side (Figures 25H-I), which was previously shown to promote feeding and reduce stress-induced grooming⁶¹. Collectively, these results indicate that glutamate release from PVH neurons drive a scalable increase in escape behavior, while both glutamate and non-glutamate action contribute to self-grooming.

PVH projections to the midbrain area drive escape behavior and avoidance

To probe potential PVH targets for the observed behaviors, we injected cre-dependent, synaptophysin constructs (AAV-FLEX-Syn::EGFP) to PVH neurons of Sim1-Cre mice for anterograde tracing²²⁸ (Figures 27A-B). We observed dense projections in previously reported sites, such as the median eminence (ME), periaqueductal gray (PAG)/dorsal raphe (DR), parabrachial nucleus (PBN), and locus coeruleus (LC) (Figure 28). Interestingly, we observed substantial puncta in the midbrain area, both within and surrounding the VTA, most notably in the area medial to VTA and above the mammillary nucleus (supramammillary nucleus, SUM) and caudally into the VTA area (thereafter called midbrain) (Figures 27C and 28B-C). Puncta were in close proximity to tyrosine-hydroxylase (TH) positive neurons in the VTA, indicating possible connections with dopaminergic neurons (Figure 27C). To evaluate functional connectivity, we photostimulated local PVH^{Sim1-ChR2} fibers in the midbrain (Figure 27D), which evoked time-locked, excitatory post-synaptic currents in midbrain neurons, indicating glutamatergic transmission (Figure 27E). Following PVH→midbrain photostimulation in live animals, we found that compared to GFP controls (Sim1-Cre::ChR2^{GFP->mdbrn}), Sim1-Cre::ChR2^{PVH->mdbrn} had a greater number of cFos-labeled neurons in the midbrain and SUM (Figures 27F-G). Fewer cFos-labeled cells were detected in the VTA region proper (Figure 27F, bottom), which overlapped with very few TH+ cells

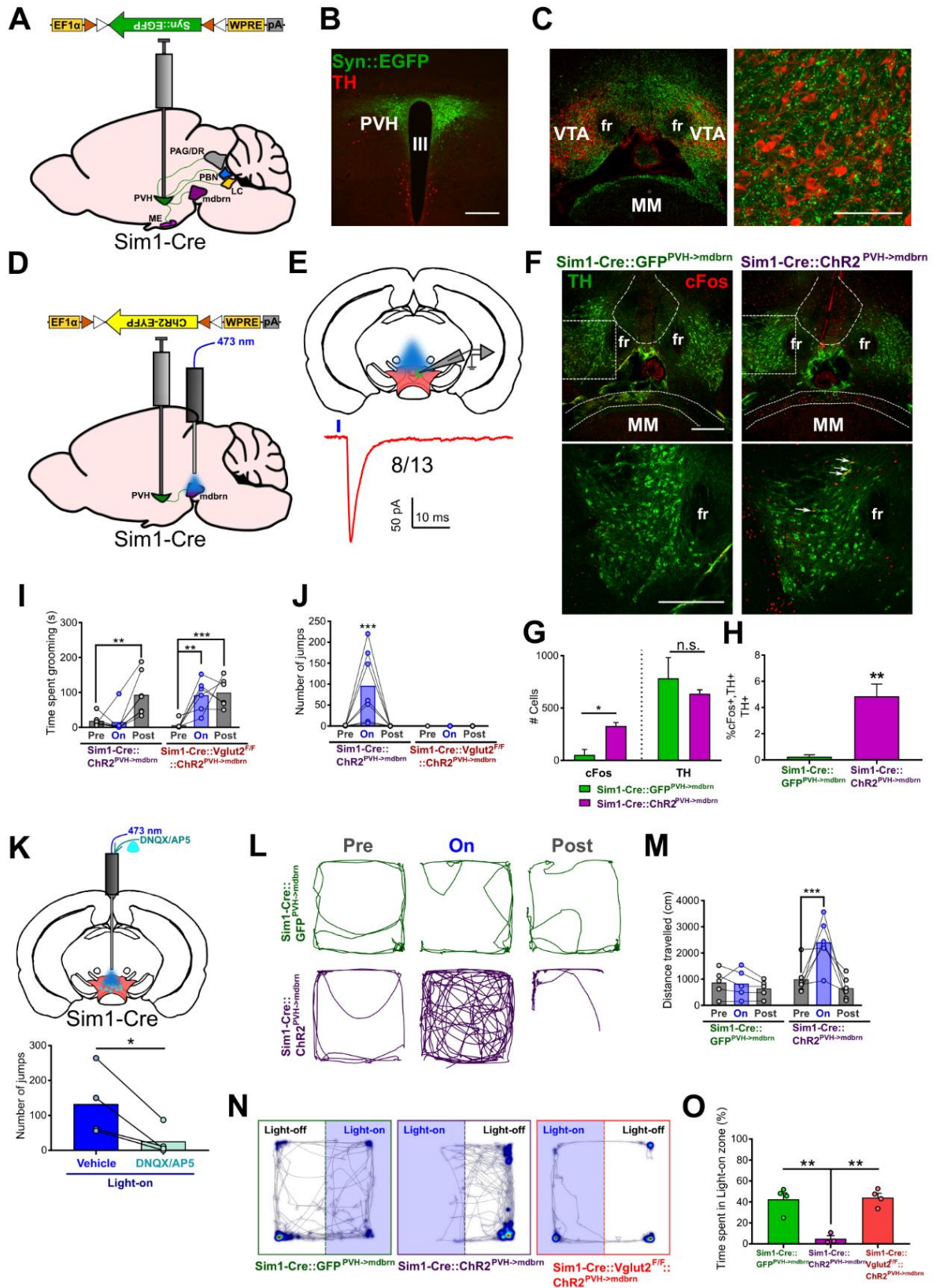


(Figure 27H), consistent with tracing results showing a substantial portion of PVH

Figure 27. Glutamatergic Transmission from PVH to Midbrain Drives Flight and Escape. (A) Anterograde tracing schematic showing downstream sites targeted by PVH projections. (B) Synaptophysin-EGFP expression in PVH neurons. III, third ventricle; PVH, paraventricular hypothalamus. Scale bar, 300 μ m. (C) Synaptophysin-EGFP puncta seen in VTA and adjacent midbrain regions (left). Higher magnification showing puncta in close proximity to tyrosine-hydroxylase (TH) positive neurons (right). fr, fasciculus retroflexus; MM, medial mammillary nucleus; VTA, ventral tegmental area. Scale bar, 100 μ m. (D) Optogenetic activation schematic of PVH \rightarrow midbrain circuit. (E) Schematic of whole cell recordings (top) showing light-evoked excitatory post synaptic current trace in VTA/midbrain neuron (bottom). Red trace is representative of 8/13 neurons showing oEPSCs. 5/13 neurons showed no response. Holding potential = -70 mV. Figure used with permission from Yungang Lu. (F) Coronal brain slice images of cFos and TH staining in GFP and ChR2 mice receiving PVH \rightarrow midbrain photostimulation prior to sacrifice. Bottom panels represent higher magnification of dashed rectangular area shown in top panels. Arrows point to cells with co-localization of cFos and TH. Scale bars, 300 μ m. (G) Quantification of number of cells showing cFos and TH staining in GFP and ChR2 mice. (H) Quantification of cells showing dual staining of cFos and TH, with respect to total number of TH cells. (I) Time spent grooming before, during, and after PVH \rightarrow midbrain photostimulation. (J) Quantification of number of jumps elicited by PVH \rightarrow midbrain photostimulation. (K) (Top) Schematic of pharmacological blockade of glutamate receptors in VTA/midbrain area prior to photostimulation in live animals. (Bottom) Number of jumps evoked by PVH \rightarrow midbrain photostimulation following microinjection of vehicle or glutamate receptor antagonists to midbrain. (L) Representative locomotion tracks in response to light activation of PVH \rightarrow midbrain circuit. (M) Distance travelled during locomotion assay in (L). (N) Representative heatmaps of time spent in each location superimposed over tracks during RTPP/A assay, where one side of chamber was paired with light activation of PVH \rightarrow midbrain. (O) Quantification of time spent in the light zone during RTPP/A assay. Repeated measures 2-way ANOVA, paired or unpaired t-tests, and 1-way ANOVA for statistical comparisons, * $p < 0.05$, ** $p < 0.005$, *** $p < 0.0005$. Error bars represent SEM. See also Figures 28 and 29.

projections terminating in the SUM and midline portions of VTA.

Empirically, we found that 20 Hz photostimulation of the PVH \rightarrow midbrain circuit in live Sim1-Cre::ChR2^{PVH \rightarrow mdbrn} animals resulted in the most obvious behavioral changes, including increased grooming behavior post-stimulation (Figure 27I), and escape-jumping similar to that seen with PVH photostimulation (Figure 27J). The same photostimulation failed to enact obvious repetitive grooming and escape-jumping in GFP controls (Figures 30A-B). In contrast, Sim1-Cre::Vglut2^{F/F}::ChR2^{PVH \rightarrow mdbrn} (KO) mice exhibited a significant increase in grooming during and after the photostimulation period, but showed no jumping behavior (Figures 27I-J). We found that microinfused glutamate receptor antagonists to the midbrain prior to photostimulation in Sim1-Cre::ChR2^{PVH \rightarrow mdbrn} mice significantly reduced the

escape-jumping in response to photostimulation (Figure 27K), confirming that midbrain neurons mediate the behavior. Similar to PVH activation, we also noted that photostimulation of PVH fibers in midbrain promoted locomotor activity in Sim1-

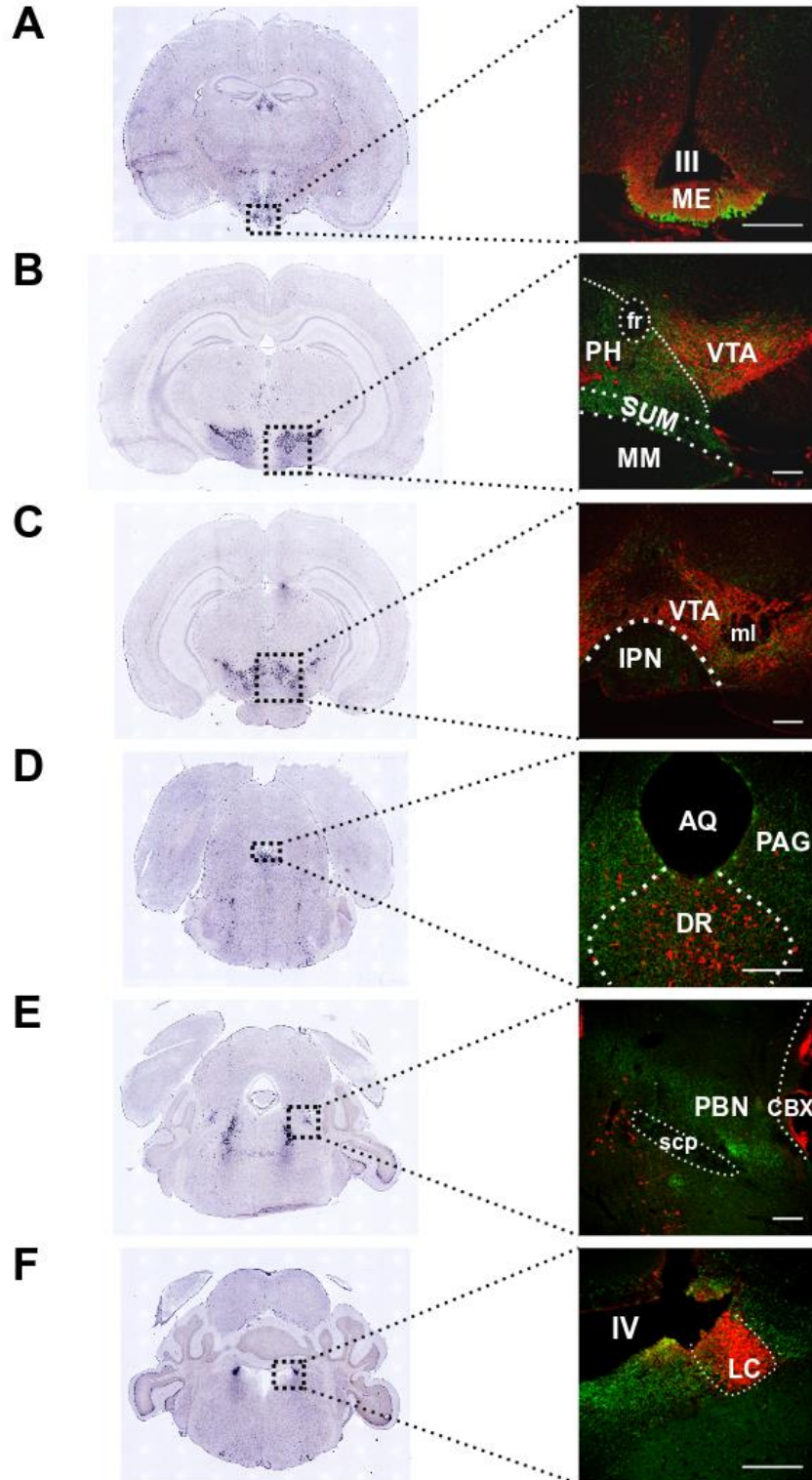


Figure 28. PVH Projections in Downstream Brain Sites. Related to Figure 27. Coronal brain slice images showing *in situ* hybridization for tyrosine hydroxylase (TH)¹ (left) and Synaptophysin-EGFP signal/immunostaining for TH (right). (A) Synaptophysin-EGFP puncta in the median eminence (ME). Scale bar, 200 μ m. (B) Synaptophysin-EGFP puncta in anterior section of VTA. (C) Synaptophysin-EGFP puncta in posterior section of VTA. (D) Synaptophysin puncta in the periaqueductal gray (PAG)/dorsal raphe (DR) region. (E) Synaptophysin signal in parabrachial nucleus (PBN). (F) Synaptophysin signal in locus coeruleus (LC). Scale bars, 200 μ m. III, third ventricle; IV, fourth ventricle; AQ, cerebral aqueduct, CBX, cerebellar cortex; IPN, interpeduncular nucleus; fr, fasciculus retroflexus; ml, medial lemniscus; MM, medial mammillary nucleus; PH, posterior hypothalamus; SUM, supramammillary nucleus; scp, superior cerebellar peduncles. *In situ* hybridization images were taken from the Allen Institute. www.alleninstitute.org, ID: Th – RP_Baylor_103073 – coronal.

Cre::ChR2^{PVH->mdbrn} mice, but not in GFP controls (Figures 27L-M and 29F) or KO mice (Figures 29C-E), suggesting an essential role for glutamate release in promoting locomotor activity.

Interestingly, we found that place avoidance caused by PVH→midbrain photostimulation in the RTPP/A assay required glutamatergic transmission (Figures 27N-O), but did not affect the total distance travelled during the assay (Figure 29G). These results suggest that glutamatergic transmission from PVH→midbrain promotes a state of negative valence, coupled by a drive for flight and escape.

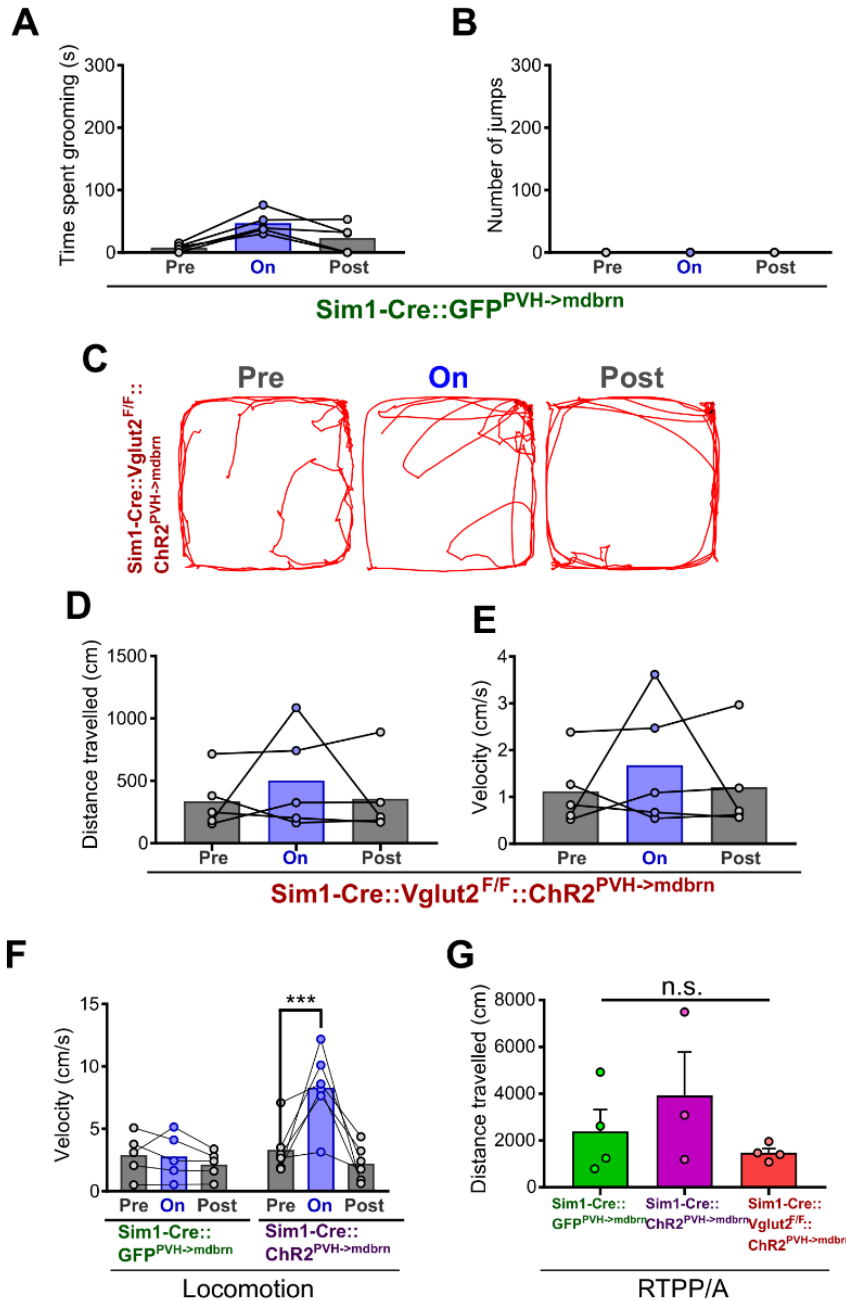


Figure 29. Photoactivation of PVH→Midbrain Circuit in Grooming and Locomotion. Related to Figure 27. (A) Time spent grooming in response to 20 Hz-10 ms photostimulation of PVH→midbrain circuit in GFP control mice. (B) Number of jumps evoked by 20 Hz-10 ms photostimulation in the same mice. (C) Locomotion tracks of *Sim1-Cre::Vglut2^{F/F}* mice before, during, and after 20 Hz-10 ms photostimulation in PVH→midbrain. (D) Quantification of distance travelled during locomotion assay in the same mice. (E) Average velocity during the locomotion assay in the same mice. (F) Average velocity during the locomotion assay in Figures 27L-M. (G) Distance travelled during Real Time Place Preference/Avoidance Assay (RTTP/A) in Figures 27N-O. Repeated measures or regular 1-way ANOVA, and repeated measures 2-way ANOVA for statistical comparisons ***p<0.0005, n.s.-Not Significant. Error bars represent SEM.

Activation of PVH→midbrain circuit suppresses food intake due to intense avoidance and promotes aversion learning

We previously demonstrated that photostimulation of PVH neurons abruptly halts ongoing feeding, and in turn promotes repetitive grooming, a phenomenon that was reversible upon light termination⁶¹. To examine whether place avoidance elicited by PVH neuron activation would alter fast-refeeding, we modified the RTPP/A assay by placing food in a corner of the light-paired side of the arena (Figure 30A). Following a 24h fast, GFP control mice approached the light-paired side of the chamber and proceeded to consume the food (Figures 30B-E, S4A). In contrast, ChR2 mice attempted to approach the food zone (Figure 31A), but spent significantly less time in the light-on side and food zone (Figures 30B-D), and consequently ate significantly less than controls (Figure 30E). Given that total locomotion during the assay was unchanged between groups (Figure 31B), together these data suggest that negative valence triggered by PVH photostimulation was sufficient to repel mice from an extremely salient goal, i.e., re-feeding after a long fast. We next performed the same assay on mice with photostimulation of local PVH fibers in midbrain, and similarly found that Sim1-Cre::ChR2^{PVH->mdbrn} mice spent significantly less time in the light-paired side

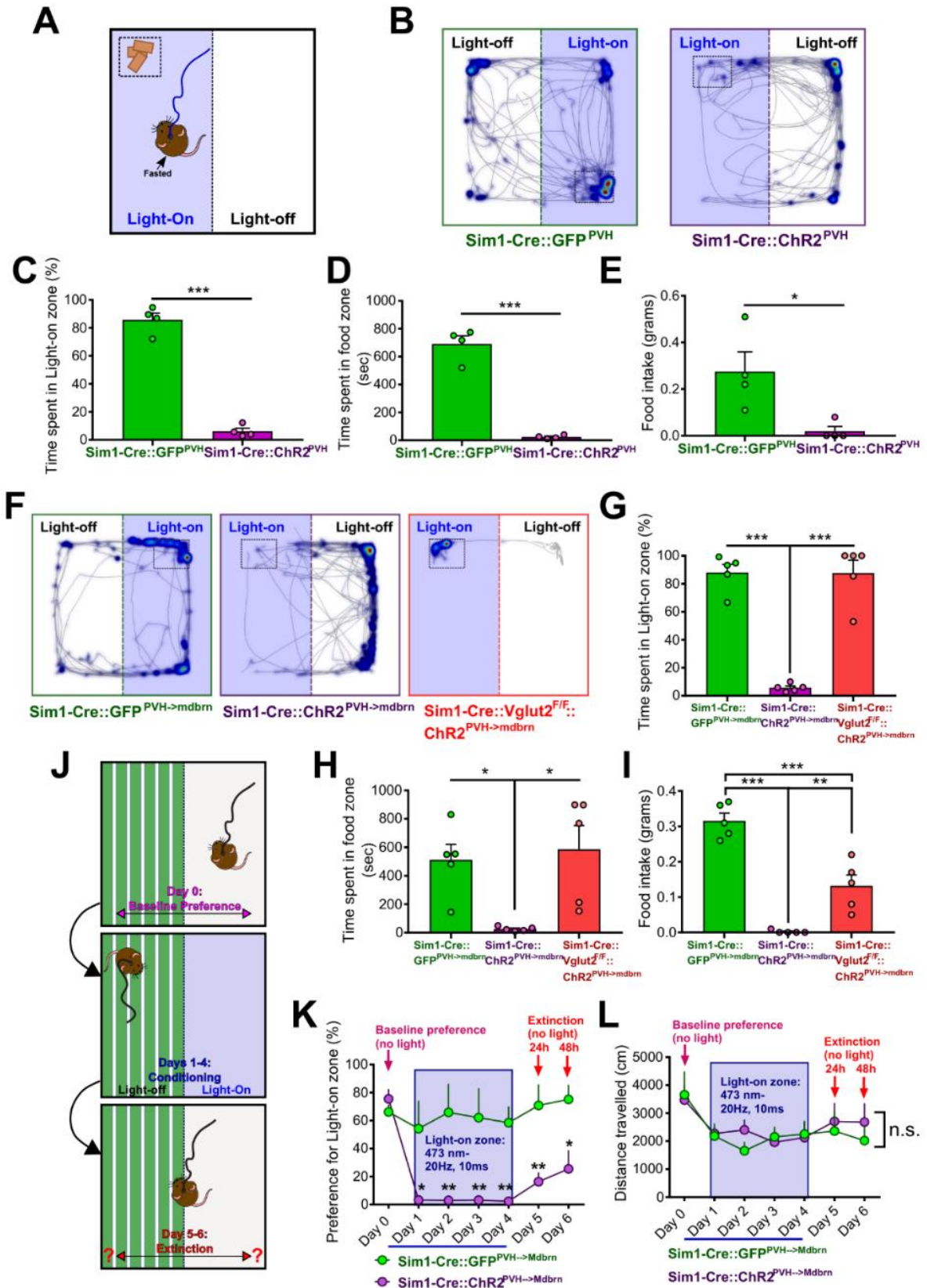


Figure 30. PVH→Midbrain Activation on Fast-Refeeding and Aversive Conditioning. (A) Schematic of fast-refeeding experiment where food is placed in a corner of the light-paired side of the arena. (B) Representative heatmaps of time spent in arena location superimposed over tracks during fast-refeeding assay. Dashed rectangular area denotes food zone. One side of the chamber was paired with PVH photostimulation. (C) Percent of total testing time spent in light-paired zone during fast-refeeding assay. (D) Time spent in food zone during fast-refeeding assay. (E) Amount of food eaten during fast-refeeding assay. (F) Representative heatmaps and activity tracks during fast-refeeding assay, where one side of the chamber containing food was paired with PVH→midbrain photostimulation. Dashed rectangular area denotes food zone. (G) Percent of time spent in light-on zone during fast-refeeding assay for PVH→midbrain photostimulation. (H) Time spent in food zone during fast-refeeding assay. (I) Amount of food eaten during the same assay. (J) Schematic timeline showing experimental conditions during days of aversive conditioning and extinction tests. The initially most preferred side of a chamber containing contextual flooring cues was paired with PVH→midbrain photostimulation on the subsequent days of conditioning. (K) Preference for light-paired side across conditioning days and extinction. (L) Distance travelled during the conditioning assay for each day. Unpaired t-tests, 1-way ANOVA, and 2-way ANOVA for statistical comparisons, * $p < 0.05$, ** $p < 0.005$, *** $p < 0.0005$. Error bars represent SEM. See also Figure 31.

and food zone (Figures 30F-H), and consumed significantly less (Figure 30I), despite attempts in approaching the food zone (Figure 31C). On the other hand, upon locating food, KO mice with the same stimulation tended to remain in the light-paired side (Figures 30F, 31C), and spent a similar amount of time in the light-on side and food zone as GFP controls (Figure 30G-H). Surprisingly, however, their food intake was significantly less (Figure 30I). The total distance travelled during the assay was unchanged between GFP control and Sim1-Cre::ChR2^{PVH->mdbrn} mice, but was significantly reduced in KO mice (Figure 31D), suggesting a role for non-glutamatergic transmission in the PVH→midbrain circuit in suppressing feeding and locomotion during the fasted state.

Given the known role for the midbrain in learning, we next tested whether the aversion associated with light stimulation of PVH→midbrain could be learned. Sim1-Cre::ChR2^{PVH->mdbrn} and GFP control mice were conditioned across several consecutive days by pairing a previously preferred side of a chamber with light stimulation (Figure 30J). As expected, Sim1-Cre::ChR2^{PVH->mdbrn} mice avoided the light-paired side during the four days of conditioning, spending significantly less time in that side (Figure 30K). Interestingly, Sim1-

Cre::ChR2^{PVH→mdbrn} mice persisted in avoiding the light-paired side during 24h and 48h extinction tests, when light was no longer applied (Figure 30K). Day-to-day changes in locomotion during the entire testing session was unchanged between groups (Figure 30L). Thus, the PVH→midbrain circuit participates in a learned aversion process.

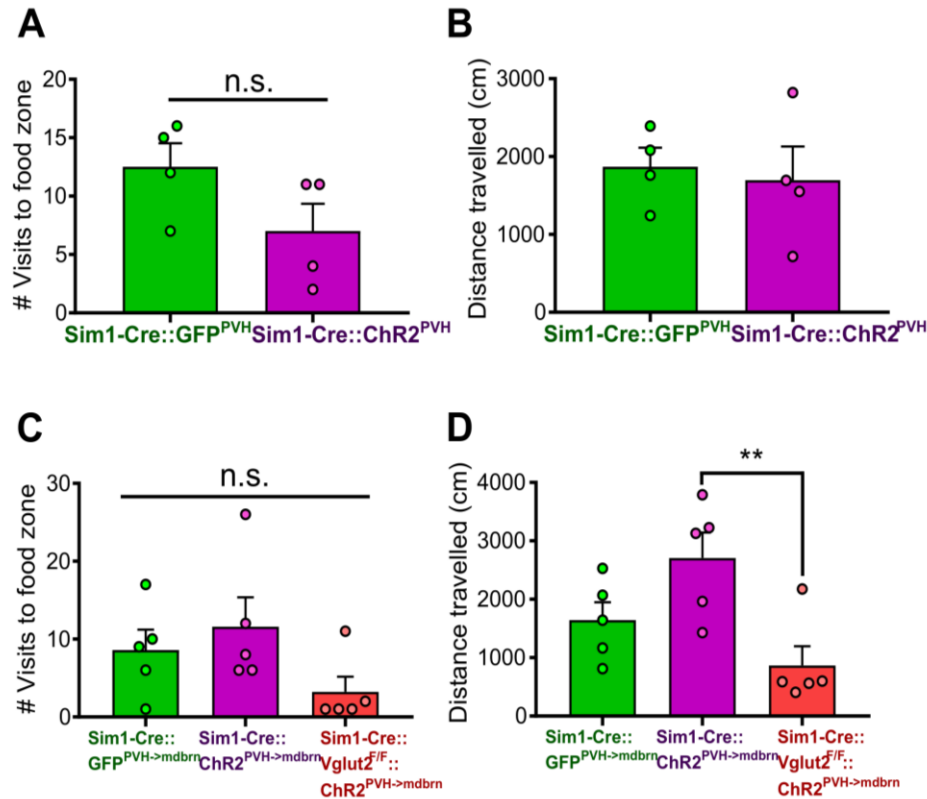


Figure 31. PVH and PVH→Midbrain Photostimulation Does Not Impact Approach to Food or Locomotion after Fasting. Related to Figure 30. (A) The number of times mice occupied the food zone during fast-refeeding assay in Figures 3B-E. (B) Distance travelled during the fast-refeeding assay in the same mice. (C) Number of times mice occupied the food zone during fast-refeeding assay in Figures 30F-I. (D) Distance travelled during the fast-refeeding assay in the same mice. Unpaired t-tests and 1-way ANOVA for statistical comparisons, **p<0.005, n.s.-Not Significant. Error bars represent SEM.

Glutamatergic midbrain neurons are activated by PVH projections to drive escape behavior

Previous studies reported that glutamatergic neurons in the VTA respond to aversive cues²⁵², and their projections to the nucleus accumbens and lateral habenula drive aversion

^{253, 254}. Hence, we tested whether PVH projections target glutamatergic neurons in the midbrain to promote aversion and escape behaviors. Since Sim1-Cre co-localizes with the majority of Vglut2 neurons in the PVH ⁵⁷, we used a Vglut2-ires-Cre mouse model ²⁵⁵ to target PVH-Sim1 neurons. To determine circuit connectivity, we delivered AAV-FLEX-ChR2-EYFP viruses to the PVH, and AAV-FLEX-GFP to the midbrain to visualize glutamatergic neurons. We performed whole-cell recordings on glutamatergic neurons in the midbrain, while photostimulating local PVH-Vglut2 fibers expressing ChR2 (Figure 32A). Surprisingly, we found that all GFP+ neurons patched showed excitatory post-synaptic currents (oEPSCs) (Figure 32B). The currents could be blocked by bath application of tetrodotoxin

(TTX), and subsequently rescued by 4-aminopyridine (4-AP), suggesting monosynaptic

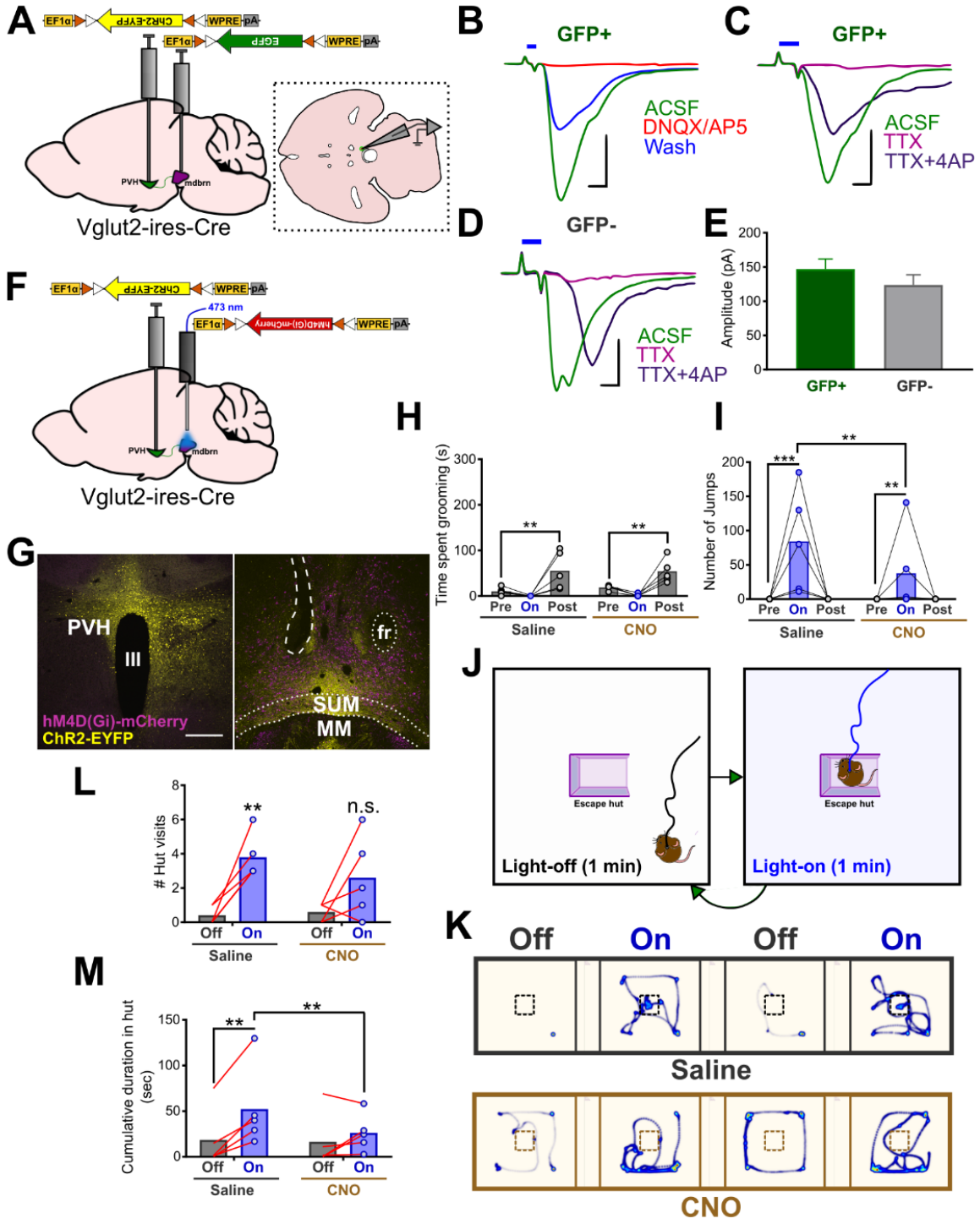


Figure 32. Activation of Glutamatergic-Midbrain Neurons in Escape Behaviors.

(A) Schematic showing viral delivery of ChR2-EYFP to PVH and EGFP to the midbrain in Vglut2-ires-Cre mice. Inset shows schematic of horizontal slice recordings in midbrain area. (B) Light-evoked excitatory post-synaptic responses (oEPSCs) in 20/20 GFP+ cells receiving input from PVH. Red traces showing oEPSCs blocked by glutamate receptor blockers, and partial recovery after wash-out of drugs (blue traces). Scale bar: vertical, 100 pA, horizontal, 2 seconds. (C) Light-evoked oEPSCs are blocked by TTX and recovered with addition of 4-AP in GFP+ cells. Scale bar: vertical, 100 pA, horizontal, 2 seconds. (D) Light-evoked oEPSCs are blocked by TTX and recovered with addition of 4-AP in GFP- cells. Scale bar: vertical, 50 pA, horizontal, 2 seconds. (E) Comparison of averaged oEPSC amplitude in GFP+ and GFP- cells. Figures B-E used with permission from Zhiying Jiang. (F) Experimental schematic for inhibition of midbrain glutamatergic neurons during PVH→midbrain photostimulation. (G) Brain slice images of Vglut2-ires-Cre mice showing ChR2-EYFP expression in PVH (left), and hM4D(Gi)-mCherry expression in midbrain area (right). Dashed area shows optic fiber implant trace. III, third ventricle; fr, fasciculus retroflexus; MM, mammillary nucleus; SUM, supramammillary nucleus. Scale bar, 300 μ m. (H) Time spent grooming before, during, and after photostimulation of PVH→midbrain following i.p. injection of saline or CNO. (I) Number of jumps counted during PVH→midbrain photostimulation tests above, following i.p. injection of saline or CNO. (J) Schematic for escape-hut assay. Light-off and light-on epochs alternated for eight minutes. (K) Representative heatmap traces, showing relative time spent in each arena location during the escape-hut assay. The first four minutes of the test is shown. (L) Quantification of the number of times animals visited the escape hut following i.p. injection of saline or CNO. Number of hut visits were summed across four 1-minute light-off periods and four 1-minute light-on periods. (M) Cumulative duration inside the hut during the escape-hut assay. Time spent inside the hut was summed across four 1-minute light-off and four 1-minute light-on epochs. Unpaired t-tests, and repeated measures 2-way ANOVA for statistical comparisons, ** $p < 0.005$, *** $p < 0.0005$, n.s.-Not Significant. Error bars represent SEM. See also Figure 33.

connectivity (Figure 32C). We noted that the majority of GFP- cells patched (18/20) also received monosynaptic excitatory input from PVH (Figure 32D), with a comparable latency and amplitude to GFP+ cells (Figure 32E), suggesting diffusive innervation of PVH fibers onto midbrain neurons. To examine the function of glutamatergic midbrain neurons, we silenced them prior to photostimulation by administering clozapine-n-oxide (CNO) in Vglut2-ires-Cre mice injected with AAV-FLEX-hM4D(Gi)-mCherry virus into the midbrain and AAV-FLEX-ChR2-EYFP into the PVH (Figures 32F-G). Injection of CNO prior to PVH→midbrain photostimulation reduced cFos expression in the midbrain region (Figures 33A-B), and also failed to affect self-grooming behavior (Figure 32H), place avoidance (Figure 33C-D), and increased locomotion (Figure 33E-F) evoked by photostimulating PVH→midbrain circuit.

However, CNO significantly reduced light-evoked escape-jumping (Figure 32I), indicating that midbrain glutamatergic neurons play a significant role in escape, but not in other

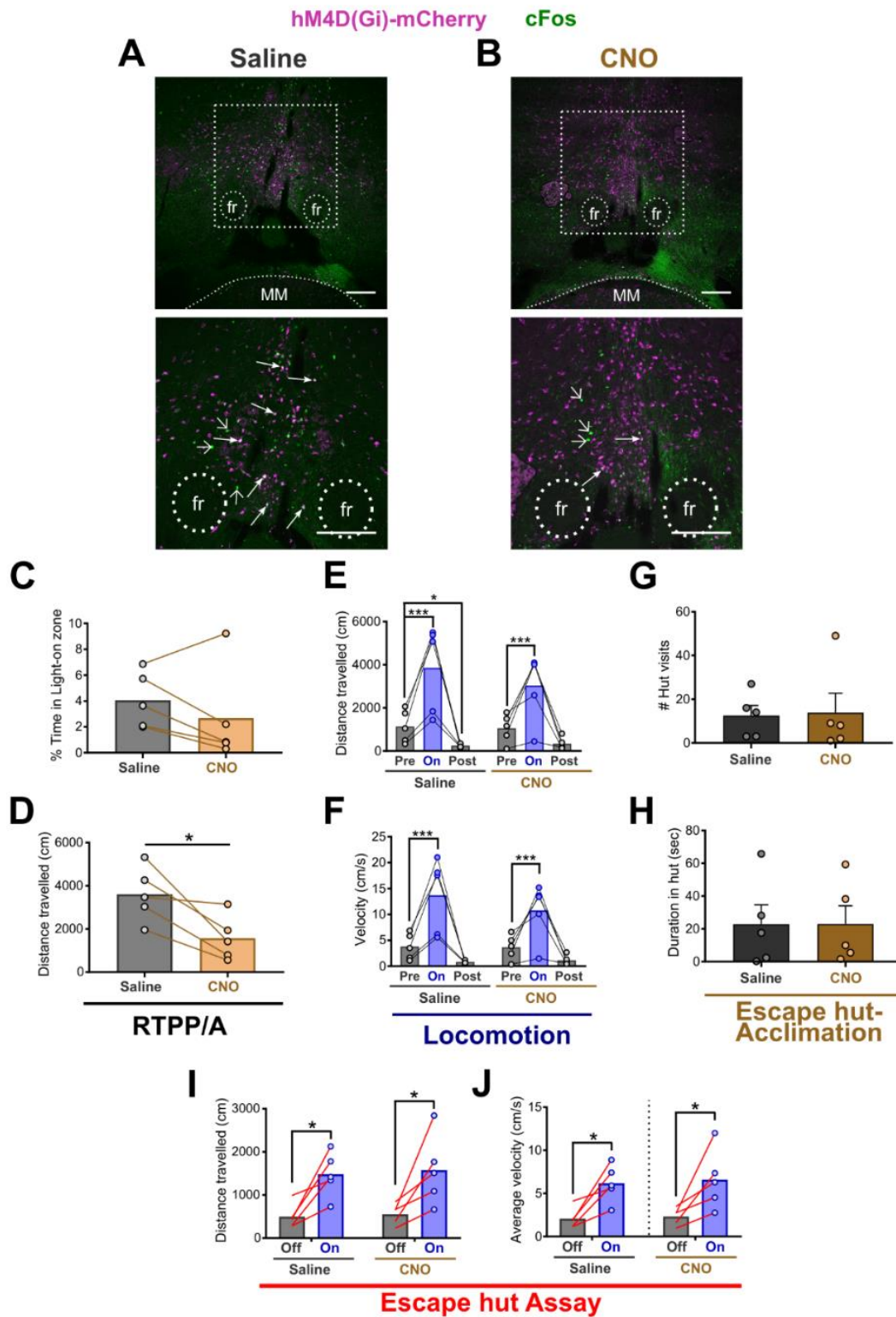


Figure 33. Activation of Glutamatergic-Midbrain Neurons is Not Required For PVH→Midbrain-Evoked Hyperlocomotion and Avoidance. Related to Figure 32. (A) cFos immunostaining in the midbrain following intraperitoneal (i.p.) injection of saline prior to PVH→midbrain photostimulation in mice expressing inhibitory DREADD (hM4D(Gi)-mCherry) in midbrain. Bottom image shows higher magnification of outlined box in top image. Filled arrowheads point to mCherry positive/cFos overlapping cells; unfilled arrows point to cells positive for cFos only. Scale bars, 200 μ m. (B) cFos immunostaining in the midbrain following i.p. injection of CNO prior to PVH→midbrain photostimulation in mice expressing inhibitory DREADD (hM4D(Gi)-mCherry) in midbrain. Bottom image shows higher magnification of outlined box in top image. Filled arrowheads point to mCherry positive/cFos overlapping cells; unfilled arrows point to cells positive for cFos only. Scale bars, 200 μ m. fr, fasciculus retroflexus; MM, medial mammillary nucleus. (C) Percent time spent in the light-on zone during the Real Time Place Preference/Avoidance (RTPP/A) assay in mice receiving i.p. injection of saline or CNO prior to testing. (D) Distance travelled during the RTPP/A assay in the same mice. (E) Distance travelled during the locomotion assay following i.p. injection of saline or CNO. (F) Average velocity during the locomotion assay in the same mice. (G) Number of times mice approached and entered an escape hut, placed in the center of the testing arena, during a seven-minute period prior to performing optogenetic stimulation tests. Mice were i.p. injected with saline or CNO prior to this acclimation period. (H) Time spent inside the hut during the acclimation period in the same mice. (I) Distance travelled during the escape hut assay in Figures 32J-M, following i.p. injection of saline or CNO. (J) Average velocity during the escape hut assay in Figures 4J-M. Paired t-tests and repeated measures 2-way ANOVA for statistical comparisons, * $p < 0.05$, *** $p < 0.0005$. Error bars represent SEM.

defensive behaviors evoked by light stimulation.

A recent study showed that mice consistently and predictably return to a previously memorized shelter location upon experiencing threatening stimuli²⁵⁶, so we next sought to explore the function of midbrain glutamatergic neurons in this type of escape strategy. Towards this, we first injected Vglut2-ires-Cre mice with dual viral constructs as above, and then placed them in a testing chamber containing a shelter (“escape hut”) located in the middle of the arena (Figure 32J). Mice were acclimated to the testing environment for 7 minutes to allow spontaneous discovery of the shelter²⁵⁶ (Figures 33G-H), then were exposed to 1 minute periods of no light, followed by 1 minute intervals of light-on, repeated for eight minutes (Figure 32J). Light was pulsed at a lower frequency (5-10 Hz) during light-on periods to preclude potential interference from jumping activity. Remarkably, mice injected with saline prior to the trial consistently approached and hid in the shelter during the light-on epochs (Figures 32K-M). In contrast, although most mice

injected with CNO approached the shelter during light-on periods (Figure 32L) and displayed similar increases in locomotion upon light stimulation during the assay (Figure 33I-J), they spent significantly less time hiding in the shelter (Figure 32M). These findings provide further evidence that PVH projections onto midbrain glutamatergic neurons drive escape behaviors.

Population dynamics of glutamatergic midbrain neurons during a fearful and aversive situation

Given that midbrain glutamatergic neurons participate in escape behaviors, we next explored *in vivo* responses of these neurons during a situational encounter with fear and aversion. Because exposure to open arms of a t-maze provokes intense fear²⁵⁷, we performed a modified elevated t-maze test (Figure 34A) on Vglut2-ires-Cre mice injected with AAV-FLEX-GCaMP6m in the midbrain area (Figure 34B), while simultaneously monitoring real-time neuronal population calcium dynamics via fiber photometry. For this, mice were placed at the base of the open arm, and allowed to freely explore the apparatus for three minutes. We noted an abrupt increase in neural activity in response to this initial exposure (“first open”; Figure 34C), an event that was consistent across all mice tested (Figure 34D), and persisted for at least 15 seconds after placement in the open arm (Figure 34E). On average, mice spent 40.8 ± 8.077 S.E.M. seconds in the open arm before exiting to the closed arm for the first time. Subsequent transitions from closed to open arms were accompanied by spikes in calcium transients (Figure 34C). Surprisingly, drops in neural activity occurred after mice concluded the three minute session upon final exiting to the closed arm, which was defined as remaining in the closed arm for at least 15 seconds with no re-entry into the open arm (Figures 34C and 34F). A significant decrease in the averaged calcium signal occurred by the last five seconds of the 15 second recording window following the last exit to closed arm (Figure 34G). These findings indicate that

glutamatergic midbrain neurons signal threat by increasing their activity during a fear-provoking situation, and decrease their activity once safety is determined.

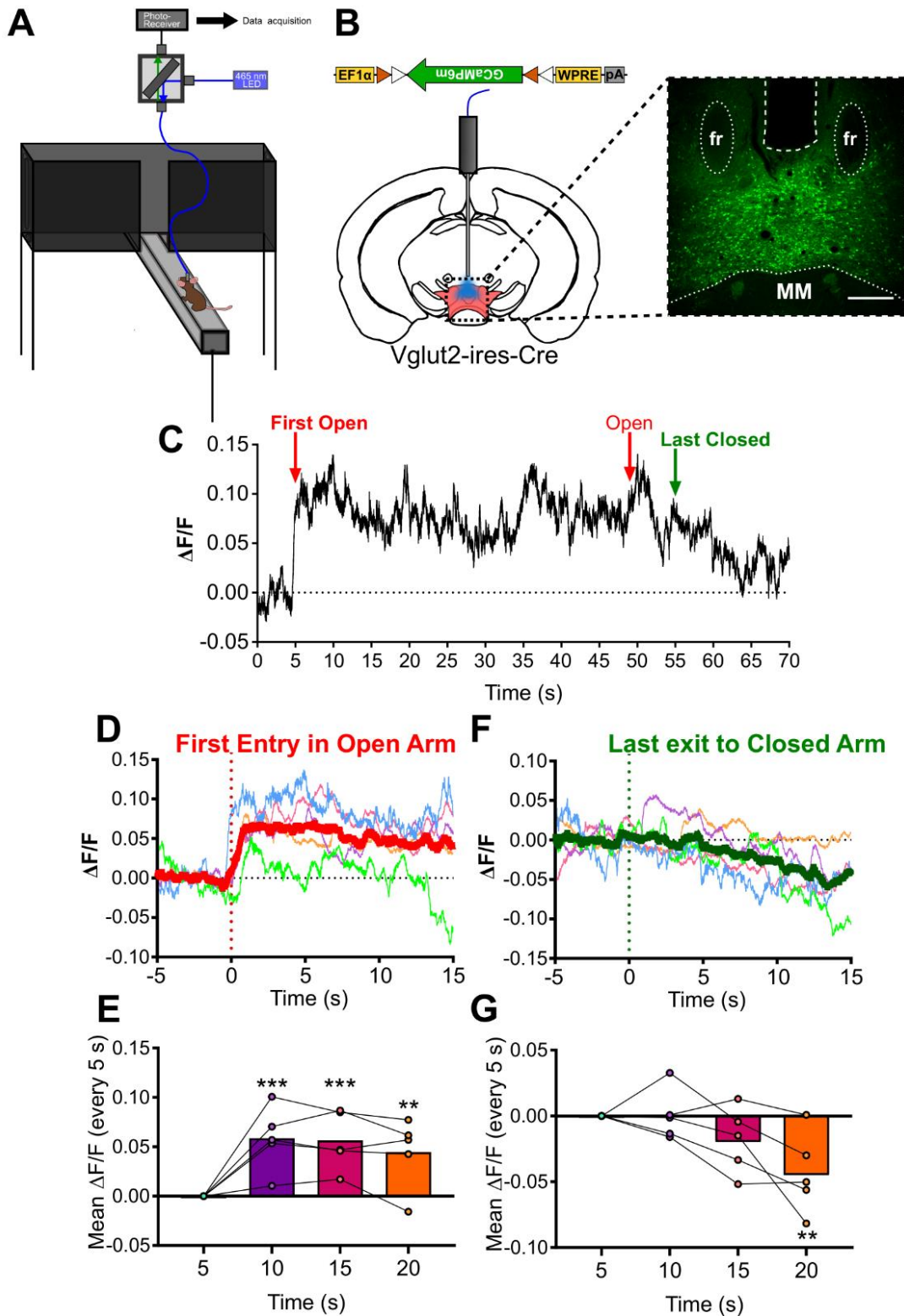


Figure 34. Population Dynamics of Glutamatergic Midbrain Neurons in Response to Fear. (A) Schematic of experimental procedure used to monitor Vglut2-midbrain neural activity during a modified elevated t-maze test. (B) (Left) Schematic for delivery of GCaMP6m calcium indicators into the midbrain area in Vglut2-ires-Cre mice. (Right) Representative brain slice image showing GCaMP6m expression in midbrain/VTA area. fr, fasciculus retroflexus; MM, mammillary nucleus. Scale bar, 300 μ m. (C) Representative traces showing GCaMP6m signal ($\Delta F/F$) during exploration of the t-maze apparatus. (D) Individual (multi-colored, thin traces) and averaged (thick, red line) GCaMP6m traces from mice exploring the t-maze, aligned to the first exposure in the open arm. (E) Mean changes in fluorescent signal during each 5-second window of the recording period in (D). (F) Individual and averaged GCaMP6m traces aligned to the last exit to an enclosed arm at the conclusion of the testing period. (G) Mean changes in fluorescent signal during each 5-second window of the recording period in (F). 1-way ANOVA for statistical comparisons, ** $p < 0.005$, *** $p < 0.0005$.

Discussion

Threatening stimuli prompt a state of fear, leading to various defensive behavioral strategies, such as flight, avoidance, freezing, risk assessment and other behaviors, and compete with ongoing activities to promote survival²⁴⁰. In this study, we describe a novel hypothalamic-midbrain circuit engaged in triggering a classic set of emotional and behavioral aspects typical of defense. Notably, we found that the PVH→midbrain connection drives acute and learned aversion, and is capable of increasing locomotion, and escape behaviors. Further, the aversive properties of PVH→midbrain activation can override intrinsic homeostatic drive for feeding. Receiving glutamatergic input from the PVH, midbrain glutamatergic neurons were shown to respond to a fear-provoking and aversive context, and drive escape behaviors. From these results, we propose that the PVH to midbrain circuit is part of the neural circuitry that underlies the behavioral and emotional processes that facilitate survival in a threatening situation.

We and others have previously shown that PVH neurons and specific neural subsets constitute a critical node for evoking idiosyncratic behaviors, such as self-grooming, following stress^{61, 168}. Our data here support the idea that PVH signals aversion, and is

sufficient to produce stress-like and defensive responses. Given that repeated encounters with stressful situations may lead to a state of fear and avoidance ²⁴¹, it is not surprising that the same neural populations transmit interrelated messages. Although the hypothalamus has been previously regarded as a relay station for unconditioned defensive behaviors ²⁵⁸, our study and others ^{26, 109, 171} support the idea that discrete hypothalamic nuclei are sufficient for generating underlying emotional states concurrent with behavioral output. Given that subsets of PVH neurons drive the autonomic and neuroendocrine components of stress, the possibility of PVH neuron collaterals to brain sites that promote associated behaviors is becoming increasingly clear ¹⁶⁸. Stress alters defensive expression ^{259, 260}; therefore, neural circuits responsive to stress may modulate behavioral action based on context and/or experience. Supporting this, our findings show that the PVH to midbrain circuit drives different defensive behaviors based on the testing environment. Distinct VTA circuits have been shown to drive emotional learning processes ^{156, 158, 253, 254, 261}, and alter behavioral output in response to stress ^{262, 263}, consistent with our findings that midbrain neurons are the downstream site of action for aversion learning and stress-related behaviors.

The majority of PVH neurons use glutamate as a neurotransmitter ⁵⁷. Glutamatergic transmission from PVH onto midbrain neurons was required for defensive behaviors seen here, but was not required for the evoked grooming response, suggesting non-glutamatergic, and likely neuropeptidergic action. Delayed postsynaptic responses inherent to neuropeptide signaling ²⁶⁴ may indeed explain the persistence in grooming following light cessation, as well as the delayed initiation of grooming following light stimulation of PVH in the absence of glutamate release. Provided that activation of corticotropin-releasing hormone (CRH) cells in PVH promotes grooming ¹⁶⁸, and that VTA neurons expressing CRH receptors play a role in stress-induced alterations in behavior ²⁶⁵, it is possible that CRH signaling from PVH onto midbrain neurons drives the evoked grooming behavior observed

here. Nevertheless, future investigation will be needed to identify the specific neuropeptide populations involved.

Despite extensive research on the impact on behavior via changes in midbrain neuron activity, specific upstream sites for glutamatergic transmission onto midbrain glutamate neurons remain largely unexplored²⁵⁰. Here, we identified the PVH as a source of glutamatergic input onto glutamate and non-glutamate cells in the midbrain region. Silencing experiments indicated that although PVH activation of non-glutamatergic midbrain cells was sufficient in promoting avoidance and hyperactivity, glutamatergic neurons are the likely population that drive escape behaviors. However, glutamatergic neural silencing failed to completely suppress light-evoked escape behaviors. One of underlying reasons may be due to inherent caveats of less than one hundred percent transfection with hM4D-Gi via viral targeting; thus, incomplete silencing of glutamatergic neurons may have insufficiently precluded escape responses. Alternatively, given that hM4D-Gi-silenced mice still approached the escape hut during PVH→midbrain activation, it is possible that non-glutamatergic midbrain neurons drive initial escape responses, but do not maintain continued escape behavior during ongoing threat encounters. Nevertheless, the importance of glutamatergic-midbrain neurons in processing threat is supported by *in vivo* population recordings that show increased activity when the animal encountered danger (open arm exposure), and decreased activity once the animal was perceived safety (final exit to closed arm). Given these findings, we posit that midbrain glutamatergic neurons participate in threat detection and active defense strategies, whereas midbrain non-glutamatergic populations promote a general state of unease and agitation. GABA-releasing VTA neurons are a good candidate for future interrogation, as they have been shown to respond to aversive stimuli²⁶⁶ and drive aversion processes^{266, 267}. Although our data suggests that only a small number of dopamine neurons are activated by PVH inputs, given their known

role in behavior, it is possible dopamine cells also contribute to aversive properties ²⁶¹ and increased locomotion ²⁶⁸ in response to PVH-activation.

The PVH projects to several brainstem regions, some of which have been implicated in various defensive behaviors ¹⁸⁰ and threat detection ¹⁷⁸. For example, the periaqueductal gray (PAG) has been shown to participate in freezing, flight, and avoidance behaviors ^{179, 180}. Recently, a specific neural subset in the parabrachial nucleus (PBN), a major relay for sensory information, was implicated in defensive expression following recall of fearful memories ¹⁷⁸. Our current study and others ^{59, 62} have shown that PVH projects to the PAG and PBN. Since the PVH to midbrain projection promotes defensive behaviors, it is conceivable that PVH projections to the PAG and PBN may also exert a similar function. Notably, given an incomplete reversal in behavioral phenotypes by either midbrain glutamate receptor antagonism or inhibition of midbrain glutamatergic neurons, it is possible that PVH-collateral fiber activation, due to back propagation, may have resulted in activation of PAG and/or PBN. Ultimately, this may lead to redundant manifestation of the observed residual defensive behaviors. This possibility is supported by the role of these projections in feeding suppression ^{51, 59}, and our results showing that activation of PVH→midbrain prevents feeding. Future functional tracing and behavioral studies will help delineate how distinct PVH projections are coordinated in the generation of defense and feeding in response to changing environments.

Defensive behaviors such as shelter-seeking and escape are crucial, and represent innate behavioral components that are essential for survival. Maladaptive coping strategies in people, such as social avoidance and behavioral compulsions, may be illustrative of hardwired responses gone awry in a modern world posing an onslaught of novel environmental challenges. Thus, it has become increasingly important to investigate the neural basis of such behaviors, as they can often lead to paralyzing mental disorders such as generalized anxiety ²⁶⁹. Here, we have uncovered a hypothalamic-midbrain pathway that

drives and/or promotes conditioned aversion and escape, adding to the accumulating picture of how the brain integrates and produces emotions and behaviors underlying adaptive, and possibly maladaptive, strategies for survival.

Chapter 4.

Materials and Methods

Methods for Chapter 2

Animal care

Mice were housed at 21°C–22°C with a 12 h light/12 h dark cycle with standard pellet chow and water provided *ad libitum* unless otherwise noted for fasting experiments. Animal care and procedures were approved by the University of Texas Health Science Center at Houston Institutional Animal Care and Use Committee. *Pdx1-Cre* and *Sim1-Cre* mice were described previously^{50, 226}. Mice with the conditional allele of vesicular GABA transporter (*Vgat*, also named *Slc32a1*), and mice with the conditional allele of vesicular glutamate transporter 2 (*Vglut2*, also named *Slc17a6*) were reported previously^{270, 271}. Mice containing GABA-A receptor 2 subunit ($\gamma 2$) conditional allele were also reported previously²⁷². The following breeding pairs were maintained to generate study subjects: 1.

Pdx1^{cre/+}::Vgat^{flox/+} X *Vgat^{flox/flox}*; 2. *Pdx1^{cre/+}::Vglut2^{flox/+}* X *Vglut2^{flox/flox}*; 3. *Pdx1^{cre/+}:: $\gamma 2$ ^{flox/flox}* X *Sim1^{cre/+}:: $\gamma 2$ ^{flox/flox}*; 4. *Sim1^{cre/+}::Vglut2^{flox/+}* X *Vglut2^{flox/flox}*. Additionally, in most breeding pairs, either male or female breeders (or both) contained the Ai9 reporter gene to allow RFP expression in the presence of cre recombination²⁷³. Both male and female mice were used as study subjects. Mice used in experiments were obtained from multiple litters and were at least 6 weeks old.

Surgeries and viral constructs

Stereotaxic surgeries to deliver viral constructs and for optical fiber implantation were performed as previously described²⁷⁴. Briefly, mice were anesthetized with a ketamine/xylazine cocktail (100 mg/kg and 10 mg/kg, respectively), and their heads affixed to a stereotaxic apparatus. Viral vectors were delivered through a 0.5 μ L syringe (Neuros Model 7000.5 KH, point style 3; Hamilton, Reno, NV, USA) mounted on a motorized stereotaxic injector (Quintessential Stereotaxic Injector; Stoelting, Wood Dale, IL, USA) at a rate of 40 nL/min. Viral preparations were titered at $\sim 10^{12}$ particles/mL. Viral delivery was

targeted to the LH (200-400 nL/side; anteroposterior (AP): -1.0 mm; mediolateral (ML): \pm 1.1 to 1.3 mm; dorsoventral (DV): -5.0 mm) or PVH (65-150 nL/side; AP: -0.5 to -0.6 mm; ML: \pm 0.2 to 0.3 mm; DV: -5.0 mm). Uncleaved fiber optic cannulae (\varnothing 1.25 mm Stainless Ferrule, \varnothing 200 μ m Core, 0.39 NA; ThorLabs, Newton, New Jersey, USA) were pre-cut to 4.5-4.8 mm and implanted above the PVH (AP: -0.5 to -0.6 mm; ML: 0 mm). Optical fibers were secured on the head with dental cement.

For blue-light dependent activation of LH \rightarrow PVH fibers and PVH neurons, *AAV-EF1 α -DIO-hChR2(H134R)-EYFP-WPRE-hGHpA* (Addgene, plasmid number 20298) serotype 2/9²²⁸ or *AAV-EF1 α -DIO-hChR2(H134R)-EYFP-WPRE-pA* serotype 2/5 (University of North Carolina Vector Core, Chapel Hill, NC, USA) (general name used throughout text for ChR2 virus: AAV-FLEX-ChR2-EYFP) was injected unilaterally or bilaterally into the LH of *Pdx1-Cre*, *Pdx1-Cre::Vgat^{flox/flox}*, *Pdx1-Cre::Vglut2^{flox/flox}*, *Pdx1-Cre:: γ 2^{flox/flox}*, and *Pdx1-Cre::Sim1-Cre:: γ 2^{flox/flox}* or PVH of *Sim1-Cre* and *Sim1-Cre::Vglut2^{flox/flox}* mice. For light-dependent inhibition of LH \rightarrow PVH fibers, *AAV-CAG-DIO-eArchT3.0-EGFP* (general name used throughout text for eArchT3.0 virus: AAV-FLEX-eArchT3.0-[E]GFP) serotype 2/9 was delivered bilaterally into LH of *Pdx1-Cre::Vglut2^{flox/flox}* and *Pdx1-Cre::Vgat^{flox/flox}* mice. For PVH^{*Sim1*} inhibition experiments, *AAV-EF1 α -DIO-iC++-EYFP* (University of North Carolina Vector Core, Chapel Hill, NC, USA) (general name used throughout text for iC++ virus: AAV-FLEX-iC++-EYFP) was injected bilaterally into the PVH of *Sim1-Cre* mice. *AAV-EF1 α -DIO-EGFP* (general name used throughout text for GFP virus: AAV-FLEX-[E]GFP) serotype DJ8 was injected into the LH and PVH of *Pdx1-Cre* mice and *Sim1-Cre* mice, respectively, and used as an opsin-negative control for behavioral experiments. For electrophysiology recordings testing suppression of light-evoked current response, *Pdx1-Cre* mice received a cocktail injection containing 50:50 mix of cre-dependent ChR2 + eArchT3.0 viruses to the LH. For anterograde viral tracing, *AAV-EF1 α -FLEX-Syn::EGFP-WPRE-hGHpA*, serotype DJ/8²²⁸ (general name used for Synaptophysin virus: AAV-FLEX-Synaptophysin-GFP) was

injected unilaterally into LH of *Pdx1-Cre::Sim1-Cre::Ai9* mice. Cre-dependent viruses cited from²²⁸ as well as eArchT3.0 and GFP were made in-house by Dr. Ben Arenkiel's lab.

Brain slice electrophysiological recordings

Coronal brain slices (250-300 μm) containing the PVH from mice that had received stereotaxic injections of AAV-FLEX-ChR2-YFP or AAV-FLEX-ChR2-YFP + AAV-FLEX-eArchT3.0-GFP to LH or PVH at least 3 weeks prior to the recording were cut in ice-cold artificial cerebrospinal fluid (aCSF) containing the following (in mM): 125 NaCl, 2.5 KCl, 1 MgCl_2 , 2 CaCl_2 , 1.25 NaH_2PO_4 , 25 NaHCO_3 , and 11 D-glucose bubbling with 95% O_2 /5% CO_2 . Slices containing the PVH were immediately transferred to a holding chamber and submerged in oxygenated aCSF. Slices were maintained for recovery for at least 1 h at 32-34°C before transferring to a recording chamber. Individual slices were transferred to a recording chamber mounted on an upright microscope (Olympus BX51WI) and continuously superfused (2 ml/min) with ACSF warmed to 32-34°C by passing it through a feedback-controlled in-line heater (TC-324B; Warner Instruments). Cells were visualized through a 40X water-immersion objective with differential interference contrast (DIC) optics and infrared illumination. Whole cell voltage-clamp recordings were made from neurons within the sub-regions of the PVH that showed the highest density of ChR2-eYFP+ axonal fibers. Patch pipettes (3–5 M Ω) were filled with a Cs⁺-based low Cl⁻ internal solution containing (in mM) 135 CsMeSO₃, 10 HEPES, 1 EGTA, 3.3 QX-314, 4 Mg-ATP, 0.3 Na₂-GTP, 8 Na₂-Phosphocreatine (pH 7.3 adjusted with CsOH; 295 mOsm) for voltage-clamp. For current-clamp recordings, pipettes were filled with a K⁺-based low Cl⁻ internal solution containing (in mM) 145 KGlu, 10 HEPES, 0.2 EGTA, 1 MgCl_2 , 4 Mg-ATP, 0.3 Na₂-GTP, 10 Na₂-Phosphocreatine (pH 7.3 adjusted with KOH; 295 mOsm). Membrane potentials were corrected for ~10mV liquid junction potential. To activate ChR2 or ChR2+eArchT3.0-expressing fibers from LH or ChR2-expressing neurons in PVH, light from a 447 nm or 473 nm laser (Opto Engine LLC, Midvale, UT, USA) was focused on the area of the recorded

PVH neuron to produce spot illumination through optic fiber. Brief pulses of light (blue light [1-2ms] and/or yellow light [556nm, 200ms]; 1-2mW/mm²) were delivered at the recording site at 10-15 s intervals under control of the acquisition software. GABA_A (10 μM) or CNQX + APV (20 μM and 50 μM) drugs (Abcam) were bath-applied to block GABA-A receptors or AMPA, kainate, and NMDA receptors, respectively, during voltage-clamp recordings of photostimulation-induced inhibitory or excitatory current responses. TTX (0.5 μM; Alomone labs, Jerusalem, Israel), and 4-AP (100 μM; ACROS Organics, Fisher Scientific, Pittsburgh, PA, USA) were bath-applied during voltage-clamp recordings of photostimulation-induced inhibitory and excitatory current responses to block action potentials and inhibit network activity. Following established protocols for loose-patch recordings in voltage clamp mode²⁷⁵, pipettes (2-3 MΩ) were filled with ACSF and the seal resistance was kept at 20–100 MΩ. The holding potential was routinely monitored and adjusted to maintain a holding current close to 0 pA in order to avoid changing the membrane potential of the cell being recorded. To activate iC++-expressing fibers²³⁰, blue light (473 nm, 5mW/mm², 10 sec) was applied during AP firing induced by current injection of 10-30 pA, at 30 sec intervals intervals under control of the acquisition software.

Behavioral Experiments

Behavioral testing was conducted during the light cycle following a minimum 3 week recovery period post-surgery. For *in vivo* photostimulation/inhibition experiments, an integrated rotary joint patch cable connected the ferrule end of optic fiber cannula with a Ø1.25 mm ferrule end of the patch cable via a mating ceramic sleeve (ThorLabs, Newton, New Jersey, USA). At the other end of the rotary joint, an FC/PC connector was connected to a 447 nm, 473 nm or 556 nm diode-pumped solid state (DPSS) laser (Opto Engine LLC, Midvale, Utah, USA). Light pulses were controlled by Master-8 pulse stimulator (A.M.P.I., Jerusalem, Israel). For Real Time Place Preference Assays, a commutator (rotary joint; Doric, Québec, Canada) was attached to a patch cable via FC/PC adaptor. The patch cable

was then attached to the optic fiber cannula ferrule end via a ceramic mating sleeve. Another patch cable containing FC/PC connections at both ends allowed the connection between the commutator and the laser, which was controlled by the Master-8 pulse stimulator. During testing, mice were placed in a fresh cage with no bedding. For RTPP assays, mice were placed into a clean testing chamber that was wiped down with 70% isopropyl alcohol between tests.

Feeding and Grooming Assays

For optogenetic stimulation-feeding/grooming experiments, mice were *ad libitum* fed prior to testing (excluding competition experiments; see below). Mice underwent 15-min trials consisting of three consecutive 5-min epochs (pre-light, light-on, and post-light). During pre-light and post-light periods, the laser was turned off. During the light-on period, blue light (473 nm, ~5-10 mW/mm²) was pulsed at 5 Hz, with each pulse-width duration lasting 10 or 100 ms. Food intake was measured and recorded after the completion of each epoch during the 15-min trial. A video was recorded for each trial. Trials were repeated for each mouse at least 3 times on separate days to verify repeatability. An observer blind to the experimental conditions watched the videos and manually calculated the time spent grooming (see paragraph below), feeding, and/or licking with a stopwatch. Feeding time was counted when mice were actively engaged in biting, chewing, swallowing, or licking food. Licking time in the absence of food was counted when the tongue moved across the surface of the cage floors and walls.

For grooming quantification, an observer blind to genotype condition watched the 15-min videos and manually quantified the time spent grooming during each epoch with a stopwatch. Grooming time was counted when the mouse engaged in forelimb paw strokes made near the nose, eyes, and head and during paw, body, tail, and genital licking. Rodent grooming is typically classified as a stereotypical chain of events that progresses from paw and nose grooming, to face grooming, to head grooming, and finally to body grooming¹⁶⁹.

To assess whether grooming induced by light activation of LH^{Pdx-ChR2}→PVH fibers results in abnormal patterning of grooming events, an observer watched 5 Hz, 10 ms videos of *Pdx1-Cre* and *Pdx1-Cre::Vgat^{flox/flox}* mice and quantified the number of grooming bouts, bout interruptions, and changes in grooming transitions using a grooming analysis algorithm described in²²⁷ during pre-light and light-on (5Hz, 10ms) conditions. To analyze small changes in grooming patterns, the observer watched videos on Quick Time Player (Apple), which easily allows for manual manipulation of video speed and pausing.

Real Time Place Preference (RTPP)

Pdx1-Cre::Vglut2^{flox/flox} and *Pdx1-Cre-GFP* controls, injected with cre-dependent ChR2 or GFP viruses, respectively, and implanted with optic fibers above PVH, were placed in a clean 45 cm X 45 cm X 50 cm chamber equipped with a camera mounted on top of the chamber and optical fiber patch cable attached to a commutator. Prior to starting experiments, the patch cable was attached to optic fiber ferrule end of the mouse's cannula. At the start of the experiment, mice were placed in the light-off zone, in which no light was applied. Then, for twenty minutes, the mice were allowed to freely roam the enclosure, which was divided into two equal zones containing the light-off zone and a light-on zone, in which 5Hz, 100 ms (473nm, ~5-10mW/mm²) light pulses were delivered. The side paired with photostimulation was counterbalanced between mice. Tracking data, including time spent in each zone, were collected and analyzed by Ethovision XT software (version 11.5; Noldus, Wageningen, Netherlands). Preference for one of either side was determined by comparing the percentage of time spent in each zone.

Inotropic GluR blockade experiment

Custom-made guide cannulae (Doric, Québec, Canada) allowing for interchangeable fluid and light delivery were implanted above PVH in *Pdx1-Cre* mice containing ChR2 in LH^{Pdx1} neurons. Prior to testing, the dummy cannula was removed from the guiding cannula and the fluid-delivery cannula was inserted via a screw-on top mechanism. Either 100 nL

vehicle (15% sterile DMSO in 0.9% saline) or 100 nL drugs (Tocris) containing 50 nL [61 mM D-AP5 solution in saline] + 50 nL [24 mM DNQX solution in 25-30% DMSO] were delivered via syringe (5 μ L, Model 75 RN SYR, Small Removable NDL, 26s ga, 2 in, point style 2; Hamilton, Reno, NV, USA). A plastic tube (RenaSil Silicone Rubber Tubing, .025 OD X .012 ID; Braintree Scientific, INC, Braintree, MA, USA) joined the syringe to the fluid-delivery cannula, and vehicle or drugs were manually infused at a rate of 100 nL/min. To prevent backflow of fluid, the fluid-delivery cannula was left screwed-on for an additional 2-3 min after infusion. Thereafter, the fluid-delivery cannula was screwed-off and the optical-fiber cannula was screwed on and attached to a fiber optic patch cable for light delivery and subsequent behavioral testing. Light was pulsed at 5 Hz, 10-50 ms (473nm, 2-6 mW/mm²) for a 5-min trial, in which a video was recorded and later quantified for time spent grooming. Vehicle and drug trials were performed on separate days, and order of trial condition was randomized. Pulse duration for each mouse was determined by the lowest duration (starting at 10 ms) that would induce the maximal amount of grooming without inducing feeding.

Inhibition Experiments

Pdx1-Cre::Vglut2^{flox/flox} mice containing eArchT3.0 in LH^{*Pdx1*} neurons and optic fiber implants over PVH underwent two 10-min trials: for Mock Inhibition trials, mice were fasted for 24 h and re-fed under “mock inhibition” (optic fiber cable attached to head but no light delivered) for 10 mins. For +Light trials, mice were fasted for 24 h and re-fed during alternating, consecutive light-off (1 min) followed by light-on (556 nm, ~10mW/mm²; constant-on for 1 min) periods for 10 mins. Trials were done at least a week apart. Mock inhibition trial was repeated a second time to verify randomness of time spent eating in each time period. Videos were recorded during trials and later manually quantified for time spent feeding and grooming by an observer.

Pdx1-Cre::Vgat^{flox/flox} mice containing eArchT3.0 in LH^{*Pdx1*} neurons and optic fiber implants over PVH performed 4 trials (performed on separate days, in randomized order): Trial A, Using a spray bottle filled with sterile water, mice were water sprayed with two squirts directed to the face, belly, and back (two squirts per area) to induce grooming²²². They were then placed in a bare cage with a single food pellet and observed for 10 mins, with laser cable attached to the head delivering continuous 447 nm light pulses (10 seconds light-on, followed by 2 seconds light-off, 5-15 mW/mm²); Trial B, same as trial A, except 556 nm light pulses were delivered instead (10 seconds light-on, followed by 2 seconds light-off, 5-15 mW/mm²); Trials C and D, either 447nm or 556 nm light was delivered during testing as in trials above; however, although mice were handled similarly to water spray experiments before testing, they did not receive any water sprays during these trials. Mice were acclimated to the bare cage with optic fiber cables attached to the head for 5 mins prior to water spray or handling. Videos were recorded for each trial and later analyzed for grooming and feeding behaviors.

Sim1-Cre mice injected with AAV-FLEX-EGFP or AAV-FLEX-iC++-EYFP virus in the PVH were used in feeding and stress-induced grooming assays. For food intake assays, mice were first acclimated to a bare testing cage with optic fiber cables attached to the head for 10 mins. Following acclimation, a pellet of food was added to the cage, and 473 nm light was pulsed continuously (2 seconds light-on, 1 second light-off; 10-15 mW/mm²) for 30 mins. Food weight was measured before and after 30 min tests. For baseline grooming tests (No Stress + Mock Inhibition trials), mice were placed in a bare testing cage with optic fiber cables attached to head, and observed for 15 mins. For stress-induced grooming assays, mice were immobilized on a cutting board with autoclave tape for 10 mins to induce anxiety and stress. They were then placed in a bare testing cage with optic fiber cables attached to the head and observed for 15 mins with light pulsed continuously (2 seconds

light-on, 1 second light-off; 10-15 mW/mm²). Videos were taken to later quantify time spent grooming. For food intake tests, baseline grooming, and stress-induced grooming experiments, GFP and iC++ mice were tested side-by-side and in pairs when possible.

Feeding vs. Grooming Competition Experiments

To study whether photostimulation of glutamatergic LH^{Pdx1-ChR2}→PVH fibers affects fast- refeeding, *Pdx1-Cre::Vgat^{flox/flox}* mice receiving ChR2 injections in LH^{Pdx1} neurons and optic fiber implants over PVH were placed in a bare testing cage with a pellet of food approximately 1-3 h before the beginning of the dark cycle. The same mice underwent 3 separate trials, lasting 30 mins each. Food intake was measured following each 30-min trial and videos were recorded for grooming behavior analysis. For one of the trials, food intake was measured for *ad libitum*-fed mice following 30 mins of mock stimulation (Trial A). In Trial B, mice were fasted for 24 h and re-fed under mock stimulation. For Trial C, mice were fasted for 24 h and then re-fed under light-on conditions (473nm, ~5-10 mW/mm² light: 5Hz, 100ms) for the final trial. The order of trials A-C was not the same for every mouse (to ensure a level of randomization), and mice were never fasted more than once per week. During mock stimulation trials, optic fiber cables were attached to the heads of the mice but no light was delivered. Trial A and Trial B or C occurred at least 24 hours apart, and Trials B and C occurred at least a week apart. An observer blind to the experimental conditions manually quantified the time spent grooming during each 30 min trial.

To study the effects of photostimulating GABAergic LH^{Pdx1-ChR2}→PVH fibers during self-grooming, *Pdx1-Cre::Vglut2^{flox/flox}* mice containing ChR2 in LH^{Pdx1} neurons and optic fiber implants over PVH underwent three 11-min trials, consisting of alternating consecutive 1 minute light-off followed by 1 minute light-on (473nm, ~5-10 mW/mm² light: 5Hz, 100ms) periods or mock stimulation (optic fiber cable attached to head but no light delivered). Prior to the trials, mice received either no water sprays or sterile water sprays with a spray bottle

directed to the face, belly, and back (2 squirts per area) to induce grooming. During the first trial, mice received water sprays and then were tested with mock stimulation. For the second trial, mice received water sprays prior to testing with light-off/light-on. For the third trial, no water spray was delivered and mice were tested with light-off/light-on. During trials, videos were recorded and time spent grooming and feeding was later quantified by an observer blind to the experimental conditions. Trials were performed on separate days. To test if photostimulation of PVH^{Sim1-ChR2} neurons interferes with fast-refeeding, *Sim1-Cre* and *Sim1-Cre::Vglut2^{flox/flox}* containing ChR2 in PVH neurons and optic fibers over PVH were fasted for 24 h and re-fed during alternating consecutive light-off (1 min) followed by light-on (473nm, ~5-10 mW/mm² light: 5Hz, 10ms) periods for 11 mins. Videos of the trials were recorded and time spent grooming and feeding was later quantified by an observer blind to genotype.

In situ hybridization (ISH)

Manual RNAscope® assay (Advanced Cell Diagnostics, INC., Newark, CA, USA) was used to visualize *Vglut2* and *Vgat* transcript in fresh frozen brain slices. The digoxigenin-labeled cRNA probes were generated against mouse *Vgat* mRNA and *Vglut2* mRNA sequence covering exon 2, which is flanked by two *loxP* sites. ISH was performed as we previously described for validating the deletion of *Vglut2* mRNA in *Sim1* neurons^{57, 276}. Briefly, fresh brain was harvested from *Vglut2^{flox/flox}* and *Pdx1-Cre::Vglut2^{flox/flox}* animals and frozen on dry ice prior to embedding in cryo-embedding medium (OCT). Brains in OCT were immediately frozen over dry ice. Embedded tissue was then equilibrated at -20°C for 30 min-1h prior to sectioning on a cryostat. 15 µm-thick fresh frozen sections were cut with the cryostat and mounted onto slides. The slides were then immersed in chilled 10% buffered formalin for 15 min at 4°C. Thereafter, the sections were dehydrated by immersing in 50% EtOH, 70% EtOH, and 100% EtOH for 5 min each at room temperature. After allowing slides to dry, a hydrophobic barrier was drawn around tissue with a

hydrophobic barrier pen. The slides were then placed on a hybridization humidifying rack and treated with protease pretreatment solution for 30 mins at room temperature. After pretreatment, slides were washed twice with fresh 1X PBS in a slide rack. PBS was gently tapped away from slides prior to applying the hybridization probe for *Vglut2*. The slides were placed in the humidifying rack and allowed to incubate for 2 h at 40 °C in a hybridization incubator. After hybridization, slides went through a series of washes with 1X RNAscope® wash buffer, followed by 4 amplification steps of the hybridization signal. After the wash and amplification step, slides were counterstained with DAPI and cover-slipped with Prolong Gold Anti-fade mounting medium (Life Technologies). *Vglut2* signal in matched sections of control and knockout groups was visualized with confocal microscopy (Leica TCS SP5; Leica Microsystems, Wetzlar, Germany).

Brain tissue preparation, imaging, and post-hoc analysis

After behavioral experiments were completed, study subjects were anesthetized with a ketamine/xylazine cocktail (100 mg/kg and 10 mg/kg, respectively) and subjected to transcardial perfusion. During perfusion, animals were flushed with 20 mL of saline prior to fixation with 20 mL of 10% buffered formalin. Freshly fixed brains were then extracted and placed in 10% buffered formalin in 4°C overnight for post-fixation. The next day, brains were transferred to 30% sucrose solution and allowed to rock at room temperature for 24 h prior to sectioning. Brains were frozen and sectioned into 30 µm slices with a sliding microtome and mounted onto slides for post-hoc visualization of injection sites and cannula placements. Injection sites were marked on an atlas where –EYFP or –EGFP fusion products were the densest. The location of cannula implants were noted by prominent lesion sites that extended over the rostro-caudal axis of the PVH. Mice with missed injections to the LH or misplaced optic fibers over the PVH were excluded from behavioral analysis. Representative pictures of LH and PVH injection sites and cannula placements were visualized with confocal microscopy (Leica TCS SP5; Leica Microsystems, Wetzlar,

Germany). Microinjection delivery to PVH was confirmed by injecting blue ink through the fluid injection cannula prior to perfusion. Blue ink perfusion in the PVH area was confirmed with a bright field microscope (Zeiss Axio Scope with AxioCam 506 color camera; Carl Zeiss Microscopy, Jena, Germany).

Statistics

GraphPad Prism 7.00 (GraphPad Software, Inc., La Jolla, CA, USA) was used for all statistical analyses and construction of graphs. Two-way repeated measures or regular two-way ANOVA followed by Dunnett's or Sidak's multiple comparisons tests were used for group comparisons. Single variable comparisons were made by paired or unpaired two-tailed Student's t-tests, ratio paired t-tests, Mann Whitney tests, or one-way ANOVA followed by Dunnett's or Tukey's multiple comparison post-hoc tests. Error bars in graphs were represented as mean \pm s.e.m. Sample size was chosen based on previously published work. All tests met assumptions for normal distribution, with similar variance between groups that were statistically compared. N values represent final number of animals used in experiments following genotype verification and post-hoc brain validation of injection sites/cannula placements.

Methods for Chapter 3

Subjects and Experimental Models

Animal care and procedures were approved by the University of Texas Health Science Center at Houston Institutional Animal Care and Use Committee. Mice were housed at 21-22°C on a 12 h light/ 12 h dark cycle (7 A.M. to 7 P.M. light), with ad libitum access to standard pellet chow, unless otherwise stated during fasting experiments. Sim1-Cre mice⁵⁰ were bred to Ai9 reporter mice²⁷³ to generate Sim1-Cre::Ai9; some of the subjects used in behavioral experiments contained the reporter gene for post-hoc visualization purposes. Sim1-Cre::Vglut2^{flox/flox} mice were generated as previously described⁵⁷. Vglut2-ires-Cre mice²⁵⁵ were purchased from Jackson Labs (stock no. 016963) and bred to C57 mice to generate Vglut2-ires-Cre subjects used in the experiments. Mice were at least 6 weeks old prior to surgeries and testing, and were chosen from multiple litters. All experiments were done during the light cycle, between the early afternoon hours (12 P.M.) and early evening before the start of the dark cycle.

Viruses and Surgery

The following viral constructs were delivered to the PVH via stereotactic surgery: For optogenetic experiments, AAV-EF1 α -DIO-hChR2(H134R)-EYFP-WPRE-hGHpA serotype 2/9 (IDDRC Neuroconnectivity Core, Baylor College of Medicine, Houston, Texas); AAV-EF1 α -DIO-EGFP serotype DJ8 (IDDRC Neuroconnectivity Core, Baylor College of Medicine, Houston, Texas); AAV-EF1 α -DIO-iC++-EYFP (University of North Carolina Vector Core, Chapel Hill, NC, USA); For anterograde tracing, AAV-EF1 α -FLEX-Syn::EGFP-WPRE-hGHpA, serotype DJ/8 (IDDRC Neuroconnectivity Core, Baylor College of Medicine, Houston, Texas);

For *ex vivo* electrophysiological recordings of Vglut2 positive and negative neurons in the midbrain, Chr2 virus as above was injected to PVH and AAV-EF1 α -DIO-EGFP serotype DJ8 virus was injected to the midbrain to label Vglut2 positive cells;

For combined optogenetic/DREADD-mediated inhibition, Chr2 virus as above was injected to PVH and AAV1-EF1 α -DIO-hM4D(Gi)-mCherry EYFP (University of North Carolina Vector Core, Chapel Hill, NC, USA) was injected in the midbrain-VTA area.

For fiber photometry experiments, AAV-EF1 α -FLEX-GCaMP6m (IDDRC Neuroconnectivity Core, Baylor College of Medicine, Houston, Texas) was delivered to the midbrain-VTA area. All viral preparations were tittered to at least 10¹¹ particles/mL.

Stereotaxic surgeries to deliver viral constructs and for optical fiber implantation were performed as previously described. Briefly, mice were anesthetized with a ketamine/xylazine cocktail (100 mg/kg and 10 mg/kg, respectively), and their heads affixed to a stereotaxic apparatus. Viral vectors were delivered through a 0.5 μ L syringe (Neuros Model 7000.5 KH, point style 3; Hamilton, Reno, NV, USA) mounted on a motorized stereotaxic injector (Quintessential Stereotaxic Injector; Stoelting, Wood Dale, IL, USA) at a rate of 40 nL/min. Viral delivery was targeted to the PVH (100 nL/side; AP: -0.5 mm; ML: \pm 0.2 mm; DV: -5.0 mm) or midbrain/VTA area (200-300 nL/side AP: -2.4 mm; ML: \pm 0.5 mm; DV: -4.6 mm). Uncleaved fiber optic cannulae (\emptyset 1.25 mm Stainless Ferrule, \emptyset 200 μ m Core, 0.39 NA; ThorLabs, Newton, New Jersey, USA) were precut to 4.5–4.8 mm and implanted above the PVH (AP: -0.5 mm; ML: 0 mm) or precut to 4.3-4.5 mm and implanted above midbrain/VTA (AP: -2.4 mm; ML: +0.5 mm). For glutamate receptor blockade experiments, a single cannula system allowing for interchangeable optic fiber and fluid delivery (Plastics1, Roanoke, VA) was implanted above the midbrain/VTA area. For fiber photometry, uncleaved fiber optic cannulae (\emptyset 1.25 mm Stainless Ferrule, \emptyset 400 μ m Core, 0.39 NA; ThorLabs, Newton, New Jersey, USA) were precut to 4.3-4.5 mm and implanted above the midbrain/VTA area. All cannulae implants

were secured on the head with adhesive gel (Loctite 454) and dental cement.

Experiments were conducted on subjects after a 3-4 week recovery period following surgery.

Acute Brain Slices Preparation and *in vitro* Electrophysiology Recordings.

For Sim1-Cre recordings, coronal brain slices (250–300 μm) containing the PVH or VTA from mice that had received stereotaxic injections of AAV-FLEX-ChR2-EYFP to PVH at least 3 weeks prior to the recording were cut in ice-cold artificial cerebrospinal fluid (aCSF) containing the following (in mM): 125 NaCl, 2.5 KCl, 1 MgCl₂, 2 CaCl₂, 1.25 NaH₂PO₄, 25 NaHCO₃, and 11 D-glucose bubbling with 95% O₂/5% CO₂. Slices containing the PVH were immediately transferred to a holding chamber and submerged in oxygenated aCSF. Slices were maintained for recovery for at least 1 h at 32–34 °C before transferring to a recording chamber. Individual slices were transferred to a recording chamber mounted on an upright microscope (Olympus BX51WI) and continuously superfused (2 ml/min) with ACSF warmed to 32–34 °C by passing it through a feedback-controlled in-line heater (TC-324B; Warner Instruments). Cells were visualized through a 40X water-immersion objective with differential interference contrast (DIC) optics and infrared illumination. Whole cell current-clamp recordings were made from neurons within the regions of the PVH showing high density of ChR2-EYFP expression, and whole cell voltage-clamp recordings in VTA/midbrain region were performed on cells surrounded by dense ChR2-EYFP expressing fibers. Pipettes were filled with a K⁺-based low Cl⁻ internal solution containing (in mM) 145 K₂Glu, 10 HEPES, 0.2 EGTA, 1 MgCl₂, 4 Mg-ATP, 0.3 Na₂-GTP, 10 Na₂-Phosphocreatine (pH 7.3 adjusted with KOH; 295 mOsm) for current clamp recordings. For voltage-clamp recordings, Patch pipettes (3–5 M Ω) were filled with a Cs⁺-based low Cl⁻ internal solution containing (in mM) 135 CsMeSO₃, 10

HEPES, 1 EGTA, 3.3 QX-314, 4 Mg-ATP, 0.3 Na₂-GTP, 8 Na₂-Phosphocreatine (pH 7.3 adjusted with CsOH; 295 mOsm). Membrane potentials were corrected for ~10 mV liquid junction potential. To activate ChR2-expressing neurons in PVH or CHR2-fibers in VTA/midbrain, light from a 473 nm laser (Opto Engine LLC, Midvale, UT, USA) was focused on the area of the recorded PVH neuron to produce spot illumination through optic fiber. Brief pulses of light (blue light, 1–2 ms, 1–2 mW/mm²) were delivered at the recording site at 10–15 s intervals under control of the acquisition software.

Vglut2-ires-cre mice, at least 3 weeks following virus infection, were anesthetized with Avertin (i.p) and transcardially perfused with ice-cold cutting solution containing the following (in mM): 75 sucrose, 73 NaCl, 26 NaHCO₃, 2.5 KCl, 1.25 NaH₂PO₄, 15 Glucose, 7 MgCl₂, and 0.5 CaCl₂, saturated with 95% O₂/5% CO₂. Horizontal slices (250 μm) containing the VTA were sectioned using a Leica VT 1000S vibratome, and transferred to a holding chamber with artificial cerebrospinal fluid (aCSF) containing (in mM): 123 NaCl, 26 NaHCO₃, 2.5 KCl, 1.25 NaH₂PO₄, 10 glucose, 1.3 MgCl₂, and 2.5 CaCl₂, and saturated with 95% O₂/5% CO₂ at 32°C for 1h, then maintained at room temperature for to allow for recovery prior to any electrophysiological recordings. Individual slices were transferred from the holding chamber to a heated recording chamber (31-33°C, Luigs-Neumann), in which they were submerged and continuously perfused with oxygenated aCSF at a rate of 2-3ml/min. Recordings were performed under infrared-differential interference contrast visualization on a fixed stage, upright microscope (Olympus BX51WI) equipped with a water immersion 40x objective. Pipettes with resistance 3-5 MΩ were pulled from borosilicate glass (OD 1.5 mm, ID 1.1 mm, Sutter Instruments) using a horizontal puller (Sutter P-1000), and filled with an internal patch solution containing (in mM): 142 K-gluconate, 10 HEPES, 1 EGTA, 2.5 MgCl₂, 0.25 CaCl₂, 4 Mg-ATP, 0.3 Na-GTP, and 10 Na₂-phosphocreatine, adjusted to pH 7.25-7.35, osmolality 295-305 with KOH. Whole-cell patch-clamp recordings data were digitized and collected using Multiclamp 700B amplifier, and Digidata 1550B digitizer, and Clampex 10

(Molecular Devices). Membrane potential were held at -60mV. The liquid junction potential was not corrected, and series resistance (Rs) was bridge balanced. Offline data analysis was performed using Clampfit 10 (Molecular Devices). To excite channelrhodopsin in brain slices, we illuminated the brain slices every 30s with blue light pulses (473 nm PSU-III-LED laser system, Optoengine), of short duration (1-3ms) through 40x water-immersion objective lens.

Optogenetic Experimental Parameters

For *in vivo* photostimulation/inhibition, an integrated rotary joint patch cable connected the ferrule end of optic fiber cannula with a Ø1.25 mm ferrule end of the patch cable via a mating ceramic sleeve (ThorLabs, Newton, New Jersey, USA). At the other end of the rotary joint, an FC/PC connector was connected to a 473 nm diode-pumped solid state (DPSS) laser (Opto Engine LLC, Midvale, Utah, USA). Light pulses were controlled by Master-8 pulse stimulator (A.M.P.I., Jerusalem, Israel). For behavioral experiments requiring a large chamber (Real Time Place Preference/Avoidance, locomotion, and escape hut assays) a commutator (rotary joint; Doric, Québec, Canada) was attached to a patch cable via FC/PC adapter. The patch cable was then attached to the optic fiber cannula ferrule end via a ceramic mating sleeve. Another patch cable containing FC/PC connections at both ends allowed the connection between the commutator and the laser, which was controlled by the Master-8 pulse stimulator. During testing, mice were placed in a clean, high-walled enclosure or in a large chamber wiped down with 70% isopropyl alcohol. Light power was measured before starting experiments each day with an optical power meter (ThorLabs), and adjusted to emit an output of 5-15 mW from the end of the mating sleeve.

Behavioral Analysis

Grooming and Escape-Jumping

To measure the effects of photostimulation on baseline behavior, mice were placed in a clean, high-walled enclosure, which prevented escape from the chamber. Sim1-Cre mice were observed for grooming and recorded with a hand-held camera for a 15 minute period with the following protocol: 5 minutes, no light (Pre), 5 minutes, light-on (On), and 5 minutes post-light (Post). A 6 minute observation period for jumping behavior in Sim1-Cre mice was performed following 2 minutes pre-light, 2 minutes light-on, and 2 minutes post-light. Vglut2-ires cre mice were observed for grooming and jumping during the 15 minute protocol.

For PVH photostimulation, light was pulsed at a 5 Hz frequency with 10 or 100 ms pulse-width duration, and 20 Hz- 10 ms for PVH→midbrain photostimulation. Behavioral changes were annotated by watching the videos using QuickTime Player (Apple). Time spent grooming was carefully annotated by noting the video timestamps at the beginning of grooming bouts and end of grooming bouts. Beginning of bouts was defined as the moment the animal started engaging in forelimb paw strokes made near the nose, eyes, and head, and licking of paw, body, tail, or genitals, and the end of bouts was noted when grooming was interrupted for at least 6 seconds. The latency to start grooming was defined as the precise time mice started grooming following the first pulse of light. Number of jumps during the 15 minute test was quantified by watching videos in slow motion and counting each jump mice made, as defined by removal of limbs from the floor of the cage and complete suspension of the body in air. Grooming and escape-jumping observations were performed one hour following intraperitoneal (i.p.) injection of saline or CNO (1 mg/kg) in Vglut2-ires-Cre mice expressing hM4D(Gi)-mCherry in the midbrain.

Glutamate Receptor Blockade

Mice implanted with interchangeable fluid delivery/optic fiber cannula system (Plastics1, Roanoke, VA) were anesthetized with isoflurane and placed in a stereotactic apparatus. A microinjection volume of 100 nL, directed to the midbrain/VTA area, was slowly infused at an approximate rate of 33 nL/min. Three minutes following infusion, fluid delivery cannula were removed from the guiding cannula and replaced with optic fiber cannula, and mice were allowed to recover from anesthesia for 10-15 minutes prior to testing. Mice were then placed in a high-walled enclosure and video recorded for 5 minutes during photostimulation (20 Hz, 10 ms pulses). Jumping behavior was annotated as described above. Two separate trials were performed in the same mice on separate days: a control (vehicle injection) trial and drug (glutamate receptor blockade injection) trial. Vehicle injections consisted of 15% DMSO, while drug injections consisted of 300 ng D-AP5 + 150 ng DNQX (Tocris, Minneapolis, MN) suspended in 15% DMSO.

Locomotion

Mice were placed in a large (45 X 45 X 50 cm³) chamber, equipped with an overhead infrared camera (PhenoTyper system 3.0, Noldus, Wageningen, the Netherlands), and allowed to freely roam during a 15 minute test, consisting of 5 minutes no-light, 5 minutes light-on, and 5 minutes post-light. Light was pulsed at 5 Hz, 10 ms for PVH photostimulation, and 20 Hz, 10 ms for PVH→midbrain photostimulation. Locomotion assays were performed one hour following intraperitoneal (i.p.) injection of saline or CNO (1 mg/kg) in Vglut2-ires-Cre mice expressing hM4D(Gi)-mCherry in the midbrain. Locomotion data, including total distance travelled and average velocity, was collected by tracking software (EthoVision XT 11.5, Noldus) for each 5 minute period. Activity tracks were visualized by plotting movement of the mouse based on center-point location, as captured by the overhead camera.

Real Time Place Preference/Avoidance Assays

For RTPP/A assays, mice were allowed to freely explore a large 45 X 45 X 50 cm³ chamber, as detailed above, during a 20 minute testing period. The chamber was evenly divided into two sectors, one of which was randomly assigned as the light-on side. Crossing over and occupying the light-paired side of the chamber triggered continuous pulsing of light (5 Hz, 100 ms light pulses for PVH photostimulation, and 20 Hz, 10 ms pulses for PVH→midbrain photostimulation), which ceased once animals returned to the light-off side. The side of the chamber paired with light was counterbalanced during experiments for each mouse. RTPP/A assays were performed one hour following intraperitoneal (i.p.) injection of saline or CNO (1 mg/kg) in *Vglut2-ires-Cre* mice expressing hM4D(Gi)-mCherry in the midbrain. The percent time spent on each side and time spent in the food zone, as well as the tracking data, were collected by EthoVision tracking software (Noldus). Heatmaps detailing proportion of time spent in each location of the arena, as well as activity tracks, were visualized based on the data collected.

Modified RTPP/A Assay-Fast Refeed

Mice were fasted 24h prior to testing fast-refeeding in a large chamber containing food in one corner of the arena. The location of food was rotated amongst four corners of the cage, and the light-paired side was counterbalanced for each mouse tested. Upon crossing into the light-paired side, light was pulsed through the optical fiber into the brain at 5 Hz, 10 ms for PVH activation or 20 Hz, 10 ms for PVH→midbrain activation, and ceased upon exit into the light-unpaired side. Total testing time lasted 15 minutes. The percent time spent on each side and time spent in the food zone, as well as the tracking data, were collected by EthoVision tracking software (Noldus). Heatmaps detailing proportion of time spent in each location of the arena, as well as activity tracks, were visualized based on the data collected.

Conditioning Assay

Sim1-Cre mice with ChR2 injected into the PVH and optical fibers placed over the midbrain, were placed in a large testing chamber with flooring on one side lined with several columns of green tape spanning the top to bottom edges of the cage. On day 0, mice tethered to an optic fiber cable delivering no light, were allowed to freely explore the arena for 20 minutes; the side most preferred, as determined by percent time spent on each side, was noted and assigned as the light-paired side for the subsequent days of conditioning. For the next 4 days of conditioning, mice were tested approximately at the same time for 20 minutes, during which optic fiber cable delivered 20 Hz, 10 ms photostimulation upon crossing the light-paired side of the chamber, and ceased once mice traversed to the light-off side. Mice were thereafter tested for 20 minutes on days 5-6 for extinction, during which light was no longer delivered through the optic fiber. The preference for the light-on zone, initially the most preferred side, was calculated as the percent time mice spent in the light-paired side of the chamber for each trial. Locomotion data to calculate the distance travelled during testing sessions were collected by EthoVision tracking software (Noldus).

Escape Hut Assay

For this assay, an “escape hut”, equipped with a single entry and three 9.5 cm walls with no “roof” (in order to maintain top-down visualization of tracking from the overhead camera) was placed in the center of a large chamber. Testing was performed one hour following intraperitoneal (i.p.) injection of saline or CNO (1 mg/kg) in Vglut2-ires-Cre mice expressing hM4D(Gi)-mCherry in the midbrain. Mice were first acclimated to the novel environment for seven minutes, which allowed sufficient time for spontaneous discovery of the hut. After acclimation, an eight-minute testing period immediately followed, in

which light was continuously pulsed at 5-10 Hz (10 ms pulse width) every other minute. The number of hut visits (defined as the number of times the animal approached and entered the hut) and duration in the hut (quantified as the time spent inside the hut enclosure) were quantified by EthoVision software (Noldus). Number of hut visits and total time spent inside the hut across each time interval (Off vs. On) was combined for statistical analysis. Total distance travelled during each time interval was also combined for analysis, and velocity was averaged across each light-off and light-on periods to reveal average velocity during the two light conditions. Heatmaps across time intervals were constructed based on tracking data collected by EthoVision software.

Fiber Photometry and Modified T-maze

Fiber photometry system was purchased from Doric Lenses (Québec, Canada). In short, mice with optic fiber implants were attached to fiber-optic patch cords, connected to 465 nm LED light modulated by fluorescence mini cubes containing beam splitters that combine excitation wavelengths and separate emission wavelengths. Fluorescence emission was collected by a photodetector capable of sensing low-intensity light. A single console synchronized output control over external LED drivers and acquisition of input data. Doric Neuroscience Studio software was used to collect data over the course of recording sessions. Following handling, mice were placed in a pre-experimental habituation cage for two minutes. GcaMP6m recording commenced at the end of the two minute habituation, a few seconds prior to placing mice on the t-maze. The t-maze was modified to include one open arm and two closed arms, allowing for a two-way escape strategy. Baseline fluorescence, F_0 , was defined as the non-linear regression fit (to horizontal line) of fluorescence data collected in the first 10 seconds of the recording period. After collection of baseline recordings, mice were placed at the base of the open arm and allowed to freely explore the apparatus for three minutes. Changes in neural activity over time were quantified by subtracting instantaneous fluorescence from

baseline fluorescence and dividing by baseline $((F-F_0)/F_0, \text{ or } \Delta F/F)$. For data quantification and representation purposes, mean changes in fluorescence occurring in the first five seconds was subtracted from $\Delta F/F$ for each time point, and were aligned to the first exposure to the maze and the final exit to a closed arm. Changes in fluorescence were averaged in five second time windows occurring just before, and 15 seconds after the alignment period to allow quantitative comparison across time.

Immunohistochemistry and Imaging

After behavioral experiments were completed, study subjects were anesthetized with a ketamine/xylazine cocktail (100 mg/kg and 10 mg/kg, respectively) and subjected to transcardial perfusion. During perfusion, animals were flushed with 20 mL of saline prior to fixation with 20 mL of 10% buffered formalin. Freshly fixed brains were then extracted and placed in 10% buffered formalin in 4 °C overnight for post-fixation. The next day, brains were transferred to 30% sucrose solution and allowed to rock at room temperature for 24 h prior to sectioning. Brains were frozen and sectioned into 30 μm slices with a sliding microtome and mounted onto slides for post-hoc visualization of injection sites and cannula placements. Injection sites were determined by the densest regions of –EYFP, –EGFP, or mCherry fusion products. The location of cannula implants were noted by prominent lesion sites that extended over the rostro-caudal axis of the PVH or VTA/midbrain area. Mice with missed injections to the PVH or VTA/midbrain, or those with misplaced optic fibers over the areas of interest were excluded from behavioral analysis. Representative pictures of PVH, PVH projections, and VTA/midbrain injection sites were visualized with confocal microscopy (Leica TCS SP5; Leica Microsystems, Wetzlar, Germany). Brain sections used for immunohistochemistry (IHC) were stained with the following primary antibodies, followed by secondary antibodies: mouse anti-tyrosine hydroxylase (TH) (Millipore, MAB318)/Alexa Fluor 488, donkey anti-mouse or Alexa Fluor 594 donkey anti-mouse; rabbit anti-cFos (Cell Signal #2250)/Alexa Fluor 488

donkey anti-rabbit or Alexa Fluor 594 donkey anti-rabbit. Sections were washed three times, ten minutes each, in 1XPBS, and then blocked with 5% normal donkey serum (NDS) in a solution containing 0.3% triton-X-100 (TX-100) in 1XPBS for 1 hour at room temperature. After blocking, blocking serum was removed and primary antibody diluted in fresh 5% NDS was added to sections and then transferred to a shaking rocker in 4°C for overnight incubation. The next day, primary antibody solution was removed and sections were washed three times, ten minutes each, in a solution containing 0.1% TX-100 in 1XPBS. Upon removing the last wash, secondary antibody, diluted in fresh 5% NDS solution, was then added to sections, and allowed to rock at room temperature for two hours. Following secondary antibody incubation, sections were washed three times with 0.1% TX-100/1X PBS solution and mounted on slides for imaging. Sim1-Cre mice used for cFos analysis were placed separately in clean testing cages, provided with food, water, and bedding for two hours prior to photostimulation. Mice were then photostimulated with 20 Hz light pulses (10 ms pulse-width duration) for five seconds, followed by five seconds of no light, repeated for 15 minutes. Following photostimulation, mice were subjected to transcardial perfusion 1.5 hours later and brain sections processed for IHC. Vglut2-ires-Cre mice used for cFos analysis were first i.p. injected with CNO, and placed in clean testing cages 30 minutes prior to photostimulation. Photostimulation was then applied for 15 minutes (20 Hz, 10 ms pulses every five seconds), and mice were transcardially perfused 1.5 hours later.

Statistics

GraphPad Prism 7 software (La Jolla, CA) was used for statistical analysis. Two-way repeated measures ANOVA, followed by Dunnett's or Sidak's multiple comparisons tests, and ordinary or repeated measures one-way ANOVA tests, followed by Dunnett's or Tukey's multiple comparisons test, were used for comparisons of more than two groups. Paired or unpaired two-tailed t-tests were used for comparing two groups. Pearson correlation (two-

tailed) was used to analyze correlation between two variables. A cubic spline function was used to smooth GCaMP6m signal in graphs showing individual and averaged traces. Data in figures, text and legends were expressed as means \pm SEMs. Significance levels were denoted by asterisks: * $p < 0.05$, ** $p < 0.01$, *** $p < 0.001$, **** $p < 0.0001$.

Chapter 5.

Discussion

Intrahypothamic circuits regulate feeding and stress-related behavior in an antagonistic manner

Our study identified the significance of LH→PVH circuit in feeding regulation and behavioral manifestation of stress, particularly repetitive self-grooming. Using genetic tools that allowed access to both GABA and glutamate neuron populations in the LH, along with optogenetics, electrophysiology, and behavioral assays, we identified novel circuit components that selectively and antagonistically drive one behavior over the other. Specifically, photostimulation of GABAergic LH fibers in PVH rapidly evoked intense feeding behavior, whereas inhibition of the circuit significantly reduced feeding after a 24 hour fast. Additionally, photostimulation of the circuit promptly halted ongoing grooming, and in turn, promoted a drive to feed, an effect that was reversible upon termination of photostimulation. In parallel, photostimulation of glutamatergic LH fibers in PVH induced blatant repetitive self-grooming behavior shortly after the first pulse of light. Detailed behavioral analysis revealed a stereotypical stress-like pattern of the evoked grooming, which was corroborated by inhibition experiments that showed silencing of the circuit significantly reduced repetitive grooming induced by a mild stressor (water spray). Activation of the glutamatergic LH→PVH circuit suppressed feeding after a fast, and promoted repetitive self-grooming instead. Genetic and pharmacological experiments, coupled with optogenetic behavioral assays, revealed the necessity of GABA and glutamate release from LH neurons onto PVH in promoting the evoked behaviors.

Recent studies have identified the PVH as a central hub for integrating information on energy status and producing appropriate behavioral and autonomic output, via relays to downstream brainstem nuclei⁴⁶. Acute inhibition of PVH neurons using chemogenetic techniques have shown that suppressing PVH neural activity is sufficient to induce increased feeding behavior (see Table 2). Until recently, main inhibitory input onto PVH neurons for driving feeding was thought to emanate from Arc^{AgRP} neurons; however, a

previous study by our group suggested that additional sources of GABAergic input from non-Agrp neurons and other hypothalamic sites were required for feeding regulation^{64, 69}. Indeed, recent publications, as well as our study here, prove that inhibitory input onto PVH from nearby hypothalamic sites other than Arc^{Agrp} neurons drives feeding behavior^{61, 69, 72}.

Oppositely, studies have shown activation of PVH neurons suppresses feeding (see Table 2), and our research supports this finding, identifying a novel source of glutamatergic input for PVH action on feeding suppression.

Classic electrical stimulation studies of the PVH suggested a role for this nucleus in complex behaviors other than in feeding, including self-grooming²⁷⁷. Indeed, recent studies have shown that activation of hypothalamic centers including Arc^{Agrp} and LH produces emotional and motivational changes^{35, 107, 163}, suggesting that homeostatic brain centers function dually in emotional regulation and feeding¹³³. In line with many recent reports¹³³, activation of a feeding-promoting circuit (LH^{GABA}→PVH) induced behavioral approach, indicating positive valence, whereas activation of a feeding-suppressive circuit (LH^{Glutamate}→PVH) encodes behaviors indicative of aversion or negative valence (in this case, stress-related grooming). Although the valence of activating the LH^{Glutamate}→PVH pathway in this study was not formally tested (the rigidity of stationary repetitive self-grooming evoked by photostimulation precluded free movement in the RTPP chamber), our experiments indicated that suppressing PVH neural activity following a highly stressful and aversive event (immobilization stress) significantly reduced behavioral expression (i.e., repetitive self-grooming) following the aversive experience. This suggests that increased activity of PVH neurons is required for elicitation of at least one type stress-related behavior. Future experiments will be needed to identify the role of PVH neurons in other behavioral manifestations of stress.

PVH neurons are heterogeneously composed of many different neural populations, many of which express neuropeptides that are essential for hormonal functions⁴⁶.

Additionally, some of these neuropeptide-expressing populations, such as those expressing oxytocin and vasopressin, have roles in complex behaviors outside of hormonal regulation through interactions with other brain areas^{278, 279}. Interestingly, our study does not support a role for neuropeptides in the competitive action of feeding vs. self-grooming by manipulating PVH activity. Instead, the antagonistic nature of behaviors through PVH action relied upon glutamate release. Notably, glutamate release was also required for feeding-inhibiting effects of PVH activation, suggesting that glutamatergic transmission from PVH neurons onto downstream sites, such as in the PBN⁵¹, is essential for satiety regulation. However, we cannot completely rule out a role for neuropeptides in grooming, as photoactivation in mice lacking Vglut2 in PVH still produced grooming behavior, although evoked grooming was significantly reduced compared to intact Vglut2 animals. Future studies will be needed to clarify whether the evoked grooming in the presence or absence of glutamate release are phenotypically the same (but differ in degree) or differing in subtype. For example, it may be possible that neuropeptide-driven grooming may promote a grooming subtype that is part of a behavioral satiety sequence (grooming following a meal)²⁸⁰ and unrelated to stress.

Recent studies have supported appetite-stimulating and rewarding roles for LH^{GABA} neurons¹⁰⁷, in part via projections to the VTA^{111, 156}, and appetite-suppressing and aversive roles for LH^{Glutamate} neurons (via projections to the VTA and lateral habenula)^{110, 156}. Our study provides additional evidence that bidirectional control of feeding, concurrent with changes in emotional valence, are controlled by two separate populations in a single hypothalamic region. However, as suggested by another recent publication, GABA and glutamate LH projections to other brain regions, in this case, the PAG, may produce differing behavioral outcomes (prey pursuit vs. defensive behavior in the form of evasion) but encode similar emotional output (negative valence in this example)¹⁶². Thus, it appears that GABA and glutamate LH neurons generally produce opposing behavioral states and encode positive or negative emotions based on projection site.

Repetitive grooming behavior in mice is used as a behavioral read-out for maladaptive compulsivity, and is analogous to pathological behaviors in human psychiatric conditions like obsessive-compulsive disorder (OCD)²⁸¹. Association between OCD, compulsivity and eating disorders in humans suggests a shared neural basis for these conditions, though a clear mechanism is presently unknown^{282, 283}. Given the results of our findings, that showed the replacement of hunger-driven feeding with a stress-like compulsive behavior (i.e., repetitive self-grooming), one may posit that synchronous over-activation of neurotransmission in the LH→PVH circuit may underlie maladaptive compulsivity and anorexia. Alternatively, insufficient signaling via the GABA component in the LH→PVH circuit may also lead to changes in behavior that negatively impact normal adaptations to stress and hunger. The basis for these and many other brain disorders are bound to be much more complex than malfunction in one circuit, but in the context of larger neural ensembles, a single component may prove to be a significant contributing factor²⁸⁴.

Defensive behaviors driven by a novel hypothalamic-midbrain circuit suppress feeding

In order to deal with a myriad of environmental challenges, the brain has developed sophisticated and redundant pathways for the manifestation of defensive behaviors²⁴². These include fleeing, freezing, defensive aggression, and other related behaviors, which are strategically employed depending on the context²⁴⁰. Using markers of neuronal activation, previous research identified brain regions activated by threatening stimuli *post-hoc*^{285, 286}. These included certain nuclei of the hypothalamus, brainstem and amygdala^{285, 286}. Subsequent studies were able to confirm causal involvement of some of these nuclei (including the VMH, AHN, and PAG) in the repertoire of defensive responses^{171, 172, 179, 180}. As shown by post-hoc analysis studies, additional hypothalamic sites not traditionally deemed as part of the medial hypothalamic zone defensive system²⁵⁸ were responsive to

predator threat²⁸⁶. This included the PVH region²⁸⁶, a critical site involved in feeding regulation as described throughout this thesis. The first study presented here described a role for PVH in stress-related grooming behavior; extending those findings, we desired in this study to map downstream projection sites targeted by PVH neurons that were responsible for stress-related behavior.

Previous work identified another hypothalamic to midbrain circuit projection in defensive behavior (VMH→PAG)¹⁷². However, photoactivation of this projection elicited freezing-type behavior and not escape¹⁷². Here, we identified a role for the PVH in escape behavior, via projections to a separate midbrain region in and surrounding the VTA. Interestingly, PVH neurons project to the PAG and have a role in satiety through this projection⁵⁹; however a behavioral role for PVH→PAG circuit has not been described. Given that photostimulation of the PVH→midbrain (VTA) circuit, as shown in this work, promoted active defense responses (flight and escape), it would be interesting if collateral or non-collateralized projections to the PAG evokes a separate set of defensive responses, like freezing. Indeed, broad optogenetic activation of PAG neurons induced a mix of defensive behaviors (freezing, flight, and avoidance)¹⁷⁹, and *in vivo* recordings showed that different subsets of neurons in PAG differentially correlate with different defensive behaviors¹⁷⁹. Given that VMH→PAG circuit favors freezing¹⁷², it is possible that separate PAG neural subsets that promote escape and/or flight are targeted by PVH. Because glutamate receptor blockade in the VTA/midbrain region only partially blocked light-evoked escape behavior, it is possible that PVH promotes this subtype of defense by activating PAG and/or other brain sites. Future studies will be needed to delineate if redundant PVH circuits contribute to defensive behaviors observed here.

Extending the first study described in Chapter 3, we aimed to explore whether PVH neurons regulate other subtypes of stress-related behavior in addition to repetitive self-grooming. We found that more intense photostimulation of PVH neurons favored transition

from self-grooming to defensive responses (escape-jumping), and that evoked behaviors were negatively correlated during photostimulation sessions. The reason for transition between the two behaviors concomitant with mounting intensity of photostimulation is unknown; however, the phenomenon could be due to 1) greater recruitment of ChR2-expressing cells in infected PVH neurons; or 2) a greater activation gain in the same ChR2-cells in response to higher intensity of light; or 3) a combination of both factors. Supporting that at least hypothesis 2 may be correct, electrophysiological recordings in PVH neurons showed prolonged depolarization in proportion to the longer light pulse. Prolonged depolarization in the form of plateau potentials, as evident by our data, indicates greater calcium flux, and therefore greater neurotransmitter release²⁸⁷. Thus, greater flux of glutamate from PVH onto downstream brain sites favored elicitation of escape behavior. This point is supported by empirical findings that PVH→midbrain photostimulation required higher frequency light pulses for eliciting obvious behavioral change. Notably, frequencies less than 20 Hz (5 and 10 Hz, data not shown) was not sufficient in producing overt escape-jumping or repetitive grooming across mice. It was indeed interesting that repetitive grooming appeared *following* light stimulation of PVH→midbrain circuit, as opposed to during light stimulation of PVH neurons directly. However, in the absence of glutamate release, PVH→midbrain photostimulation evoked repetitive grooming during and after the light-on period, suggesting that neuropeptidergic transmission in this circuit plays a significant role in grooming behavior. Glutamate release was necessary for light-evoked jumping, but not grooming, suggesting that PVH regulates two distinct, and competing stress-related behaviors, possibly by distinct or the same neural populations (as certain neuropeptide-expressing cells can also use glutamate as a neurotransmitter^{58, 168, 288}). Future studies will be required to decipher precise neural subsets in PVH mediating the two behaviors.

Interestingly, a hunger state (induced by activating Arc^{AgRP} neurons, or simply fasting) is reported to reduce anxiety and fear states, supposedly by imposing a direct competition in survival circuits for favoring adaptive responses to imminent threats^{164-166, 289}. This would allow a greater chance of survival, for example, if an animal proceeded to embark on unfamiliar, possibly dangerous territory in search for food if death would be otherwise forthcoming in the face of starvation and scarcity. At the same time, a neural basis for placing greater priority on defensive responses and risk assessment over feeding would be required in other situations, even during hunger. For example, taken the situation described above, if the animal found food in the dangerous location, and proceeded to eat, one would expect rapid cessation of ongoing feeding and flight away from the site if an immediate threat appeared (e.g., a predator). Our study revealed the participation of PVH→midbrain circuit in this latter scenario, as activation of glutamatergic signaling in the pathway severely interfered with intense attempts to approach and eat food that was placed in a location paired with photostimulation of the circuit. Notably, during testing in the RTPP/A assay, mice did not automatically display escape-jumping, but instead quickly learned to avoid the light-paired side. Thus, it appears that activation of the PVH→midbrain circuit promotes emotional components of aversion independent of evoking escape-jumping behaviors. These findings suggest, that like VMH populations in defense¹⁷¹, PVH neurons function simultaneously in adaptive behaviors and related emotional states.

Future Directions

Technological advances in neuroscience have made probing brain function increasingly more accessible, and further development will surely help pave the way to more precise interrogation of neural circuit function in emotion and behavior²⁹⁰. Combined with genetic tools and better animal models for human neurological and psychiatric illnesses, we will start to unravel the neural underpinnings behind prevalent conditions in which there are

no cures or effective treatment options^{284, 291}. The studies described here have implications for the neural basis behind conditions such as eating and feeding-related disorders, compulsive disorders, and obesity. However, in order to prove causality for these brain disorders, testing the significance of the described circuit components during pathological behaviors or animal models of disease would be necessary. Employing dual use of *in vivo* imaging, as described in the last experiment of Chapter 3, along with optogenetics in a closed-loop system would prove useful for predicting neuronal activity abnormalities that precede maladaptive behaviors, which could be modified with optogenetic techniques²⁹². For example, a feasible experiment, using a post-traumatic stress disorder model in mice^{293, 294}, would monitor changes in PVH neural activity during recall of a fearful memory; the activity patterns indicative of stress may precede maladaptive coping behaviors or impaired extinction of fear-associated cues, which may be mediated by downstream sites in the midbrain/VTA area. Implanting an optic fiber over the midbrain area, and inhibiting glutamatergic-midbrain neurons immediately when this pattern is detected may be able to block pathological behavioral changes. If mice can be wired in a way that precludes the interference from patch cables and cords^{295, 296}, then a closed-loop control of neural activity can be achieved long-term in the living environment, and alter phenotypic expression of common features in fear-based disorders, such as depressive behavior and anhedonia^{210, 293}. Analogously, a similar system could be set up for monitoring and modifying LH^{GABA}→PVH circuit in a binge-eating model, in order to probe the causality and necessity of neural circuit activity in binge-eating behavior. Given that these tools are forthcoming, future studies will be able to delve deeper into the intricacies of neural circuit dynamics for a range of motivated behaviors and emotional states.

Bibliography

- [1] Lein ES, Hawrylycz MJ, Ao N, Ayres M, Bensinger A, Bernard A, Boe AF, Boguski MS, Brockway KS, Byrnes EJ, Chen L, Chen L, Chen TM, Chin MC, Chong J, Crook BE, Czaplinska A, Dang CN, Datta S, Dee NR, Desaki AL, Desta T, Diep E, Dolbeare TA, Donelan MJ, Dong HW, Dougherty JG, Duncan BJ, Ebbert AJ, Eichele G, Estin LK, Faber C, Facer BA, Fields R, Fischer SR, Fliss TP, Frensley C, Gates SN, Glattfelder KJ, Halverson KR, Hart MR, Hohmann JG, Howell MP, Jeung DP, Johnson RA, Karr PT, Kawal R, Kidney JM, Knapik RH, Kuan CL, Lake JH, Laramée AR, Larsen KD, Lau C, Lemon TA, Liang AJ, Liu Y, Luong LT, Michaels J, Morgan JJ, Morgan RJ, Mortrud MT, Mosqueda NF, Ng LL, Ng R, Orta GJ, Overly CC, Pak TH, Parry SE, Pathak SD, Pearson OC, Puchalski RB, Riley ZL, Rockett HR, Rowland SA, Royall JJ, Ruiz MJ, Sarno NR, Schaffnit K, Shapovalova NV, Sivisay T, Slaughterbeck CR, Smith SC, Smith KA, Smith BI, Sodt AJ, Stewart NN, Stumpf KR, Sunkin SM, Sutram M, Tam A, Teemer CD, Thaller C, Thompson CL, Varnam LR, Visel A, Whitlock RM, Wohnoutka PE, Wolkey CK, Wong VY, Wood M, Yaylaoglu MB, Young RC, Youngstrom BL, Yuan XF, Zhang B, Zwingman TA, Jones AR: Genome-wide atlas of gene expression in the adult mouse brain. *Nature* 2007, 445:168-76.
- [2] Hill JO, Peters JC: Environmental contributions to the obesity epidemic. *Science (New York, NY)* 1998, 280:1371-4.
- [3] Corsica JA, Hood MM: Eating disorders in an obesogenic environment. *Journal of the American Dietetic Association* 2011, 111:996-1000.
- [4] Gonzalez-Muniesa P, Martinez-Gonzalez MA, Hu FB, Despres JP, Matsuzawa Y, Loos RJF, Moreno LA, Bray GA, Martinez JA: Obesity. *Nature reviews Disease primers* 2017, 3:17034.
- [5] Drewnowski A, Darmon N: Food choices and diet costs: an economic analysis. *The Journal of nutrition* 2005, 135:900-4.
- [6] Murray S, Tulloch A, Gold MS, Avena NM: Hormonal and neural mechanisms of food reward, eating behaviour and obesity. *Nature reviews Endocrinology* 2014, 10:540-52.
- [7] Volkow ND, Wise RA, Baler R: The dopamine motive system: implications for drug and food addiction. *Nature reviews Neuroscience* 2017, 18:741-52.
- [8] Richard D: Cognitive and autonomic determinants of energy homeostasis in obesity. *Nature reviews Endocrinology* 2015, 11:489-501.
- [9] Monteleone P, Maj M: Dysfunctions of leptin, ghrelin, BDNF and endocannabinoids in eating disorders: beyond the homeostatic control of food intake. *Psychoneuroendocrinology* 2013, 38:312-30.
- [10] Waterson MJ, Horvath TL: Neuronal Regulation of Energy Homeostasis: Beyond the Hypothalamus and Feeding. *Cell metabolism* 2015, 22:962-70.
- [11] Sternson SM, Nicholas Betley J, Cao ZF: Neural circuits and motivational processes for hunger. *Current opinion in neurobiology* 2013, 23:353-60.
- [12] Fischer EK, O'Connell LA: Modification of feeding circuits in the evolution of social behavior. *The Journal of experimental biology* 2017, 220:92-102.
- [13] Sweeney P, Yang Y: Neural Circuit Mechanisms Underlying Emotional Regulation of Homeostatic Feeding. *Trends in endocrinology and metabolism: TEM* 2017, 28:437-48.
- [14] Sohn JW, Elmquist JK, Williams KW: Neuronal circuits that regulate feeding behavior and metabolism. *Trends in neurosciences* 2013, 36:504-12.
- [15] Zhang X, van den Pol AN: Dopamine/Tyrosine Hydroxylase Neurons of the Hypothalamic Arcuate Nucleus Release GABA, Communicate with Dopaminergic and Other Arcuate Neurons, and Respond to Dynorphin, Met-Enkephalin, and Oxytocin. *The Journal of neuroscience : the official journal of the Society for Neuroscience* 2015, 35:14966-82.

- [16] Aponte Y, Atasoy D, Sternson SM: AGRP neurons are sufficient to orchestrate feeding behavior rapidly and without training. *Nature neuroscience* 2011, 14:351-5.
- [17] Atasoy D, Betley JN, Su HH, Sternson SM: Deconstruction of a neural circuit for hunger. *Nature* 2012, 488:172-7.
- [18] Krashes MJ, Koda S, Ye C, Rogan SC, Adams AC, Cusher DS, Maratos-Flier E, Roth BL, Lowell BB: Rapid, reversible activation of AgRP neurons drives feeding behavior in mice. *The Journal of clinical investigation* 2011, 121:1424-8.
- [19] Zhan C, Zhou J, Feng Q, Zhang JE, Lin S, Bao J, Wu P, Luo M: Acute and long-term suppression of feeding behavior by POMC neurons in the brainstem and hypothalamus, respectively. *The Journal of neuroscience : the official journal of the Society for Neuroscience* 2013, 33:3624-32.
- [20] Dodd GT, Decherf S, Loh K, Simonds SE, Wiede F, Balland E, Merry TL, Munzberg H, Zhang ZY, Kahn BB, Neel BG, Bence KK, Andrews ZB, Cowley MA, Tiganis T: Leptin and insulin act on POMC neurons to promote the browning of white fat. *Cell* 2015, 160:88-104.
- [21] Luquet S, Perez FA, Hnasko TS, Palmiter RD: NPY/AgRP neurons are essential for feeding in adult mice but can be ablated in neonates. *Science (New York, NY)* 2005, 310:683-5.
- [22] Bewick GA, Gardiner JV, Dhillo WS, Kent AS, White NE, Webster Z, Ghatei MA, Bloom SR: Post-embryonic ablation of AgRP neurons in mice leads to a lean, hypophagic phenotype. *FASEB journal : official publication of the Federation of American Societies for Experimental Biology* 2005, 19:1680-2.
- [23] Gropp E, Shanabrough M, Borok E, Xu AW, Janoschek R, Buch T, Plum L, Balthasar N, Hampel B, Waisman A, Barsh GS, Horvath TL, Bruning JC: Agouti-related peptide-expressing neurons are mandatory for feeding. *Nature neuroscience* 2005, 8:1289-91.
- [24] Vink T, Hinney A, van Elburg AA, van Goozen SH, Sandkuijl LA, Sinke RJ, Herpertz-Dahlmann BM, Hebebrand J, Remschmidt H, van Engeland H, Adan RA: Association between an agouti-related protein gene polymorphism and anorexia nervosa. *Molecular psychiatry* 2001, 6:325-8.
- [25] Krude H, Biebermann H, Gruters A: Mutations in the human proopiomelanocortin gene. *Annals of the New York Academy of Sciences* 2003, 994:233-9.
- [26] Sternson SM: Hypothalamic survival circuits: blueprints for purposive behaviors. *Neuron* 2013, 77:810-24.
- [27] Kim KS, Seeley RJ, Sandoval DA: Signalling from the periphery to the brain that regulates energy homeostasis. *Nature reviews Neuroscience* 2018, 19:185-96.
- [28] Konner AC, Janoschek R, Plum L, Jordan SD, Rother E, Ma X, Xu C, Enriori P, Hampel B, Barsh GS, Kahn CR, Cowley MA, Ashcroft FM, Bruning JC: Insulin action in AgRP-expressing neurons is required for suppression of hepatic glucose production. *Cell metabolism* 2007, 5:438-49.
- [29] van den Top M, Lee K, Whyment AD, Blanks AM, Spanswick D: Orexigen-sensitive NPY/AgRP pacemaker neurons in the hypothalamic arcuate nucleus. *Nature neuroscience* 2004, 7:493-4.
- [30] Cowley MA, Smart JL, Rubinstein M, Cerdan MG, Diano S, Horvath TL, Cone RD, Low MJ: Leptin activates anorexigenic POMC neurons through a neural network in the arcuate nucleus. *Nature* 2001, 411:480-4.
- [31] Qiu J, Zhang C, Borgquist A, Nestor CC, Smith AW, Bosch MA, Ku S, Wagner EJ, Ronnekleiv OK, Kelly MJ: Insulin excites anorexigenic proopiomelanocortin neurons via activation of canonical transient receptor potential channels. *Cell metabolism* 2014, 19:682-93.
- [32] Cowley MA, Smith RG, Diano S, Tschop M, Pronchuk N, Grove KL, Strasburger CJ, Bidlingmaier M, Esterman M, Heiman ML, Garcia-Segura LM, Nillni EA, Mendez P, Low MJ, Sotonyi P, Friedman JM, Liu H, Pinto S, Colmers WF, Cone RD, Horvath TL: The distribution and mechanism of action of ghrelin in the CNS demonstrates a novel hypothalamic circuit regulating energy homeostasis. *Neuron* 2003, 37:649-61.

- [33] Chen Y, Knight ZA: Making sense of the sensory regulation of hunger neurons. *BioEssays : news and reviews in molecular, cellular and developmental biology* 2016, 38:316-24.
- [34] Chen Y, Lin YC, Kuo TW, Knight ZA: Sensory detection of food rapidly modulates arcuate feeding circuits. *Cell* 2015, 160:829-41.
- [35] Betley JN, Xu S, Cao ZF, Gong R, Magnus CJ, Yu Y, Sternson SM: Neurons for hunger and thirst transmit a negative-valence teaching signal. *Nature* 2015, 521:180-5.
- [36] Mandelblat-Cerf Y, Ramesh RN, Burgess CR, Patella P, Yang Z, Lowell BB, Andermann ML: Arcuate hypothalamic AgRP and putative POMC neurons show opposite changes in spiking across multiple timescales. *eLife* 2015, 4.
- [37] Krashes MJ, Lowell BB, Garfield AS: Melanocortin-4 receptor-regulated energy homeostasis. *Nature neuroscience* 2016, 19:206-19.
- [38] Buch TR, Heling D, Damm E, Gudermann T, Breit A: Pertussis toxin-sensitive signaling of melanocortin-4 receptors in hypothalamic GT1-7 cells defines agouti-related protein as a biased agonist. *The Journal of biological chemistry* 2009, 284:26411-20.
- [39] Ollmann MM, Wilson BD, Yang YK, Kerns JA, Chen Y, Gantz I, Barsh GS: Antagonism of central melanocortin receptors in vitro and in vivo by agouti-related protein. *Science (New York, NY)* 1997, 278:135-8.
- [40] Nijenhuis WA, Oosterom J, Adan RA: AgRP(83-132) acts as an inverse agonist on the human-melanocortin-4 receptor. *Molecular endocrinology (Baltimore, Md)* 2001, 15:164-71.
- [41] Ghamari-Langroudi M, Digby GJ, Sebag JA, Millhauser GL, Palomino R, Matthews R, Gillyard T, Panaro BL, Tough IR, Cox HM, Denton JS, Cone RD: G-protein-independent coupling of MC4R to Kir7.1 in hypothalamic neurons. *Nature* 2015, 520:94-8.
- [42] Schioth HB, Mutulis F, Muceniece R, Prusis P, Wikberg JE: Discovery of novel melanocortin4 receptor selective MSH analogues. *British journal of pharmacology* 1998, 124:75-82.
- [43] Krashes MJ, Shah BP, Koda S, Lowell BB: Rapid versus delayed stimulation of feeding by the endogenously released AgRP neuron mediators GABA, NPY, and AgRP. *Cell metabolism* 2013, 18:588-95.
- [44] Fenselau H, Campbell JN, Versteegen AM, Madara JC, Xu J, Shah BP, Resch JM, Yang Z, Mandelblat-Cerf Y, Livneh Y, Lowell BB: A rapidly acting glutamatergic ARC-->PVH satiety circuit postsynaptically regulated by alpha-MSH. *Nature neuroscience* 2017, 20:42-51.
- [45] Zhang X, van den Pol AN: Hypothalamic arcuate nucleus tyrosine hydroxylase neurons play orexigenic role in energy homeostasis. *Nature neuroscience* 2016, 19:1341-7.
- [46] Sutton AK, Myers MG, Jr., Olson DP: The Role of PVH Circuits in Leptin Action and Energy Balance. *Annual review of physiology* 2016, 78:207-21.
- [47] Shor-Posner G, Azar AP, Insinga S, Leibowitz SF: Deficits in the control of food intake after hypothalamic paraventricular nucleus lesions. *Physiology & behavior* 1985, 35:883-90.
- [48] Leibowitz SF, Hammer NJ, Chang K: Hypothalamic paraventricular nucleus lesions produce overeating and obesity in the rat. *Physiology & behavior* 1981, 27:1031-40.
- [49] Sims JS, Lorden JF: Effect of paraventricular nucleus lesions on body weight, food intake and insulin levels. *Behavioural brain research* 1986, 22:265-81.
- [50] Balthasar N, Dalgaard LT, Lee CE, Yu J, Funahashi H, Williams T, Ferreira M, Tang V, McGovern RA, Kenny CD, Christiansen LM, Edelstein E, Choi B, Boss O, Aschkenasi C, Zhang CY, Mountjoy K, Kishi T, Elmquist JK, Lowell BB: Divergence of melanocortin pathways in the control of food intake and energy expenditure. *Cell* 2005, 123:493-505.
- [51] Garfield AS, Li C, Madara JC, Shah BP, Webber E, Steger JS, Campbell JN, Gavrilova O, Lee CE, Olson DP, Elmquist JK, Tannous BA, Krashes MJ, Lowell BB: A neural basis for melanocortin-4 receptor-regulated appetite. *Nature neuroscience* 2015, 18:863-71.

- [52] Huszar D, Lynch CA, Fairchild-Huntress V, Dunmore JH, Fang Q, Berkemeier LR, Gu W, Kesterson RA, Boston BA, Cone RD, Smith FJ, Campfield LA, Burn P, Lee F: Targeted disruption of the melanocortin-4 receptor results in obesity in mice. *Cell* 1997, 88:131-41.
- [53] Yeo GS, Farooqi IS, Aminian S, Halsall DJ, Stanhope RG, O'Rahilly S: A frameshift mutation in MC4R associated with dominantly inherited human obesity. *Nature genetics* 1998, 20:111-2.
- [54] Vaisse C, Clement K, Guy-Grand B, Froguel P: A frameshift mutation in human MC4R is associated with a dominant form of obesity. *Nature genetics* 1998, 20:113-4.
- [55] Shah BP, Vong L, Olson DP, Koda S, Krashes MJ, Ye C, Yang Z, Fuller PM, Elmquist JK, Lowell BB: MC4R-expressing glutamatergic neurons in the paraventricular hypothalamus regulate feeding and are synaptically connected to the parabrachial nucleus. *Proceedings of the National Academy of Sciences of the United States of America* 2014, 111:13193-8.
- [56] Kim MS, Rossi M, Abusnana S, Sunter D, Morgan DG, Small CJ, Edwards CM, Heath MM, Stanley SA, Seal LJ, Bhatti JR, Smith DM, Ghatei MA, Bloom SR: Hypothalamic localization of the feeding effect of agouti-related peptide and alpha-melanocyte-stimulating hormone. *Diabetes* 2000, 49:177-82.
- [57] Xu Y, Wu Z, Sun H, Zhu Y, Kim ER, Lowell BB, Arenkiel BR, Xu Y, Tong Q: Glutamate mediates the function of melanocortin receptor 4 on Sim1 neurons in body weight regulation. *Cell metabolism* 2013, 18:860-70.
- [58] Krashes MJ, Shah BP, Madara JC, Olson DP, Strohlic DE, Garfield AS, Vong L, Pei H, Watabe-Uchida M, Uchida N, Liberles SD, Lowell BB: An excitatory paraventricular nucleus to AgRP neuron circuit that drives hunger. *Nature* 2014, 507:238-42.
- [59] Stachniak TJ, Ghosh A, Sternson SM: Chemogenetic synaptic silencing of neural circuits localizes a hypothalamus-->midbrain pathway for feeding behavior. *Neuron* 2014, 82:797-808.
- [60] Singru PS, Wittmann G, Farkas E, Zseli G, Fekete C, Lechan RM: Refeeding-activated glutamatergic neurons in the hypothalamic paraventricular nucleus (PVN) mediate effects of melanocortin signaling in the nucleus tractus solitarius (NTS). *Endocrinology* 2012, 153:3804-14.
- [61] Mangieri LR, Lu Y, Xu Y, Cassidy RM, Xu Y, Arenkiel BR, Tong Q: A neural basis for antagonistic control of feeding and compulsive behaviors. *Nature communications* 2018, 9:52.
- [62] Geerling JC, Shin JW, Chimenti PC, Loewy AD: Paraventricular hypothalamic nucleus: axonal projections to the brainstem. *The Journal of comparative neurology* 2010, 518:1460-99.
- [63] Ziegler DR, Edwards MR, Ulrich-Lai YM, Herman JP, Cullinan WE: Brainstem origins of glutamatergic innervation of the rat hypothalamic paraventricular nucleus. *The Journal of comparative neurology* 2012, 520:2369-94.
- [64] Kim ER, Wu Z, Sun H, Xu Y, Mangieri LR, Xu Y, Tong Q: Hypothalamic Non-AgRP, Non-POMC GABAergic Neurons Are Required for Postweaning Feeding and NPY Hyperphagia. *The Journal of neuroscience : the official journal of the Society for Neuroscience* 2015, 35:10440-50.
- [65] Sutton AK, Pei H, Burnett KH, Myers MG, Jr., Rhodes CJ, Olson DP: Control of food intake and energy expenditure by Nos1 neurons of the paraventricular hypothalamus. *The Journal of neuroscience : the official journal of the Society for Neuroscience* 2014, 34:15306-18.
- [66] Pei H, Sutton AK, Burnett KH, Fuller PM, Olson DP: AVP neurons in the paraventricular nucleus of the hypothalamus regulate feeding. *Molecular metabolism* 2014, 3:209-15.
- [67] Liu J, Conde K, Zhang P, Lilascharoen V, Xu Z, Lim BK, Seeley RJ, Zhu JJ, Scott MM, Pang ZP: Enhanced AMPA Receptor Trafficking Mediates the Anorexigenic Effect of Endogenous Glucagon-like Peptide-1 in the Paraventricular Hypothalamus. *Neuron* 2017, 96:897-909.e5.
- [68] D'Agostino G, Lyons DJ, Cristiano C, Burke LK, Madara JC, Campbell JN, Garcia AP, Land BB, Lowell BB, Dileone RJ, Heisler LK: Appetite controlled by a cholecystokinin nucleus of the solitary tract to hypothalamus neurocircuit. *eLife* 2016, 5.

- [69] Wu Z, Kim ER, Sun H, Xu Y, Mangieri LR, Li DP, Pan HL, Xu Y, Arenkiel BR, Tong Q: GABAergic projections from lateral hypothalamus to paraventricular hypothalamic nucleus promote feeding. *The Journal of neuroscience : the official journal of the Society for Neuroscience* 2015, 35:3312-8.
- [70] Sweeney P, Li C, Yang Y: Appetite suppressive role of medial septal glutamatergic neurons. *Proceedings of the National Academy of Sciences of the United States of America* 2017, 114:13816-21.
- [71] Luo SX, Huang J, Li Q, Mohammad H, Lee CY, Krishna K, Kok AM, Tan YL, Lim JY, Li H, Yeow LY, Sun J, He M, Grandjean J, Sajikumar S, Han W, Fu Y: Regulation of feeding by somatostatin neurons in the tuberal nucleus. *Science (New York, NY)* 2018, 361:76-81.
- [72] Otgon-Uul Z, Suyama S, Onodera H, Yada T: Optogenetic activation of leptin- and glucose-regulated GABAergic neurons in dorsomedial hypothalamus promotes food intake via inhibitory synaptic transmission to paraventricular nucleus of hypothalamus. *Molecular metabolism* 2016, 5:709-15.
- [73] Anand BK, Brobeck JR: Localization of a "feeding center" in the hypothalamus of the rat. *Proceedings of the Society for Experimental Biology and Medicine Society for Experimental Biology and Medicine (New York, NY)* 1951, 77:323-4.
- [74] Grossman SP, Dacey D, Halaris AE, Collier T, Routtenberg A: Aphagia and adipsia after preferential destruction of nerve cell bodies in hypothalamus. *Science (New York, NY)* 1978, 202:537-9.
- [75] Grossman SP, Grossman L: Ionophoretic injections of kainic acid into the rat lateral hypothalamus: effects on ingestive behavior. *Physiology & behavior* 1982, 29:553-9.
- [76] Stricker EM, Swerdloff AF, Zigmond MJ: Intrahypothalamic injections of kainic acid produce feeding and drinking deficits in rats. *Brain research* 1978, 158:470-3.
- [77] Stuber GD, Wise RA: Lateral hypothalamic circuits for feeding and reward. *Nature neuroscience* 2016, 19:198-205.
- [78] Leininger GM, Opland DM, Jo YH, Faouzi M, Christensen L, Cappellucci LA, Rhodes CJ, Gnegy ME, Becker JB, Pothos EN, Seasholtz AF, Thompson RC, Myers MG, Jr.: Leptin action via neurotensin neurons controls orexin, the mesolimbic dopamine system and energy balance. *Cell metabolism* 2011, 14:313-23.
- [79] Leininger GM: Lateral thinking about leptin: a review of leptin action via the lateral hypothalamus. *Physiology & behavior* 2011, 104:572-81.
- [80] Leininger GM, Jo YH, Leshan RL, Louis GW, Yang H, Barrera JG, Wilson H, Opland DM, Faouzi MA, Gong Y, Jones JC, Rhodes CJ, Chua S, Jr., Diano S, Horvath TL, Seeley RJ, Becker JB, Munzberg H, Myers MG, Jr.: Leptin acts via leptin receptor-expressing lateral hypothalamic neurons to modulate the mesolimbic dopamine system and suppress feeding. *Cell metabolism* 2009, 10:89-98.
- [81] Laque A, Zhang Y, Gettys S, Nguyen TA, Bui K, Morrison CD, Munzberg H: Leptin receptor neurons in the mouse hypothalamus are colocalized with the neuropeptide galanin and mediate anorexigenic leptin action. *American journal of physiology Endocrinology and metabolism* 2013, 304:E999-1011.
- [82] Wren AM, Small CJ, Abbott CR, Dhillon WS, Seal LJ, Cohen MA, Batterham RL, Taheri S, Stanley SA, Ghatei MA, Bloom SR: Ghrelin causes hyperphagia and obesity in rats. *Diabetes* 2001, 50:2540-7.
- [83] Olszewski PK, Li D, Grace MK, Billington CJ, Kotz CM, Levine AS: Neural basis of orexigenic effects of ghrelin acting within lateral hypothalamus. *Peptides* 2003, 24:597-602.
- [84] Scott V, McDade DM, Luckman SM: Rapid changes in the sensitivity of arcuate nucleus neurons to central ghrelin in relation to feeding status. *Physiology & behavior* 2007, 90:180-5.
- [85] Brown JA, Woodworth HL, Leininger GM: To ingest or rest? Specialized roles of lateral hypothalamic area neurons in coordinating energy balance. *Frontiers in systems neuroscience* 2015, 9:9.

- [86] Sakurai T: Orexins and orexin receptors: implication in feeding behavior. *Regulatory peptides* 1999, 85:25-30.
- [87] de Lecea L, Kilduff TS, Peyron C, Gao X, Foye PE, Danielson PE, Fukuhara C, Battenberg EL, Gautvik VT, Bartlett FS, 2nd, Frankel WN, van den Pol AN, Bloom FE, Gautvik KM, Sutcliffe JG: The hypocretins: hypothalamus-specific peptides with neuroexcitatory activity. *Proceedings of the National Academy of Sciences of the United States of America* 1998, 95:322-7.
- [88] Adamantidis AR, Zhang F, Aravanis AM, Deisseroth K, de Lecea L: Neural substrates of awakening probed with optogenetic control of hypocretin neurons. *Nature* 2007, 450:420-4.
- [89] Sakurai T, Amemiya A, Ishii M, Matsuzaki I, Chemelli RM, Tanaka H, Williams SC, Richardson JA, Kozlowski GP, Wilson S, Arch JR, Buckingham RE, Haynes AC, Carr SA, Annan RS, McNulty DE, Liu WS, Terrett JA, Elshourbagy NA, Bergsma DJ, Yanagisawa M: Orexins and orexin receptors: a family of hypothalamic neuropeptides and G protein-coupled receptors that regulate feeding behavior. *Cell* 1998, 92:573-85.
- [90] Tabuchi S, Tsunematsu T, Black SW, Tominaga M, Maruyama M, Takagi K, Minokoshi Y, Sakurai T, Kilduff TS, Yamanaka A: Conditional ablation of orexin/hypocretin neurons: a new mouse model for the study of narcolepsy and orexin system function. *The Journal of neuroscience : the official journal of the Society for Neuroscience* 2014, 34:6495-509.
- [91] Hara J, Beuckmann CT, Nambu T, Willie JT, Chemelli RM, Sinton CM, Sugiyama F, Yagami K, Goto K, Yanagisawa M, Sakurai T: Genetic ablation of orexin neurons in mice results in narcolepsy, hypophagia, and obesity. *Neuron* 2001, 30:345-54.
- [92] Gonzalez JA, Jensen LT, Iordanidou P, Strom M, Fugger L, Burdakov D: Inhibitory Interplay between Orexin Neurons and Eating. *Current biology : CB* 2016, 26:2486-91.
- [93] Jago S, Glasgow SD, Herrera CG, Ekstrand M, Reed SJ, Boyce R, Friedman J, Burdakov D, Adamantidis AR: Optogenetic identification of a rapid eye movement sleep modulatory circuit in the hypothalamus. *Nature neuroscience* 2013, 16:1637-43.
- [94] Qu D, Ludwig DS, Gammeltoft S, Piper M, Pelleymounter MA, Cullen MJ, Mathes WF, Przypek R, Kanarek R, Maratos-Flier E: A role for melanin-concentrating hormone in the central regulation of feeding behaviour. *Nature* 1996, 380:243-7.
- [95] Ludwig DS, Tritos NA, Mastaitis JW, Kulkarni R, Kokkotou E, Elmquist J, Lowell B, Flier JS, Maratos-Flier E: Melanin-concentrating hormone overexpression in transgenic mice leads to obesity and insulin resistance. *The Journal of clinical investigation* 2001, 107:379-86.
- [96] Shimada M, Tritos NA, Lowell BB, Flier JS, Maratos-Flier E: Mice lacking melanin-concentrating hormone are hypophagic and lean. *Nature* 1998, 396:670-4.
- [97] Alon T, Friedman JM: Late-onset leanness in mice with targeted ablation of melanin concentrating hormone neurons. *The Journal of neuroscience : the official journal of the Society for Neuroscience* 2006, 26:389-97.
- [98] Broberger C, De Lecea L, Sutcliffe JG, Hokfelt T: Hypocretin/orexin- and melanin-concentrating hormone-expressing cells form distinct populations in the rodent lateral hypothalamus: relationship to the neuropeptide Y and agouti gene-related protein systems. *The Journal of comparative neurology* 1998, 402:460-74.
- [99] Mickelsen LE, Kolling FWt, Chimileski BR, Fujita A, Norris C, Chen K, Nelson CE, Jackson AC: Neurochemical Heterogeneity Among Lateral Hypothalamic Hypocretin/Orexin and Melanin-Concentrating Hormone Neurons Identified Through Single-Cell Gene Expression Analysis. *eNeuro* 2017, 4.
- [100] Harthoorn LF, Sane A, Nethe M, Van Heerikhuizen JJ: Multi-transcriptional profiling of melanin-concentrating hormone and orexin-containing neurons. *Cellular and molecular neurobiology* 2005, 25:1209-23.

- [101] Chee MJ, Arrigoni E, Maratos-Flier E: Melanin-concentrating hormone neurons release glutamate for feedforward inhibition of the lateral septum. *The Journal of neuroscience : the official journal of the Society for Neuroscience* 2015, 35:3644-51.
- [102] Cooke JH, Patterson M, Patel SR, Smith KL, Ghatei MA, Bloom SR, Murphy KG: Peripheral and central administration of xenin and neurotensin suppress food intake in rodents. *Obesity (Silver Spring, Md)* 2009, 17:1135-43.
- [103] Kim ER, Leckstrom A, Mizuno TM: Impaired anorectic effect of leptin in neurotensin receptor 1-deficient mice. *Behavioural brain research* 2008, 194:66-71.
- [104] Woodworth HL, Beekly BG, Batchelor HM, Bugescu R, Perez-Bonilla P, Schroeder LE, Leininger GM: Lateral Hypothalamic Neurotensin Neurons Orchestrate Dual Weight Loss Behaviors via Distinct Mechanisms. *Cell reports* 2017, 21:3116-28.
- [105] Dergacheva O, Yamanaka A, Schwartz AR, Polotsky VY, Mendelowitz D: Optogenetic identification of hypothalamic orexin neuron projections to paraventricular spinally projecting neurons. *American journal of physiology Heart and circulatory physiology* 2017, 312:H808-h17.
- [106] Blanco-Centurion C, Bendell E, Zou B, Sun Y, Shiromani PJ, Liu M: VGAT and VGLUT2 expression in MCH and orexin neurons in double transgenic reporter mice. *IBRO Reports* 2018, 4:44-9.
- [107] Jennings JH, Ung RL, Resendez SL, Stamatakis AM, Taylor JG, Huang J, Veleta K, Kantak PA, Aita M, Shilling-Scriver K, Ramakrishnan C, Deisseroth K, Otte S, Stuber GD: Visualizing hypothalamic network dynamics for appetitive and consummatory behaviors. *Cell* 2015, 160:516-27.
- [108] Zhaofei Wu ERK, Hao Sun, Yuanzhong Xu, Leandra Mangieri, De-Pei Li, Hui-Lin Pan, Yong Xu, Benjamin Arenkiel, and Qingchun Tong: GABAergic Projections from Lateral Hypothalamus to Paraventricular Hypothalamic Nucleus Promote Feeding. *Journal of Neuroscience* 2015.
- [109] Jennings JH, Rizzi G, Stamatakis AM, Ung RL, Stuber GD: The inhibitory circuit architecture of the lateral hypothalamus orchestrates feeding. *Science (New York, NY)* 2013, 341:1517-21.
- [110] Stamatakis AM, Van Swieten M, Basiri ML, Blair GA, Kantak P, Stuber GD: Lateral Hypothalamic Area Glutamatergic Neurons and Their Projections to the Lateral Habenula Regulate Feeding and Reward. *The Journal of neuroscience : the official journal of the Society for Neuroscience* 2016, 36:302-11.
- [111] Nieh EH, Matthews GA, Allsop SA, Presbrey KN, Leppla CA, Wichmann R, Neve R, Wildes CP, Tye KM: Decoding Neural Circuits that Control Compulsive Sucrose Seeking. *Cell* 2015, 160:528-41.
- [112] Schneeberger M, Gomis R, Claret M: Hypothalamic and brainstem neuronal circuits controlling homeostatic energy balance. *The Journal of endocrinology* 2014, 220:T25-46.
- [113] King BM: The rise, fall, and resurrection of the ventromedial hypothalamus in the regulation of feeding behavior and body weight. *Physiology & behavior* 2006, 87:221-44.
- [114] Choi YH, Fujikawa T, Lee J, Reuter A, Kim KW: Revisiting the Ventral Medial Nucleus of the Hypothalamus: The Roles of SF-1 Neurons in Energy Homeostasis. *Frontiers in neuroscience* 2013, 7:71.
- [115] Unger TJ, Calderon GA, Bradley LC, Sena-Esteves M, Rios M: Selective deletion of Bdnf in the ventromedial and dorsomedial hypothalamus of adult mice results in hyperphagic behavior and obesity. *The Journal of neuroscience : the official journal of the Society for Neuroscience* 2007, 27:14265-74.
- [116] Musatov S, Chen W, Pfaff DW, Mobbs CV, Yang XJ, Clegg DJ, Kaplitt MG, Ogawa S: Silencing of estrogen receptor alpha in the ventromedial nucleus of hypothalamus leads to metabolic syndrome. *Proceedings of the National Academy of Sciences of the United States of America* 2007, 104:2501-6.
- [117] Bellingr LL, Bernardis LL: The dorsomedial hypothalamic nucleus and its role in ingestive behavior and body weight regulation: lessons learned from lesioning studies. *Physiology & behavior* 2002, 76:431-42.

- [118] Mieda M, Williams SC, Richardson JA, Tanaka K, Yanagisawa M: The dorsomedial hypothalamic nucleus as a putative food-entrainable circadian pacemaker. *Proceedings of the National Academy of Sciences of the United States of America* 2006, 103:12150-5.
- [119] Gooley JJ, Schomer A, Saper CB: The dorsomedial hypothalamic nucleus is critical for the expression of food-entrainable circadian rhythms. *Nature neuroscience* 2006, 9:398-407.
- [120] Garfield AS, Shah BP, Burgess CR, Li MM, Li C, Steger JS, Madara JC, Campbell JN, Kroeger D, Scammell TE, Tannous BA, Myers MG, Jr., Andermann ML, Krashes MJ, Lowell BB: Dynamic GABAergic afferent modulation of AgRP neurons. *Nature neuroscience* 2016, 19:1628-35.
- [121] Jeong JH, Lee DK, Jo YH: Cholinergic neurons in the dorsomedial hypothalamus regulate food intake. *Molecular metabolism* 2017, 6:306-12.
- [122] Kirchgessner AL, Sclafani A: PVN-hindbrain pathway involved in the hypothalamic hyperphagia-obesity syndrome. *Physiology & behavior* 1988, 42:517-28.
- [123] Grill HJ, Hayes MR: Hindbrain neurons as an essential hub in the neuroanatomically distributed control of energy balance. *Cell metabolism* 2012, 16:296-309.
- [124] Hayes MR, Bradley L, Grill HJ: Endogenous hindbrain glucagon-like peptide-1 receptor activation contributes to the control of food intake by mediating gastric satiation signaling. *Endocrinology* 2009, 150:2654-9.
- [125] Hayes MR, Skibicka KP, Leichner TM, Guarnieri DJ, DiLeone RJ, Bence KK, Grill HJ: Endogenous leptin signaling in the caudal nucleus tractus solitarius and area postrema is required for energy balance regulation. *Cell metabolism* 2010, 11:77-83.
- [126] Wu Q, Clark MS, Palmiter RD: Deciphering a neuronal circuit that mediates appetite. *Nature* 2012, 483:594-7.
- [127] Roman CW, Derkach VA, Palmiter RD: Genetically and functionally defined NTS to PBN brain circuits mediating anorexia. *Nature communications* 2016, 7:11905.
- [128] Carter ME, Soden ME, Zweifel LS, Palmiter RD: Genetic identification of a neural circuit that suppresses appetite. *Nature* 2013, 503:111-4.
- [129] Palmiter RD: The Parabrachial Nucleus: CGRP Neurons Function as a General Alarm. *Trends in neurosciences* 2018, 41:280-93.
- [130] Fletcher PJ, Davies M: Dorsal raphe microinjection of 5-HT and indirect 5-HT agonists induces feeding in rats. *European journal of pharmacology* 1990, 184:265-71.
- [131] Veasey SC, Fornal CA, Metzler CW, Jacobs BL: Single-unit responses of serotonergic dorsal raphe neurons to specific motor challenges in freely moving cats. *Neuroscience* 1997, 79:161-9.
- [132] Nectow AR, Schneeberger M, Zhang H, Field BC, Renier N, Azevedo E, Patel B, Liang Y, Mitra S, Tessier-Lavigne M, Han MH, Friedman JM: Identification of a Brainstem Circuit Controlling Feeding. *Cell* 2017, 170:429-42.e11.
- [133] Rossi MA, Stuber GD: Overlapping Brain Circuits for Homeostatic and Hedonic Feeding. *Cell metabolism* 2018, 27:42-56.
- [134] Liu CM, Kanoski SE: Homeostatic and non-homeostatic controls of feeding behavior: Distinct vs. common neural systems. *Physiology & behavior* 2018.
- [135] Pike KM, Dunne PE: The rise of eating disorders in Asia: a review. *Journal of eating disorders* 2015, 3:33.
- [136] Battle EK, Brownell KD: Confronting a rising tide of eating disorders and obesity: treatment vs. prevention and policy. *Addictive behaviors* 1996, 21:755-65.
- [137] Preti A, Girolamo G, Vilagut G, Alonso J, Graaf R, Bruffaerts R, Demyttenaere K, Pinto-Meza A, Haro JM, Morosini P: The epidemiology of eating disorders in six European countries: results of the ESEMeD-WMH project. *Journal of psychiatric research* 2009, 43:1125-32.
- [138] Morton GJ, Meek TH, Schwartz MW: Neurobiology of food intake in health and disease. *Nature reviews Neuroscience* 2014, 15:367-78.

- [139] Volkow ND, Wang GJ, Baler RD: Reward, dopamine and the control of food intake: implications for obesity. *Trends in cognitive sciences* 2011, 15:37-46.
- [140] Hardaway JA, Crowley NA, Bulik CM, Kash TL: Integrated circuits and molecular components for stress and feeding: implications for eating disorders. *Genes, brain, and behavior* 2015, 14:85-97.
- [141] Pavlov IP: *Conditioned reflexes*. Dover, New York 1927.
- [142] Stice E, Spoor S, Bohon C, Veldhuizen MG, Small DM: Relation of reward from food intake and anticipated food intake to obesity: a functional magnetic resonance imaging study. *Journal of abnormal psychology* 2008, 117:924-35.
- [143] Volkow ND, Wang GJ, Tomasi D, Baler RD: Obesity and addiction: neurobiological overlaps. *Obesity reviews : an official journal of the International Association for the Study of Obesity* 2013, 14:2-18.
- [144] Liu C, Lee S, Elmquist JK: Circuits controlling energy balance and mood: inherently intertwined or just complicated intersections? *Cell metabolism* 2014, 19:902-9.
- [145] Delgado JM, Anand BK: Increase of food intake induced by electrical stimulation of the lateral hypothalamus. *The American journal of physiology* 1953, 172:162-8.
- [146] Olds J, Milner P: Positive reinforcement produced by electrical stimulation of septal area and other regions of rat brain. *Journal of comparative and physiological psychology* 1954, 47:419-27.
- [147] Hoebel BG, Teitelbaum P: Hypothalamic control of feeding and self-stimulation. *Science (New York, NY)* 1962, 135:375-7.
- [148] Margules DL, Olds J: Identical "feeding" and "rewarding" systems in the lateral hypothalamus of rats. *Science (New York, NY)* 1962, 135:374-5.
- [149] Opland D, Sutton A, Woodworth H, Brown J, Bugescu R, Garcia A, Christensen L, Rhodes C, Myers M, Jr., Leininger G: Loss of neurotensin receptor-1 disrupts the control of the mesolimbic dopamine system by leptin and promotes hedonic feeding and obesity. *Molecular metabolism* 2013, 2:423-34.
- [150] Cone JJ, McCutcheon JE, Roitman MF: Ghrelin acts as an interface between physiological state and phasic dopamine signaling. *The Journal of neuroscience : the official journal of the Society for Neuroscience* 2014, 34:4905-13.
- [151] Lopez-Ferreras L, Richard JE, Anderberg RH, Nilsson FH, Olandersson K, Kanoski SE, Skibicka KP: Ghrelin's control of food reward and body weight in the lateral hypothalamic area is sexually dimorphic. *Physiology & behavior* 2017, 176:40-9.
- [152] Cassidy RM, Tong Q: Hunger and Satiety Gauge Reward Sensitivity. *Frontiers in endocrinology* 2017, 8:104.
- [153] Harris GC, Wimmer M, Aston-Jones G: A role for lateral hypothalamic orexin neurons in reward seeking. *Nature* 2005, 437:556-9.
- [154] Aston-Jones G, Smith RJ, Sartor GC, Moorman DE, Massi L, Tahsili-Fahadan P, Richardson KA: Lateral hypothalamic orexin/hypocretin neurons: A role in reward-seeking and addiction. *Brain research* 2010, 1314:74-90.
- [155] Domingos AI, Sordillo A, Dietrich MO, Liu ZW, Tellez LA, Vaynshteyn J, Ferreira JG, Ekstrand MI, Horvath TL, de Araujo IE, Friedman JM: Hypothalamic melanin concentrating hormone neurons communicate the nutrient value of sugar. *eLife* 2013, 2:e01462.
- [156] Nieh EH, Vander Weele CM, Matthews GA, Presbrey KN, Wichmann R, Leppla CA, Izadmehr EM, Tye KM: Inhibitory Input from the Lateral Hypothalamus to the Ventral Tegmental Area Disinhibits Dopamine Neurons and Promotes Behavioral Activation. *Neuron* 2016, 90:1286-98.
- [157] Ikemoto S, Panksepp J: The role of nucleus accumbens dopamine in motivated behavior: a unifying interpretation with special reference to reward-seeking. *Brain research Brain research reviews* 1999, 31:6-41.

- [158] Barbano MF, Wang HL, Morales M, Wise RA: Feeding and Reward Are Differentially Induced by Activating GABAergic Lateral Hypothalamic Projections to VTA. *The Journal of neuroscience : the official journal of the Society for Neuroscience* 2016, 36:2975-85.
- [159] O'Connor EC, Kremer Y, Lefort S, Harada M, Pascoli V, Rohner C, Luscher C: Accumbal D1R Neurons Projecting to Lateral Hypothalamus Authorize Feeding. *Neuron* 2015, 88:553-64.
- [160] Lecca S, Meye FJ, Truscel M, Tchenio A, Harris J, Schwarz MK, Burdakov D, Georges F, Mameli M: Aversive stimuli drive hypothalamus-to-habenula excitation to promote escape behavior. *eLife* 2017, 6.
- [161] Carrive P: The periaqueductal gray and defensive behavior: functional representation and neuronal organization. *Behavioural brain research* 1993, 58:27-47.
- [162] Li Y, Zeng J, Zhang J, Yue C, Zhong W, Liu Z, Feng Q, Luo M: Hypothalamic Circuits for Predation and Evasion. *Neuron* 2018, 97:911-24.e5.
- [163] Chen Y, Lin YC, Zimmerman CA, Essner RA, Knight ZA: Hunger neurons drive feeding through a sustained, positive reinforcement signal. *eLife* 2016, 5.
- [164] Dietrich MO, Zimmer MR, Bober J, Horvath TL: Hypothalamic Agrp neurons drive stereotypic behaviors beyond feeding. *Cell* 2015, 160:1222-32.
- [165] Burnett CJ, Li C, Webber E, Tsaousidou E, Xue SY, Bruning JC, Krashes MJ: Hunger-Driven Motivational State Competition. *Neuron* 2016, 92:187-201.
- [166] Padilla SL, Qiu J, Soden ME, Sanz E, Nestor CC, Barker FD, Quintana A, Zweifel LS, Ronnekleiv OK, Kelly MJ, Palmiter RD: Agouti-related peptide neural circuits mediate adaptive behaviors in the starved state. *Nature neuroscience* 2016, 19:734-41.
- [167] Herman JP, Figueiredo H, Mueller NK, Ulrich-Lai Y, Ostrander MM, Choi DC, Cullinan WE: Central mechanisms of stress integration: hierarchical circuitry controlling hypothalamo-pituitary-adrenocortical responsiveness. *Frontiers in neuroendocrinology* 2003, 24:151-80.
- [168] Fuzesi T, Daviu N, Wamsteeker Cusulin JI, Bonin RP, Bains JS: Hypothalamic CRH neurons orchestrate complex behaviours after stress. *Nature communications* 2016, 7:11937.
- [169] Kalueff AV, Stewart AM, Song C, Berridge KC, Graybiel AM, Fentress JC: Neurobiology of rodent self-grooming and its value for translational neuroscience. *Nature reviews Neuroscience* 2016, 17:45-59.
- [170] Viskaitis P, Irvine EE, Smith MA, Choudhury AI, Alvarez-Curto E, Glegola JA, Hardy DG, Pedroni SMA, Paiva Pessoa MR, Fernando ABP, Katsouri L, Sardini A, Ungless MA, Milligan G, Withers DJ: Modulation of SF1 Neuron Activity Coordinately Regulates Both Feeding Behavior and Associated Emotional States. *Cell reports* 2017, 21:3559-72.
- [171] Kunwar PS, Zelikowsky M, Remedios R, Cai H, Yilmaz M, Meister M, Anderson DJ: Ventromedial hypothalamic neurons control a defensive emotion state. *eLife* 2015, 4.
- [172] Wang L, Chen IZ, Lin D: Collateral pathways from the ventromedial hypothalamus mediate defensive behaviors. *Neuron* 2015, 85:1344-58.
- [173] Yang CF, Chiang MC, Gray DC, Prabhakaran M, Alvarado M, Juntti SA, Unger EK, Wells JA, Shah NM: Sexually dimorphic neurons in the ventromedial hypothalamus govern mating in both sexes and aggression in males. *Cell* 2013, 153:896-909.
- [174] Lee H, Kim DW, Remedios R, Anthony TE, Chang A, Madisen L, Zeng H, Anderson DJ: Scalable control of mounting and attack by Esr1+ neurons in the ventromedial hypothalamus. *Nature* 2014, 509:627-32.
- [175] Kanoski SE, Alhadeff AL, Fortin SM, Gilbert JR, Grill HJ: Leptin signaling in the medial nucleus tractus solitarius reduces food seeking and willingness to work for food. *Neuropsychopharmacology : official publication of the American College of Neuropsychopharmacology* 2014, 39:605-13.

- [176] Alhadeff AL, Grill HJ: Hindbrain nucleus tractus solitarius glucagon-like peptide-1 receptor signaling reduces appetitive and motivational aspects of feeding. *American journal of physiology Regulatory, integrative and comparative physiology* 2014, 307:R465-70.
- [177] Roman CW, Sloat SR, Palmiter RD: A tale of two circuits: CCK(NTS) neuron stimulation controls appetite and induces opposing motivational states by projections to distinct brain regions. *Neuroscience* 2017, 358:316-24.
- [178] Campos CA, Bowen AJ, Roman CW, Palmiter RD: Encoding of danger by parabrachial CGRP neurons. *Nature* 2018, 555:617-22.
- [179] Deng H, Xiao X, Wang Z: Periaqueductal Gray Neuronal Activities Underlie Different Aspects of Defensive Behaviors. *The Journal of neuroscience : the official journal of the Society for Neuroscience* 2016, 36:7580-8.
- [180] Tovote P, Esposito MS, Botta P, Chaudun F, Fadok JP, Markovic M, Wolff SB, Ramakrishnan C, Fenno L, Deisseroth K, Herry C, Arber S, Luthi A: Midbrain circuits for defensive behaviour. *Nature* 2016, 534:206-12.
- [181] Ellenbroek B, Youn J: Rodent models in neuroscience research: is it a rat race? *Disease models & mechanisms* 2016, 9:1079-87.
- [182] Harper A: Mouse models of neurological disorders--a comparison of heritable and acquired traits. *Biochimica et biophysica acta* 2010, 1802:785-95.
- [183] Dunn DA, Pinkert CA, Kooyman DL: Foundation Review: Transgenic animals and their impact on the drug discovery industry. *Drug discovery today* 2005, 10:757-67.
- [184] Sternson SM, Atasoy D, Betley JN, Henry FE, Xu S: An Emerging Technology Framework for the Neurobiology of Appetite. *Cell metabolism* 2016, 23:234-53.
- [185] Kos CH: Cre/loxP system for generating tissue-specific knockout mouse models. *Nutrition reviews* 2004, 62:243-6.
- [186] Missirlis PI, Smailus DE, Holt RA: A high-throughput screen identifying sequence and promiscuity characteristics of the loxP spacer region in Cre-mediated recombination. *BMC genomics* 2006, 7:73.
- [187] McLellan MA, Rosenthal NA, Pinto AR: Cre-loxP-Mediated Recombination: General Principles and Experimental Considerations. *Current protocols in mouse biology* 2017, 7:1-12.
- [188] Atasoy D, Aponte Y, Su HH, Sternson SM: A FLEX switch targets Channelrhodopsin-2 to multiple cell types for imaging and long-range circuit mapping. *The Journal of neuroscience : the official journal of the Society for Neuroscience* 2008, 28:7025-30.
- [189] Yizhar O, Fenno LE, Davidson TJ, Mogri M, Deisseroth K: Optogenetics in neural systems. *Neuron* 2011, 71:9-34.
- [190] Guru A, Post RJ, Ho YY, Warden MR: Making Sense of Optogenetics. *The international journal of neuropsychopharmacology* 2015, 18:pyv079.
- [191] Herman AM, Huang L, Murphey DK, Garcia I, Arenkiel BR: Cell type-specific and time-dependent light exposure contribute to silencing in neurons expressing Channelrhodopsin-2. *eLife* 2014, 3:e01481.
- [192] Mahn M, Prigge M, Ron S, Levy R, Yizhar O: Biophysical constraints of optogenetic inhibition at presynaptic terminals. *Nature neuroscience* 2016, 19:554-6.
- [193] Sternson SM, Roth BL: Chemogenetic tools to interrogate brain functions. *Annual review of neuroscience* 2014, 37:387-407.
- [194] Chen TW, Wardill TJ, Sun Y, Pulver SR, Renninger SL, Baohan A, Schreiter ER, Kerr RA, Orger MB, Jayaraman V, Looger LL, Svoboda K, Kim DS: Ultrasensitive fluorescent proteins for imaging neuronal activity. *Nature* 2013, 499:295-300.
- [195] Broussard GJ, Liang R, Tian L: Monitoring activity in neural circuits with genetically encoded indicators. *Frontiers in molecular neuroscience* 2014, 7:97.

- [196] Resendez SL, Stuber GD: In vivo calcium imaging to illuminate neurocircuit activity dynamics underlying naturalistic behavior. *Neuropsychopharmacology : official publication of the American College of Neuropsychopharmacology* 2015, 40:238-9.
- [197] Betley JN, Cao ZF, Ritola KD, Sternson SM: Parallel, redundant circuit organization for homeostatic control of feeding behavior. *Cell* 2013, 155:1337-50.
- [198] Johnston E, Johnson S, McLeod P, Johnston M: The relation of body mass index to depressive symptoms. *Canadian journal of public health = Revue canadienne de sante publique* 2004, 95:179-83.
- [199] Castellini G, Castellani W, Lelli L, Sauro CL, Dini C, Lazzeretti L, Bencini L, Mannucci E, Ricca V: Association between resting energy expenditure, psychopathology and HPA-axis in eating disorders. *World journal of clinical cases* 2014, 2:257-64.
- [200] Plodkowski RA, Nguyen Q, Sundaram U, Nguyen L, Chau DL, St Jeor S: Bupropion and naltrexone: a review of their use individually and in combination for the treatment of obesity. *Expert opinion on pharmacotherapy* 2009, 10:1069-81.
- [201] Keys A, Brožek J, Henschel A, Mickelsen O, Taylor HL: *The biology of human starvation*. (2 vols). Oxford, England: Univ. of Minnesota Press, 1950.
- [202] Godier LR, Park RJ: Compulsivity in anorexia nervosa: a transdiagnostic concept. *Frontiers in psychology* 2014, 5:778.
- [203] Haynos AF, Roberto CA, Martinez MA, Attia E, Fruzzetti AE: Emotion regulation difficulties in anorexia nervosa before and after inpatient weight restoration. *The International journal of eating disorders* 2014, 47:888-91.
- [204] Holtkamp K, Muller B, Heussen N, Remschmidt H, Herpertz-Dahlmann B: Depression, anxiety, and obsessionality in long-term recovered patients with adolescent-onset anorexia nervosa. *European child & adolescent psychiatry* 2005, 14:106-10.
- [205] Engel MM, Keizer A: Body representation disturbances in visual perception and affordance perception persist in eating disorder patients after completing treatment. *Scientific reports* 2017, 7:16184.
- [206] Eckert ED, Gottesman II, Swigart SE, Casper RC: A 57-YEAR FOLLOW-UP INVESTIGATION AND REVIEW OF THE MINNESOTA STUDY ON HUMAN STARVATION AND ITS RELEVANCE TO EATING DISORDERS. *Archives of Psychology* 2018, 2.
- [207] von Hausswolff-Juhlin Y, Brooks SJ, Larsson M: The neurobiology of eating disorders-a clinical perspective. *Acta psychiatrica Scandinavica* 2014.
- [208] Kaye WH, Bulik CM, Thornton L, Barbarich N, Masters K: Comorbidity of anxiety disorders with anorexia and bulimia nervosa. *The American journal of psychiatry* 2004, 161:2215-21.
- [209] Pallister E, Waller G: Anxiety in the eating disorders: understanding the overlap. *Clinical psychology review* 2008, 28:366-86.
- [210] American Psychiatric A, American Psychiatric A, Force DSMT: *Diagnostic and statistical manual of mental disorders : DSM-5*. 2013.
- [211] Succurro E, Segura-Garcia C, Ruffo M, Caroleo M, Rania M, Aloï M, De Fazio P, Sesti G, Arturi F: Obese Patients With a Binge Eating Disorder Have an Unfavorable Metabolic and Inflammatory Profile. *Medicine* 2015, 94:e2098.
- [212] Hsu LK, Mulliken B, McDonagh B, Krupa Das S, Rand W, Fairburn CG, Rolls B, McCrory MA, Saltzman E, Shikora S, Dwyer J, Roberts S: Binge eating disorder in extreme obesity. *International journal of obesity and related metabolic disorders : journal of the International Association for the Study of Obesity* 2002, 26:1398-403.
- [213] Wang GJ, Geliebter A, Volkow ND, Telang FW, Logan J, Jayne MC, Galanti K, Selig PA, Han H, Zhu W, Wong CT, Fowler JS: Enhanced striatal dopamine release during food stimulation in binge eating disorder. *Obesity (Silver Spring, Md)* 2011, 19:1601-8.

- [214] Kim J, Zhang X, Muralidhar S, LeBlanc SA, Tonegawa S: Basolateral to Central Amygdala Neural Circuits for Appetitive Behaviors. *Neuron* 2017, 93:1464-79.e5.
- [215] Doran CM, Kinchin I: A review of the economic impact of mental illness. *Australian health review* : a publication of the Australian Hospital Association 2017.
- [216] Moore CF, Sabino V, Koob GF, Cottone P: Pathological Overeating: Emerging Evidence for a Compulsivity Construct. *Neuropsychopharmacology* : official publication of the American College of Neuropsychopharmacology 2017.
- [217] Robinson MJ, Fischer AM, Ahuja A, Lesser EN, Maniates H: Roles of "Wanting" and "Liking" in Motivating Behavior: Gambling, Food, and Drug Addictions. *Current topics in behavioral neurosciences* 2016, 27:105-36.
- [218] Nederkoorn C, Dassen FC, Franken L, Resch C, Houben K: Impulsivity and overeating in children in the absence and presence of hunger. *Appetite* 2015, 93:57-61.
- [219] Eddy KT, Keel PK, Dorer DJ, Delinsky SS, Franko DL, Herzog DB: Longitudinal comparison of anorexia nervosa subtypes. *The International journal of eating disorders* 2002, 31:191-201.
- [220] Mattar L, Thiebaud MR, Huas C, Cebula C, Godart N: Depression, anxiety and obsessive-compulsive symptoms in relation to nutritional status and outcome in severe anorexia nervosa. *Psychiatry research* 2012, 200:513-7.
- [221] Monteiro P, Feng G: Learning From Animal Models of Obsessive-Compulsive Disorder. *Biological psychiatry* 2016, 79:7-16.
- [222] Xu P, Grueter BA, Britt JK, McDaniel L, Huntington PJ, Hodge R, Tran S, Mason BL, Lee C, Vong L, Lowell BB, Malenka RC, Lutter M, Pieper AA: Double deletion of melanocortin 4 receptors and SAPAP3 corrects compulsive behavior and obesity in mice. *Proceedings of the National Academy of Sciences of the United States of America* 2013, 110:10759-64.
- [223] Sandoval D, Cota D, Seeley RJ: The integrative role of CNS fuel-sensing mechanisms in energy balance and glucose regulation. *Annual review of physiology* 2008, 70:513-35.
- [224] Burdakov D, Karnani MM, Gonzalez A: Lateral hypothalamus as a sensor-regulator in respiratory and metabolic control. *Physiology & behavior* 2013, 121:117-24.
- [225] Fenselau H, Campbell JN, Versteegen AM, Madara JC, Xu J, Shah BP, Resch JM, Yang Z, Mandelblat-Cerf Y, Livneh Y, Lowell BB: A rapidly acting glutamatergic ARC-->PVH satiety circuit postsynaptically regulated by alpha-MSH. *Nature neuroscience* 2016.
- [226] Song J, Xu Y, Hu X, Choi B, Tong Q: Brain expression of Cre recombinase driven by pancreas-specific promoters. *Genesis* 2010, 48:628-34.
- [227] Kalueff AV, Aldridge JW, LaPorte JL, Murphy DL, Tuohimaa P: Analyzing grooming microstructure in neurobehavioral experiments. *Nature protocols* 2007, 2:2538-44.
- [228] Herman AM, Ortiz-Guzman J, Kochukov M, Herman I, Quast KB, Patel JM, Tepe B, Carlson JC, Ung K, Selever J, Tong Q, Arenkiel BR: A cholinergic basal forebrain feeding circuit modulates appetite suppression. *Nature* 2016, 538:253-6.
- [229] Kalueff AV, Tuohimaa P: Grooming analysis algorithm for neurobehavioural stress research. *Brain research Brain research protocols* 2004, 13:151-8.
- [230] Berndt A, Lee SY, Wietek J, Ramakrishnan C, Steinberg EE, Rashid AJ, Kim H, Park S, Santoro A, Frankland PW, Iyer SM, Pak S, Ahrlund-Richter S, Delp SL, Malenka RC, Josselyn SA, Carlen M, Hegemann P, Deisseroth K: Structural foundations of optogenetics: Determinants of channelrhodopsin ion selectivity. *Proceedings of the National Academy of Sciences of the United States of America* 2016, 113:822-9.
- [231] Welch JM, Lu J, Rodriguiz RM, Trotta NC, Peca J, Ding JD, Feliciano C, Chen M, Adams JP, Luo J, Dudek SM, Weinberg RJ, Calakos N, Wetsel WC, Feng G: Cortico-striatal synaptic defects and OCD-like behaviours in Sapap3-mutant mice. *Nature* 2007, 448:894-900.

- [232] Bonnavion P, Jackson AC, Carter ME, de Lecea L: Antagonistic interplay between hypocretin and leptin in the lateral hypothalamus regulates stress responses. *Nature communications* 2015, 6:6266.
- [233] Fox JR, Power MJ: Eating disorders and multi-level models of emotion: an integrated model. *Clinical psychology & psychotherapy* 2009, 16:240-67.
- [234] Feusner JD, Hembacher E, Phillips KA: The mouse who couldn't stop washing: pathologic grooming in animals and humans. *CNS spectrums* 2009, 14:503-13.
- [235] Speranza M, Corcos M, Godart N, Loas G, Guilbaud O, Jeammet P, Flament M: Obsessive compulsive disorders in eating disorders. *Eating behaviors* 2001, 2:193-207.
- [236] Park RJ, Godier LR, Cowdrey FA: Hungry for reward: How can neuroscience inform the development of treatment for Anorexia Nervosa? *Behaviour research and therapy* 2014, 62:47-59.
- [237] Sominsky L, Spencer SJ: Eating behavior and stress: a pathway to obesity. *Frontiers in psychology* 2014, 5:434.
- [238] Navarro M, Olney JJ, Burnham NW, Mazzone CM, Lowery-Gionta EG, Pleil KE, Kash TL, Thiele TE: Lateral Hypothalamus GABAergic Neurons Modulate Consummatory Behaviors Regardless of the Caloric Content or Biological Relevance of the Consumed Stimuli. *Neuropsychopharmacology : official publication of the American College of Neuropsychopharmacology* 2016, 41:1505-12.
- [239] Burgess CR, Ramesh RN, Sugden AU, Levandowski KM, Minnig MA, Fenselau H, Lowell BB, Andermann ML: Hunger-Dependent Enhancement of Food Cue Responses in Mouse Postrhinal Cortex and Lateral Amygdala. *Neuron* 2016, 91:1154-69.
- [240] Blanchard DC, Blanchard RJ: Chapter 2.4 Defensive behaviors, fear, and anxiety. *Handbook of Behavioral Neuroscience*. Edited by Blanchard RJ, Blanchard DC, Griebel G, Nutt D. Elsevier, 2008. pp. 63-79.
- [241] Steimer T: The biology of fear- and anxiety-related behaviors. *Dialogues in clinical neuroscience* 2002, 4:231-49.
- [242] Silva BA, Gross CT, Graff J: The neural circuits of innate fear: detection, integration, action, and memorization. *Learning & memory (Cold Spring Harbor, NY)* 2016, 23:544-55.
- [243] Silva BA, Mattucci C, Krzykowski P, Cuzzo R, Carbonari L, Gross CT: The ventromedial hypothalamus mediates predator fear memory. *The European journal of neuroscience* 2016, 43:1431-9.
- [244] Ferguson AV, Latchford KJ, Samson WK: The paraventricular nucleus of the hypothalamus - a potential target for integrative treatment of autonomic dysfunction. *Expert opinion on therapeutic targets* 2008, 12:717-27.
- [245] Atrens DM, Von V-R: The motivational properties of electrical stimulation of the medial and paraventricular hypothalamic nuclei. *Physiology & behavior* 1972, 9:229-35.
- [246] Lammers JH, Kruk MR, Meelis W, van der Poel AM: Hypothalamic substrates for brain stimulation-induced patterns of locomotion and escape jumps in the rat. *Brain research* 1988, 449:294-310.
- [247] Lammers JH, Meelis W, Kruk MR, van der Poel AM: Hypothalamic substrates for brain stimulation-induced grooming, digging and circling in the rat. *Brain research* 1987, 418:1-19.
- [248] Watabe-Uchida M, Zhu L, Ogawa SK, Vamanrao A, Uchida N: Whole-brain mapping of direct inputs to midbrain dopamine neurons. *Neuron* 2012, 74:858-73.
- [249] Hung LW, Neuner S, Polepalli JS, Beier KT, Wright M, Walsh JJ, Lewis EM, Luo L, Deisseroth K, Dolen G, Malenka RC: Gating of social reward by oxytocin in the ventral tegmental area. *Science (New York, NY)* 2017, 357:1406-11.
- [250] Morales M, Margolis EB: Ventral tegmental area: cellular heterogeneity, connectivity and behaviour. *Nature reviews Neuroscience* 2017, 18:73-85.

- [251] Jennings JH, Sparta DR, Stamatakis AM, Ung RL, Pleil KE, Kash TL, Stuber GD: Distinct extended amygdala circuits for divergent motivational states. *Nature* 2013, 496:224-8.
- [252] Root DH, Estrin DJ, Morales M: Aversion or Salience Signaling by Ventral Tegmental Area Glutamate Neurons. *iScience* 2018, 2:51-62.
- [253] Root DH, Mejias-Aponte CA, Qi J, Morales M: Role of glutamatergic projections from ventral tegmental area to lateral habenula in aversive conditioning. *The Journal of neuroscience : the official journal of the Society for Neuroscience* 2014, 34:13906-10.
- [254] Qi J, Zhang S, Wang HL, Barker DJ, Miranda-Barrientos J, Morales M: VTA glutamatergic inputs to nucleus accumbens drive aversion by acting on GABAergic interneurons. *Nature neuroscience* 2016, 19:725-33.
- [255] Vong L, Ye C, Yang Z, Choi B, Chua S, Jr., Lowell BB: Leptin action on GABAergic neurons prevents obesity and reduces inhibitory tone to POMC neurons. *Neuron* 2011, 71:142-54.
- [256] Vale R, Evans DA, Branco T: Rapid Spatial Learning Controls Instinctive Defensive Behavior in Mice. *Current biology : CB* 2017, 27:1342-9.
- [257] Jardim MC, Nogueira RL, Graeff FG, Nunes-de-Souza RL: Evaluation of the elevated T-maze as an animal model of anxiety in the mouse. *Brain research bulletin* 1999, 48:407-11.
- [258] Canteras NS: Chapter 3.2 Neural systems activated in response to predators and partial predator stimuli. *Handbook of Behavioral Neuroscience*. Edited by Blanchard RJ, Blanchard DC, Griebel G, Nutt D. Elsevier, 2008. pp. 125-40.
- [259] Li L, Feng X, Zhou Z, Zhang H, Shi Q, Lei Z, Shen P, Yang Q, Zhao B, Chen S, Li L, Zhang Y, Wen P, Lu Z, Li X, Xu F, Wang L: Stress Accelerates Defensive Responses to Looming in Mice and Involves a Locus Coeruleus-Superior Colliculus Projection. *Current biology : CB* 2018, 28:859-71.e5.
- [260] Mongeau R, Miller GA, Chiang E, Anderson DJ: Neural correlates of competing fear behaviors evoked by an innately aversive stimulus. *The Journal of neuroscience : the official journal of the Society for Neuroscience* 2003, 23:3855-68.
- [261] Lammel S, Lim BK, Ran C, Huang KW, Betley MJ, Tye KM, Deisseroth K, Malenka RC: Input-specific control of reward and aversion in the ventral tegmental area. *Nature* 2012, 491:212-7.
- [262] Tye KM, Mirzabekov JJ, Warden MR, Ferenczi EA, Tsai HC, Finkelstein J, Kim SY, Adhikari A, Thompson KR, Andalman AS, Gunaydin LA, Witten IB, Deisseroth K: Dopamine neurons modulate neural encoding and expression of depression-related behaviour. *Nature* 2013, 493:537-41.
- [263] Chaudhury D, Walsh JJ, Friedman AK, Juarez B, Ku SM, Koo JW, Ferguson D, Tsai HC, Pomeranz L, Christoffel DJ, Nectow AR, Ekstrand M, Domingos A, Mazei-Robison MS, Mouzon E, Lobo MK, Neve RL, Friedman JM, Russo SJ, Deisseroth K, Nestler EJ, Han MH: Rapid regulation of depression-related behaviours by control of midbrain dopamine neurons. *Nature* 2013, 493:532-6.
- [264] van den Pol AN: Neuropeptide transmission in brain circuits. *Neuron* 2012, 76:98-115.
- [265] Holly EN, Boyson CO, Montagud-Romero S, Stein DJ, Gobrogge KL, DeBold JF, Miczek KA: Episodic Social Stress-Escalated Cocaine Self-Administration: Role of Phasic and Tonic Corticotropin Releasing Factor in the Anterior and Posterior Ventral Tegmental Area. *The Journal of neuroscience : the official journal of the Society for Neuroscience* 2016, 36:4093-105.
- [266] Tan KR, Yvon C, Turiault M, Mirzabekov JJ, Doehner J, Labouebe G, Deisseroth K, Tye KM, Luscher C: GABA neurons of the VTA drive conditioned place aversion. *Neuron* 2012, 73:1173-83.
- [267] van Zessen R, Phillips JL, Budygin EA, Stuber GD: Activation of VTA GABA neurons disrupts reward consumption. *Neuron* 2012, 73:1184-94.
- [268] Boekhoudt L, Omrani A, Luijendijk MC, Wolterink-Donselaar IG, Wijbrans EC, van der Plasse G, Adan RA: Chemogenetic activation of dopamine neurons in the ventral tegmental area, but not substantia nigra, induces hyperactivity in rats. *European neuropsychopharmacology : the journal of the European College of Neuropsychopharmacology* 2016, 26:1784-93.

- [269] Kashdan TB, Barrios V, Forsyth JP, Steger MF: Experiential avoidance as a generalized psychological vulnerability: comparisons with coping and emotion regulation strategies. *Behaviour research and therapy* 2006, 44:1301-20.
- [270] Tong Q, Ye CP, Jones JE, Elmquist JK, Lowell BB: Synaptic release of GABA by AgRP neurons is required for normal regulation of energy balance. *Nature neuroscience* 2008, 11:998-1000.
- [271] Tong Q, Ye C, McCrimmon RJ, Dhillon H, Choi B, Kramer MD, Yu J, Yang Z, Christiansen LM, Lee CE, Choi CS, Zigman JM, Shulman GI, Sherwin RS, Elmquist JK, Lowell BB: Synaptic glutamate release by ventromedial hypothalamic neurons is part of the neurocircuitry that prevents hypoglycemia. *Cell metabolism* 2007, 5:383-93.
- [272] Wulff P, Goetz T, Leppa E, Linden AM, Renzi M, Swinny JD, Vekovischeva OY, Sieghart W, Somogyi P, Korpi ER, Farrant M, Wisden W: From synapse to behavior: rapid modulation of defined neuronal types with engineered GABAA receptors. *Nature neuroscience* 2007, 10:923-9.
- [273] Madisen L, Zwingman TA, Sunkin SM, Oh SW, Zariwala HA, Gu H, Ng LL, Palmiter RD, Hawrylycz MJ, Jones AR, Lein ES, Zeng H: A robust and high-throughput Cre reporting and characterization system for the whole mouse brain. *Nature neuroscience* 2010, 13:133-40.
- [274] Ung K, Arenkiel BR: Fiber-optic implantation for chronic optogenetic stimulation of brain tissue. *Journal of visualized experiments : JoVE* 2012:e50004.
- [275] Sun YG, Pita-Almenar JD, Wu CS, Renger JJ, Uebele VN, Lu HC, Beierlein M: Biphasic cholinergic synaptic transmission controls action potential activity in thalamic reticular nucleus neurons. *The Journal of neuroscience : the official journal of the Society for Neuroscience* 2013, 33:2048-59.
- [276] Xu Y, Kim ER, Zhao R, Myers MG, Jr., Munzberg H, Tong Q: Glutamate release mediates leptin action on energy expenditure. *Molecular metabolism* 2013, 2:109-15.
- [277] Kruk MR, Westphal KG, Van Erp AM, van Asperen J, Cave BJ, Slater E, de Koning J, Haller J: The hypothalamus: cross-roads of endocrine and behavioural regulation in grooming and aggression. *Neuroscience and biobehavioral reviews* 1998, 23:163-77.
- [278] Bosch OJ, Neumann ID: Both oxytocin and vasopressin are mediators of maternal care and aggression in rodents: From central release to sites of action. *Hormones and Behavior* 2012, 61:293-303.
- [279] Young LJ, Flanagan-Cato LM: Editorial comment: Oxytocin, vasopressin and social behavior. *Hormones and Behavior* 2012, 61:227-9.
- [280] Halford JC, Wanninayake SC, Blundell JE: Behavioral satiety sequence (BSS) for the diagnosis of drug action on food intake. *Pharmacology, biochemistry, and behavior* 1998, 61:159-68.
- [281] Korff S, Harvey BH: Animal models of obsessive-compulsive disorder: rationale to understanding psychobiology and pharmacology. *The Psychiatric clinics of North America* 2006, 29:371-90.
- [282] Altman SE, Shankman SA: What is the association between obsessive-compulsive disorder and eating disorders? *Clinical psychology review* 2009, 29:638-46.
- [283] Pollack LO, Forbush KT: Why do eating disorders and obsessive-compulsive disorder co-occur? *Eating behaviors* 2013, 14:211-5.
- [284] Deisseroth K: Circuit dynamics of adaptive and maladaptive behaviour. *Nature* 2014, 505:309-17.
- [285] Dielenberg RA, Hunt GE, McGregor IS: "When a rat smells a cat": the distribution of Fos immunoreactivity in rat brain following exposure to a predatory odor. *Neuroscience* 2001, 104:1085-97.
- [286] Martinez RC, Carvalho-Netto EF, Amaral VC, Nunes-de-Souza RL, Canteras NS: Investigation of the hypothalamic defensive system in the mouse. *Behavioural brain research* 2008, 192:185-90.
- [287] Oda Y, Kodama S, Tsuchiya S, Inoue M, Miyakawa H: Intracellular calcium elevation during plateau potentials mediated by extrasynaptic NMDA receptor activation in rat hippocampal CA1

pyramidal neurons is primarily due to calcium entry through voltage-gated calcium channels. *The European journal of neuroscience* 2014, 39:1613-23.

[288] Pinol RA, Jameson H, Popratiloff A, Lee NH, Mendelowitz D: Visualization of oxytocin release that mediates paired pulse facilitation in hypothalamic pathways to brainstem autonomic neurons. *PLoS one* 2014, 9:e112138.

[289] Verma D, Wood J, Lach G, Herzog H, Sperk G, Tasan R: Hunger Promotes Fear Extinction by Activation of an Amygdala Microcircuit. *Neuropsychopharmacology : official publication of the American College of Neuropsychopharmacology* 2016, 41:431-9.

[290] Kim CK, Adhikari A, Deisseroth K: Integration of optogenetics with complementary methodologies in systems neuroscience. *Nature reviews Neuroscience* 2017, 18:222-35.

[291] Kaiser T, Feng G: Modeling psychiatric disorders for developing effective treatments. *Nature medicine* 2015, 21:979-88.

[292] Grosenick L, Marshel JH, Deisseroth K: Closed-loop and activity-guided optogenetic control. *Neuron* 2015, 86:106-39.

[293] Deslauriers J, Toth M, Der-Avakian A, Risbrough VB: Current Status of Animal Models of Posttraumatic Stress Disorder: Behavioral and Biological Phenotypes, and Future Challenges in Improving Translation. *Biological psychiatry* 2018, 83:895-907.

[294] Goswami S, Rodriguez-Sierra O, Cascardi M, Pare D: Animal models of post-traumatic stress disorder: face validity. *Frontiers in neuroscience* 2013, 7:89.

[295] Lu L, Gutruf P, Xia L, Bhatti DL, Wang X, Vazquez-Guardado A, Ning X, Shen X, Sang T, Ma R, Pakeltis G, Sobczak G, Zhang H, Seo DO, Xue M, Yin L, Chanda D, Sheng X, Bruchas MR, Rogers JA: Wireless optoelectronic photometers for monitoring neuronal dynamics in the deep brain. *Proceedings of the National Academy of Sciences of the United States of America* 2018, 115:E1374-e83.

[296] Shin G, Gomez AM, Al-Hasani R, Jeong YR, Kim J, Xie Z, Banks A, Lee SM, Han SY, Yoo CJ, Lee JL, Lee SH, Kurniawan J, Tureb J, Guo Z, Yoon J, Park SI, Bang SY, Nam Y, Walicki MC, Samineni VK, Mickle AD, Lee K, Heo SY, McCall JG, Pan T, Wang L, Feng X, Kim TI, Kim JK, Li Y, Huang Y, Gereau RWt, Ha JS, Bruchas MR, Rogers JA: Flexible Near-Field Wireless Optoelectronics as Subdermal Implants for Broad Applications in Optogenetics. *Neuron* 2017, 93:509-21.e3.

Vita

Leandra Rosa Mangieri was born in the United States, the daughter of Maria and Ali Mangieri. After completing her work at Bob Jones High School, Madison, Alabama, she entered the University of Alabama at Birmingham in Birmingham, Alabama. She received bachelor's and master's degrees in biology from UAB. In August of 2013 she entered The University of Texas MD Anderson Cancer Center UTHealth Graduate School of Biomedical Sciences.

Permanent address:

120 Madison Point Place

Madison, AL 35758